Distribution Agreement

In presenting this thesis or dissertation as a partial fulfillment of the requirements for an advanced degree from Emory University, I hereby grant to Emory University and its agents the non-exclusive license to archive, make accessible, and display my thesis or dissertation in whole or in part in all forms of media, now or hereafter known, including display on the world wide web. I understand that I may select some access restrictions as part of the online submission of this thesis or dissertation. I retain all ownership rights to the copyright of the thesis or dissertation. I also retain the right to use in future works (such as articles or books) all or part of this thesis or dissertation.

Signature:

_____ _____

Chelsey Chandler Ruppersburg Date

The Ca^{2+}-activated Cl^- channel ANO1 / TMEM16A regulates primary ciliogenesis

By

Chelsey Chandler Ruppersburg
Doctor of Philosophy

Graduate Division of Biological and Biomedical Sciences
Biochemistry, Cell, and Developmental Biology

_____

Criss Hartzell, Ph.D.
Advisor

_____

Victor Faundez, MD/Ph.D.
Committee Member

_____

Michael Koval, Ph.D.
Committee Member

_____

Win Sale, Ph.D.
Committee Member

_____

James Zheng, Ph.D.
Committee Member

Accepted:

_____

Lisa A. Tedesco, Ph.D.
Dean of the James T. Laney School of Graduate Studies

_____

Date

The Ca^{2+}-activated Cl^- channel ANO1 / TMEM16A regulates primary ciliogenesis

By

Chelsey Chandler Ruppersburg
B.S., University of Georgia, 2010

Advisor: Criss Hartzell, PhD

An abstract of
A dissertation submitted to the Faculty of the
James T. Laney School of Graduate Studies of Emory University
in partial fulfillment of the requirements for the degree of
Doctor of Philosophy
in Graduate Division of Biological and Biomedical Sciences
Biochemistry, Cell, and Developmental Biology
2015

Abstract

The Ca^{2+}-activated Cl^- channel ANO1 / TMEM16A regulates primary ciliogenesis

By Chelsey Chandler Ruppersburg

The primary cilium is an evolutionarily conserved sensory organelle important in mediating several signaling pathways vital for development and tissue homeostasis. Defects in primary cilium formation and function result in a variety of human disorders including polycystic kidney disease, the most frequent autosomal dominant hereditary disorder. Many cells possess a single, non-motile, primary cilium highly enriched in receptors and signaling machinery. The primary cilium is thought to be a sensory transducer akin to a cellular antenna. Ciliogenesis involves migration of the basal body to the cell surface followed by outgrowth of the axoneme by intraflagellar transport. I have identified another early step in cilium development, formation of a novel structure - the *nimbus*. Prior to cilia extension, ANO1, a Ca^{2+}-activated Cl^- channel, is organized into a torus-shaped structure along with other ciliary proteins including the small GTPases Cdc42, Arl13b and Rab11, exocyst complex components, and acetylated α-tubulin and γ-tubulin. In collaboration with the Bassell lab at Emory University, we have recently identified the nimbus as an area of mRNA localization. The nimbus forms an interface between the microtubule cytoskeleton, that we can visualize form in real-time, and the surrounding cortical actin cytoskeleton. During ciliogenesis, the nimbus disassembles and ciliary components, including ANO1, move into the cilium. This is the first identification of the Cl^- channel ANO1 in the primary cilium and I further demonstrate that blocking its channel function pharmacologically or knocking it down with shRNA interferes with ciliogenesis. My data support a model where the nimbus provides a scaffold for staging of ciliary components for assembly very early in ciliogenesis and that Cl^- transport by ANO1 / TMEM16A is required for the genesis of primary cilia.

The Ca^{2+}-activated Cl^- channel ANO1 / TMEM16A regulates primary ciliogenesis

By

Chelsey Chandler Ruppersburg
B.S., University of Georgia, 2010

Advisor: Criss Hartzell, PhD

A dissertation submitted to the Faculty of the
James T. Laney School of Graduate Studies of Emory University
in partial fulfillment of the requirements for the degree of
Doctor of Philosophy
in Graduate Division of Biological and Biomedical Sciences
Biochemistry, Cell, and Developmental Biology
2015

Table of Contents

1. General Introduction 1

Overview & Significance 2

Section I. Proper formation and function of the primary cilium is necessary for human development and homeostasis 3

1.1 Association of primary cilia dysfunction and PKD 5

1.2 The role of polycystin channels in the primary cilium 6

1.3 The primary cilium as a specialized Ca^{2+} compartment 9

Section II. Early clues into the role of Anoctamin 1 in primary cilium biology 12

Section III. Insights into primary cilium formation 15

3.1 Epithelial cell polarization and use of cell lines 15

3.2 Polarized epithelial primary cilium formation 16

Section IV. Mechanisms to control cilia composition: the ciliary gate 19

4.1 The Transition Fibers 20

4.2 The Transition Zone (TZ) 20

Section V. The periciliary ring as a potential ciliary trafficking hub 22

5.1 Ring-like structures related to the primary cilium 23

5.2 Ciliary trafficking mechanisms 24

Section VI. The role of actin to preciliary domain formation 27

6.1 Inhibition of actin polymerization promotes preciliary domain formation 27

6.2 Linkage to the actin cytoskeleton as a ciliary composition regulator 28

Figures 34

Figure 1. Diagram illustrating primary cilium structure and formation 34

Figure 2. Two proposed mechanisms of Ca^{2+} signaling associated with the primary cilium 36

Figure 3. Polarized epithelial fluid secretion mediated by ANO1 38

Figure 4. Comparison of various ring-like apical structures 40

2. The Ca^{2+}-activated Cl^- channel ANO1 / TMEM16A regulates primary ciliogenesis 41

Abstract 42

Introduction 43

Results 45

Concentration of ANO1 in an Apical Annular Structure 45
The nimbus is an antecedent of ciliogenesis 47
Ciliary proteins in the nimbus 48
Relationship of the nimbus to the centrosome 49
The nimbus is an interface between the microtubule and actin cytoskeletons 50
Effects of block of ANO1 Cl^- current on ciliogenesis 52
Discussion 54
Materials & Methods 59
Acknowledgements 63
Figures 65
Figure 1. An annulus of ANO1 is located at the apical aspect of cultured epithelial cells 65
Figure 2. ANO1 localization and nimbus formation prior to formation of the primary cilium 67
Figure 3. The ANO1 nimbus precedes primary cilium formation and localization of ANO1 in the nascent cilium 69
Figure 4. Location of key ciliary proteins in the nimbus 71
Figure 5. Relationship of the centriole to the ANO1 nimbus 73
Figure 6. The nimbus is a hub of the microtubule cytoskeleton 74
Figure 7. Moesin marks the boundary of an F-actin-free zone that coincides with the ANO1 nimbus 76
Figure 8. Inhibitors of ANO1 channel activity have a negative effect on cilium length 78
Figure 9. Effects of shRNA knockdown of ANO1 80
Figure 10. Cartoon depicting possible mechanisms of ANO1 function in ciliogenesis 82
3. Conclusions & New Directions 84
Overview 85
What role does the nimbus play in primary cilium biology? 86
Recent experimental advancements in nimbus studies 87
What is the defined spatiotemporal relationship between the nimbus and primary cilium? 88

Are nimbus-associated proteins trafficked exclusively to the developing primary cilium? 89
Is the nimbus an obligate antecedent to the primary cilium? 90
Is the nimbus more than a site for protein localization? 93
What is the role of Cl^- channel activity in primary cilium formation? 96
Does ANO1-mediated Cl^- regulation modulate ciliary protein function and/or trafficking? 96
Are osmotic forces generated by ANO1 Cl^- flux needed in early cilium extension? 97
Does ANO1 or ANO1 channel activity contribute to the distinct ciliary Ca^{2+} levels? 98
Could ANO1 play a role in cilia-related cancer progression and polycystic kidney disease (PKD)? 100
Summary 102
Figures 104
Figure 1. Live-cell imaging of nimbus formation. 104
Figure 2. Additional nimbus components imaged using structured illumination microscopy (SIM) 105
Figure 3. Association of poly(A) RNA and RNA binding protein (RBP) with the nimbus 106
Figure 4. Model of nimbus formation & ANO1 Cl^- channel activity in stages of primary cilium formation 108
Materials & Methods 110
4. References 112

List of Figures

1. General Introduction 1

Figures 34

Figure 1. Diagram illustrating primary cilium structure and formation 34

Figure 2. Two proposed mechanisms of Ca^{2+} signaling associated with the primary cilium 36

Figure 3. Polarized epithelial fluid secretion mediated by ANO1 38

Figure 4. Comparison of various ring-like apical structures 40

2. The Ca^{2+}-activated Cl^- channel ANO1 / TMEM16A regulates primary ciliogenesis 41

Figures 65

Figure 1. An annulus of ANO1 is located at the apical aspect of cultured epithelial cells 65

Figure 2. ANO1 localization and nimbus formation prior to formation of the primary cilium 67

Figure 3. The ANO1 nimbus precedes primary cilium formation and localization of ANO1 in the nascent cilium 69

Figure 4. Location of key ciliary proteins in the nimbus 71

Figure 5. Relationship of the centriole to the ANO1 nimbus 73

Figure 6. The nimbus is a hub of the microtubule cytoskeleton 74

Figure 7. Moesin marks the boundary of an F-actin-free zone that coincides with the ANO1 nimbus 76

Figure 8. Inhibitors of ANO1 channel activity have a negative effect on cilium length 78

Figure 9. Effects of shRNA knockdown of ANO1 80

Figure 10. Cartoon depicting possible mechanisms of ANO1 function in ciliogenesis 82

3. Conclusions & New Directions 84

Figures 104

Figure 1. Live-cell imaging of nimbus formation. 104

Figure 2. Additional nimbus components imaged using structured illumination microscopy (SIM) 105

Figure 3. Association of poly(A) RNA and RNA binding protein (RBP) with the nimbus 106
Figure 4. Model of nimbus formation & ANO1 Cl^- channel activity in stages of primary cilium formation 108

CHAPTER I

GENERAL INTRODUCTION

Overview & Significance

The primary cilium is a sensory organelle important in mediating several signaling pathways vital for normal human development and tissue homeostasis (Gerdes et al., 2009a; Goetz and Anderson, 2010; Ruat et al., 2012). Defects in primary cilium formation and function underlie a spectrum of developmental abnormalities and human diseases such as polycystic kidney disease (PKD) (Fliegauf et al., 2007; Harris and Torres, 2009; Lancaster and Gleeson, 2009; Patel et al., 2009; Pazour et al., 2000; Wheway et al., 2014). While several models of cilium formation are accepted, the early stages of ciliogenesis and all of the contributing components necessary for this process remain incomplete. The work presented in this dissertation furthers our understanding of primary cilium formation through two main avenues. The first focuses on the characterization of a novel cellular structure we termed the nimbus. The second comes from identifying a new player in ciliogenesis, the chloride (Cl^-) channel Anoctamin 1 (ANO1) and the potential role of Cl^- transport in cilium formation. Knowing how the primary cilium is formed in mammalian cells will provide insight into normal tissue development and homeostasis as well as pathological mechanisms of the class of diseases termed the human ciliopathies.

This introductory chapter discusses the varying views on cilium formation. It considers the importance of the primary cilium and work on PKD (Section I), background on ANO1 (Section II), the current models and players of primary cilium formation (Section III), structural elements of the cilium that control ciliary composition (Section IV), and analysis of described ring-like structures related to the cilium and ciliary trafficking mechanisms (Section V & VI). Chapter 2 presents original research identifying the novel ring structure, the nimbus, and characterization of this structure.

Furthermore, it reveals a contribution for the Cl^- channel activity of ANO1 in primary cilium formation and proposes several models of how Cl^- channel activity could contribute to ciliogenesis. Chapter 3 integrates exciting new data about the nimbus with reviews of Chapter 2 conclusions and discussion of the remaining questions surrounding early cilium formation.

My dissertation work has led to the discovery that a distinct apical domain enriched in trafficking and cilium-associated proteins that forms prior to cilium formation and appears to be the future site of ciliogenesis. Additionally, the Cl^- channel ANO1 localizes to the nimbus and is a novel ciliary protein whose Cl^- channel activity contributes to proper cilium formation. These novel observations raise unprecedented questions about the role of the nimbus and ANO1 in primary cilium biology, as the potential contribution of Cl^- channels in regulating cilium dynamics is a new and unidentified function. In my dissertation I hypothesized that *the nimbus provides a scaffold for staging of ciliary components for assembly very early in ciliogenesis and that Cl^- transport by ANO1 is required for the genesis or maintenance of primary cilia*. The data presented in Chapter 2 strongly support an expanded model of early cilium formation that includes cellular identification of the future site of ciliogenesis where protein localization and segregation occur to form the nimbus and that Cl^- channel activity, mediated through ANO1, controls early cilium outgrowth. This expanded model of ciliogenesis and the contribution of Cl^- channel activity to cilium formation reveal new hypotheses about how defects in cilium formation occur and how these defects may lead to human disease.

Section I. Proper formation and function of the primary cilium is necessary for human development and homeostasis

The primary cilium is a specialized cellular compartment; many would call an organelle, that is commonly referred to as a "cellular antenna" due to the enrichment of signaling molecules that allow it to relay and coordinate cellular responses to changes in the external environment that are critical to development and adult tissue homeostasis (Ishikawa and Marshall, 2011; Marshall and Nonaka; Nachury, 2014; Pazour and Witman, 2003; Scholey and Anderson, 2006; Wheatley, 1995). In worms and flies primary cilia are found only on sensory neurons, however in vertebrates, the primary cilium is a ubiquitous structure, present on almost every cell type at some point in development (Gerdes et al., 2009b; Wheatley et al., 1996). The primary cilium consists of a cylindrical array of nine doublet microtubules called the axoneme that extends from its foundation, the basal body (Sorokin, 1962). Surrounding the axoneme is the ciliary membrane, which is continuous with the plasma membrane but distinct in both protein and lipid composition (Fig. 1D) (Brailov et al., 2000; Handel, 1999; Kim and Dynlacht, 2013; Pazour et al., 2002).

The organization of the axoneme microtubules determines how cilia are classified. In motile cilia, the nine doublet microtubules surround a central pair of microtubules (9+2). This central pair gives motile cilia the ability to bend and generate movement like the flagella of *Chlamydomonas reinhardtii* (*C. reinhardtii*) or sperm that allow for cell propulsion or like the multi-ciliated airway epithelia that beat to drive fluid movement in the lungs (Satir and Christensen, 2007). In contrast, the single primary cilium also referred to as a non-motile cilium does not possess this central pair (9+0) but rather functions to transduce extracellular signals into efficient cellular responses that regulate myriad cellular processes including differentiation, tissue patterning and

proliferation (Badano et al., 2006a; Christensen et al., 2007; Drummond, 2012; Oh and Katsanis, 2012; Pazour and Rosenbaum, 2002).

Section 1.1 Association of primary cilia dysfunction and polycystic kidney disease

Although the presence of primary cilia has been known for almost a century, its biological importance has not been appreciated until the discovery of a cohort of cilia related human disorders termed the ciliopathies, caused by underlying cellular defects in the structural or functional aspects of the cilia. Due to the essential functions performed by cilia on all different cell types, these defects affect diverse organ systems and present with pleiotropic and often overlapping phenotypes. More than a dozen disorders comprise the ciliopathy spectrum including autosomal dominant and recessive polycystic kidney disease (ADPKD, ARPKD), nephronophthisis (NPHP), Joubert syndrome (JS), Bardet-Biedl syndrome (BBS) and Meckel-Gruber syndrome (MKS) (Badano et al., 2006a; Brown and Witman, 2014; Fliegauf et al., 2007; Katsanis et al., 2001; Lancaster and Gleeson, 2009). JS, BBS, and MKS are all multisystem recessively-inherited human diseases which display distinct but partially overlapping phenotypes that include retinal abnormalities, polydactyly, polycystic kidneys, neuronal defects, and *situs inversus*. Many of the ciliopathies are caused by mutations in proteins localized to the cilia and basal body including proteins in JS, MKS, and NPHP that are important for the function and structure of the ciliary transition zone (TZ, discussed in more detail in Section IV) (Damerla et al., 2015; Slavotinek et al., 2000).

The first indication that structural abnormalities of the cilium can cause a wide range of hereditary disorders came from the transgenic mouse mutant Tg737. In 1994

Moyer *et al.* first described the Oak Ridge Polycystic Kidney (ORPK) disease mouse (*Tg737*^{orpk}) that came from a large-scale transgene-induced insertional mutagenesis project at the Oak Ridge National Laboratory (Moyer, 1994). The ORPK mouse was the product of a transgene insertion that created a hypomorphic allele of the *Tg737* gene that presented with severely cystic kidneys. However, the function of Tg737 was unknown until 2000 when Pazour *et al.* discovered that Tg737 was the mammalian homologue of the *C. reinhardtii* intraflagellar transport (IFT)-particle protein IFT88 (details into the discovery of IFT and the value of *C. reinhardtii* model system in cilium biology are discussed in Section 3.2) (Pazour et al., 2000). Using an insertional mutant in the *C. reinhardtii IFT88* gene, they show a requirement for IFT88 in flagella formation and hypothesize that Tg737 might be important for formation of primary cilia in the kidney. Scanning electron microscopy examination of homozygous mutant mouse kidneys revealed short stubby cilia of approximately 1 μm compared to wild-type with cilia that extended over 3 μm into the lumen. These results indicated that Tg737 plays an essential role in the assembly of primary cilia, just like IFT88 in flagellar assembly in *C. reinhardtii*. Importantly, these studies made a clear connection between ciliary dysfunction and human disease. However, what mechanisms of cilia function or signaling directly contributed to ARPKD etiology was still unknown. Work on a related renal disease, autosomal dominant polycystic kidney disease (ADPKD), added to our understanding by elucidating a role for calcium (Ca^{2+}) signaling in cilium biology.

Section 1.2 The role of polycystin channels in the primary cilium

ADPKD is the most common inherited kidney disorder affecting 1 in every 1000 individuals worldwide. ADPKD presents with progressive formation and enlargement of

epithelial lined cysts in the kidney, typically resulting in chronic renal failure (Bae et al., 2006; Grantham et al., 2006). Most cases of ADPKD are caused by mutations in the gene products of polycystin-1 (PC-1, PKD1) and polycystin-2 (PC-2, PKD2, TRPP2), encoded by *Pkd1* and *Pkd2* respectively (Hughes et al., 1995; Mochizuki et al., 1996). The polycystin proteins are divided into two structural classes: 11-transmembrane proteins (PKD1, PKD1L1 and PKD1L2) with a large extracellular N-terminal domain with putative cell adhesion domains and a G-protein-coupled receptor proteolytic site (Hughes et al., 1995). The other class consists of six-transmembrane channel proteins (PKD2, PKD2L1 and PKD2L2; TRPPs). PKD2 forms a cation-selective ion channel permeable to Ca^{2+} (Hanaoka et al., 2000; Mochizuki et al., 1996). The resemblance of PKD2 in sequence and topology to transient receptor potential (TRP) channels led to its inclusion as a subfamily of the TRP channel superfamily, TRPP (Kottgen, 2007). PKD1 and PKD2 physically interact via their respective C-terminal coiled-coil domains (Qian et al., 1997). In 1999 Barr & Steinberg demonstrated that GFP-tagged versions of the *Caenorhabditis elegans* (*C. elegans*) homologs of the vertebrate polycystins localize to male sensory neuron cilia (Barr and Sternberg, 1999). Following this discovery, studies showing the co-localization of the polycystins to the primary cilia of mouse and human kidney cells provided a potential link between the cilium and PKD (Pazour et al., 2002; Yoder et al., 2002). These observations along with the work described in the following paragraph contribute to the prevailing hypothesis that PKD1 and PKD2 form a mechanosensory complex in which the large extracellular domain of PKD1 serves as an extracellular sensor for mechanical force, such as urine flow, and subsequent conformational changes of PKD1 activate the PKD2 channel to transduce ciliary bending due to fluid flow into an

intracellular Ca^{2+} increase (Fig. 2A). Some of the key studies contributing to this model are described below.

In 2003 Praetorius & Spring demonstrated that bending the cilium either by application of negative pressure to a pipette placed near the cilium or by increasing the fluid flow rate over the apical membrane resulted in increases in intracellular Ca^{2+} levels in Madin-Darby Canine Kidney (MDCK) cells (Praetorius et al., 2003; Praetorius and Spring, 2001). The change in Ca^{2+} concentration was assessed using a fluorescent Ca^{2+} indicator, Fluo-4. Replacing the extracellular solution to a Ca^{2+}-free solution prior to measurements completely inhibits the response, indicating that the increase in intracellular Ca^{2+} from bending of the cilium requires Ca^{2+} influx from the apical surface. Additionally, Gd^{3+} can inhibit this influx, which generally inhibits nonselective cation channels permeable to Ca^{2+}. On the basis of these results, it was concluded that bending of the cilium activates a mechanosensitive channel permeable to Ca^{2+}.

Following this study, in 2003 Nauli *et al.* attempted to identify the molecules mediating this process. They demonstrated localization of PKD1 and PKD2 to mouse embryonic kidney primary cilia and that application of antibodies against the extracellular domain of PKD2 prevented the flow induced Ca^{2+} influx compared to control treatment of an antibody against the intracellular domain of PKD2 (Nauli et al., 2003). Though the data seemed consistent with the idea that PKD2 in the cilium mediated this response, a direct link was missing. Ten years later, Nauli's group showed that PKD2 is needed for this influx of Ca^{2+} using a ciliary targeted Ca^{2+} sensor made from fusing the Ca^{2+} indicator G-CaMP3 to the C-terminal tail of fibrocystin which contains a highly conserved ciliary targeting sequence (Brookes et al., 2013). Use of this sensor shows that

flow induced bending of the cilium is followed by an increase in intraciliary Ca^{2+} and thereafter an increase in cytosolic Ca^{2+}. Coupling the use of this sensor to Cy5-tagged *Pkd2* siRNA transfected into the kidney proximal tubule cell line LLC-PK, they follow in live cells the responses to flow-induced ciliary bending, which show a significant decrease in both intraciliary and cytosolic Ca^{2+} concentration changes in the PKD2 knockdown cells.

Section 1.3 The primary cilium as a specialized Ca^{2+} compartment

Two recent articles by David Clapham's group significantly contributed to our understanding of Ca^{2+} signaling in the cilium by providing evidence that PKD1L1-PKD2L1 heteromeric channels establish the primary cilium as a unique Ca^{2+} compartment within the cell (DeCaen et al., 2013; Delling et al., 2013). Using telomerase-immortalized human retinal pigmented epithelial cells (htRPE) stably expressing EGFP-tagged Smoothened (htRPE SMO-EGFP) they visualize cilia by confocal microscopy and then use whole-cilia patch clamping to record ciliary channel activity. When the tip of the ciliary membrane is ruptured, they record a large, outwardly rectifying, non-inactivating current with a 96-pS conductance. The calculated density of the channel in primary cilia is comparable to endogenous channel density in the plasma membrane of excitable cells. These observations were confirmed using isolated primary cells mouse RPE and embryonic fibroblasts (MEFs) from a transgenic mouse expressing EGFP-tagged Arl13b (*Arl13B-EGFP^{tg}*) to visualize cilia. Transcript analysis revealed expression of several proposed ciliary channels including PKD1, PKD2, polycystic kidney disease 1-like 1 protein (PKD1L1) and polycystic kidney disease 2-like 2 protein (PKD2L2). However, only siRNAs specific for PKD1L1 and PKD2L1 reduced the

outward currents and patch clamp analysis of homozygous PKD2L1 knockout (*PKD2-L1*$^{-/-}$) MEFs showed reduced ciliary current (DeCaen et al., 2013).

In an accompanying manuscript by Delling *et al*. they demonstrate that the cilia is a specialized Ca^{2+} compartment with a resting Ca^{2+} concentration significantly higher than the cytoplasm and contains the PKD1L1-PKD2L1 channel that they claim regulates Hedgehog signaling (Fig. 2B & C) (Delling et al., 2013). Using a genetically encoded Ca^{2+} sensor made by fusing GCaMP3 to the C-terminus of the ciliary localized protein Smoothened (Smo-mCherry-GCaMP3) they visualize a rapid increase in ciliary Ca^{2+} levels upon rupture of the ciliary membrane tip. They measure a resting ciliary Ca^{2+} concentration of 580 nM, which is significantly higher than the normal resting cytoplasmic Ca^{2+} concentration of less than 110 nM. In htRPE cells stably expressing Smo-mCherry-GCaMP3 loaded with Fluo-4, they monitor changes in cytoplasmic Ca^{2+} in relation to ciliary Ca^{2+} levels. Upon ciliary tip rupture, ciliary Ca^{2+} levels increase and after an approximately 40 second delay that increase spreads to the ciliary base but does not influence cytoplasmic Ca^{2+} concentrations. These results suggest that an ion diffusion barrier may exist between the cilium and cytosol that contributes to the role of the cilium as a functionally distinct cellular compartment.

In addition to ion channels, molecular components from a variety of signaling pathways localize to the primary cilium including those associated with Hedgehog (Hh) signaling (Huangfu and Anderson, 2005; Huangfu et al., 2003). Delling *et al*. relate the highly localized Ca^{2+} signaling to modulation of the Hh pathway. Briefly, Hh signaling participates in the patterning of a large number of tissues including the developing limb buds and neural tube (Basu and Brueckner, 2008; Huangfu and Anderson, 2005; Huangfu

et al., 2003; McGrath et al., 2003; Yuan et al., 2015). The major components of the Shh pathway dynamically localize to the cilia including Patched1 (Ptch1) a receptor for Hh ligands, Smoothened (Smo) and the Gli transcriptional effectors. In absence of the Shh ligand, Ptch1 localizes to cilia and represses the downstream effector of the pathway, Smo, from accumulating in the cilia. After Shh stimulation, Ptch1 is removed from the cilium and Smo translocates to the cilium (Corbit et al., 2005; Rohatgi et al., 2007). Additionally, activation promotes the enrichment of Gli proteins within the cilium and blocks their processing into repressor forms and results in formation of Gli2/3 in active forms that leads to transcription of downstream target genes (Haycraft, 2005; Liu et al., 2005; May, 2005). In wild-type MEF's, treatment with the Smoothened agonist (SAG) leads to increased glioma associated oncogene homolog 1 (*Gli1*) expression. In contrast, SAG activation of *PKD2-L1*$^{-/-}$ MEF's leads to only a small increase in Gli1 levels. In addition, *PKD2-L1*$^{-/-}$ × *Arl13B-EGFP*^{tg} mutant cells show a two-fold decrease in Gli2 accumulation at the ciliary tip compared to control cells. Gli2 accumulation at the distal tip of cilia is required for the activation of Gli2 and downstream transcription events (Delling et al., 2013; Endoh-Yamagami, 2009; Liem et al., 2009). Together, these results suggest that ciliary Ca^{2+} levels, as maintained by PKD2L1, may contribute to the proper functioning of the Hh-signaling pathway (Fig. 2C) (Delling et al., 2013).

Between the studies on PKD and the more recent work from the Clapham lab, accumulating evidence suggests that two types of Ca^{2+} signaling may occur in ciliated cells. One mediated by the PKD1/PKD2 channel complex to control ciliary-mediated Ca^{2+} signaling that spreads to the cytoplasm as part of the mechanosensory function of cilia (Fig. 2A). The other through the PKD1L1-PKD2L1 heteromeric channels to

regulate intraciliary Ca^{2+} signaling that may modulate cilium associated signaling pathways like Hh (Fig. 2B & C). The identification of the cilium as a specialized cellular Ca^{2+} compartment is of particular interest because the work I present in Chapter 2 of this dissertation identified the Ca^{2+}-activated Cl^- channels (CaCC) Anoctamin1 (ANO1) in developing and mature cilia. The original observations I present in Chapter 2 on the localization of ANO1 to the cilium and the studies showing contribution of ANO1 Cl^- channel activity to cilium formation opens a new line of investigation into the role of anion channels in cilium formation and function. In light of the recent observations of the cilium as a Ca^{2+} compartment, questions are raised about the potential regulation of ANO1 in the cilium and the function Cl^- channels could play in cilia biology, which I will discuss in more detail in Chapter 3. In the following section I will provide some background on the Anoctamin channels.

Section II. Early clues into the role of Anoctamin 1 in primary cilium biology

ANO1, also referred to as TMEM16A, is a member of the Anoctamin (ANO or Tmem16) superfamily. Mammalian anoctamins have 10 gene members that are well conserved across species and predicted to have similar topologies consisting of ten hydrophobic helices that are likely to be transmembrane domains with cytosolic N- and C-termini (Brunner et al., 2014). In murine tissues, ANO's 1, 6, 7, 8, 9, and 10 are expressed in a variety of epithelia, while ANO's 2, 3, 4, and 5 are more restricted to neuronal and musculoskeletal tissue (Duran and Hartzell, 2011b; Schreiber et al., 2010). Although the Cl^- channel function of ANO1 and ANO2 have been established, determining roles for the remaining anoctamins has proven difficult though currently much attention is focused on the possibility that some members of the anoctamin family

function as phospholipid scramblases (Duran and Hartzell, 2011b; Pedemonte and Galietta, 2014; Yu et al., 2015).

ANO1, also referred to as TMEM16A, and ANO2 (TMEM16B) are gated open in response to increases in intracellular Ca^{2+} and are selective for Cl^-, which led to their categorization as Ca^{2+}-activated Cl^- channels (CaCC). This discovery came in 2008 when three labs independently showed that heterologous expression of ANO1 and ANO2 recapitulated the properties of native CaCC's (Caputo et al., 2008a; Schroeder et al., 2008a; Yang et al., 2008a). The Ca^{2+} sensitivity and voltage dependency of ANO1 are similar to those of endogenous CaCC's, with an EC_{50} of 2.6 μM at −60 mV. A large push forward in the field came from Tereshima *et al.* who showed for the first time that purified ANO1 incorporated into lipid vesicles is sufficient to form a functional CaCC that is highly selective for Cl^- over cations and that additional protein components are not necessary for the activation or function of ANO1 (Terashima, 2013). They provide clear evidence for the direct activation of ANO1 by Ca^{2+} and show that the rate of Cl^- efflux of the reconstituted protein in liposomes is modulated by the Ca^{2+} concentration at levels comparable to previous descriptions of classical CaCC's. Terashima *et al.* demonstrate that two conserved glutamates on the intracellular TM6-7 loop are responsible for this Ca^{2+} sensing, consistent with work from the Hartzell lab discovering that mutation of two glutamic acids, E702 and E705, drastically alter the Ca^{2+} sensitivity of the channel (Yu et al., 2012b).

Though much is being learned about the biophysical properties of ANO1, our understanding of the exact cell biological roles of ANO1 remain unclear. In general, CaCC's play essential roles in cellular physiology including epithelial fluid transport and

secretion, sensory transduction and adaptation, regulation of vascular smooth muscle tone, control of neuronal and cardiac excitability, and nociception (Arreola et al., 1995; Duan, 2009; Duran et al., 2010b; Hartzell et al., 2005b; Hengl et al., 2010; Liu et al., 2010; Rasche et al., 2010; Stephan et al., 2009; Tarran, 2004; Tarran et al., 2002). Perhaps the best known function of the CaCC's is their role in epithelial secretion, the general principle of which involves intracellular accumulation of Cl^- above its electrochemical gradient by pumps and transporters and downhill Cl^- efflux into the lumen mediated by apical Cl^- channels (Fig. 3B). ANO1 is widely expressed in secretory epithelia where it resides predominantly in the apical membrane to provide a pathway for the transepithelial movement of Cl^- in Ca^{2+}-regulated epithelial fluid transport (Hartzell et al., 2009a; Ousingsawat et al., 2009; Yang et al., 2008b). In addition, ANO1 performs myriad functions in a variety of cell types including smooth muscle cells, retina and somatosensory neurons (Caputo et al., 2008a; Huang et al., 2009; Kunzelmann et al., 2011a; Ousingsawat et al., 2009; Rock et al., 2009; Romanenko et al., 2010b; Yang et al., 2008a).

A handful of clues suggest that ANO1 may perform specific roles in development. Jason Rock and Brian Harfe identified *Ano1* in a screen for genes expressed in the zone of polarizing activity of the embryonic mouse limb bud, an anatomical region involved in creating a gradient of the Shh morphogen (Rock et al., 2007a). A year later Rock *et al.* showed that loss of *Ano1* causes severe developmental abnormalities as *Ano1* knockout mice die quickly after birth due to morphogenesis of the trachea and loss of gastrointestinal motility (Rock et al., 2008). These early studies gave us some clues that ANO1 may be involved with the primary cilium. Results presented in this dissertation perturbing ANO1, either by knockdown or with the use of ANO1-specific inhibitors, that causes defects in

primary cilium formation suggests that ANO1 may contribute to the formation and/or function of primary cilia. In the following sections, I will give an introduction to the field of primary ciliogenesis.

Section III. Insights into primary cilium formation

Section 3.1 Epithelial cell polarization and use of cell lines

Significant insight into the process of primary cilium formation comes from work in *in vitro* cell culture models of primary or immortalized cell lines. The work from my dissertation focuses on ciliogenesis in two widely-use polarized kidney epithelial cell lines, the murine immortalized cortical collecting duct cell line (mpkCCD$_{14}$) and the mouse intramedullary collecting duct cell line (IMCD3). Both of these cell lines are commonly used to study *in vitro* epithelial cell polarization and primary cilium formation and function. Polarization, characterized by the asymmetric segregation of proteins and lipids into discrete functional domains, is critical for epithelial cells to regulate exchange between the exterior and interior milieu. The polarized state of these cells is essential for epithelial functions including vectorial transport and barrier formation.

During epithelial development apical-basal polarity is established by the selective sorting of proteins and lipids into structurally and functionally segregated domains at the apical and basolateral membranes (Fig. 3A) (Le Gall et al., 1995; Mostov, 2003). Three major polarity complexes spatiotemporally interact with the cytoskeleton and adhesion proteins to form these distinct domains that include the Par complex (Par3, Par6, aPKC, CDC42), the Scribble complex (SCRIB, DLG, LGL), and the Crumbs complex (CRB, PALS1, PATJ) (Bilder et al., 2000; Bilder et al., 2003; Kemphues et al., 1988; Nelson,

2003; Roh et al., 2003). Generally, the Crumbs complex establishes and maintains the apical domain while the Scribble complex acts on the lateral domain. The balance between these is regulated through the Par complex that promotes establishment of the apical-basal membrane border (Rodriguez-Boulan and Macara, 2014). The basolateral domain is the site of cell-cell contact points called junctions including tight junctions, adherens junctions, gap junctions and desmosomes (McCaffrey and Macara, 2011; Rodriguez-Boulan and Macara, 2014). The tight junctions are the most apical and act as a fence to prevent mixing of components between the two domains to delineate apical versus basolateral surfaces. They also form barriers between adjacent cells to limit paracellular permeability (Matter and Balda, 2003). The apical surface confronts the external environment or lumen and is the site of primary cilium formation. The emergence of a primary cilium is considered a read out of terminal polarization and the process of ciliogenesis utilizes some of the same molecular players, discussed in the following sections (Bacallao et al., 1989).

Section 3.2 Polarized epithelial primary cilium formation

In polarized epithelial cells, ciliogenesis begins with migration and docking of the mother centriole to the apical membrane to form the foundation of the primary cilium - the basal body (Fig. 1A) (Lu et al., 2015; Sorokin, 1962). Centrioles form the core of the centrosome, along with the pericentrosomal material, that functions as the microtubule organizing center (Bettencourt-Dias and Glover, 2007). When cells enter the cell cycle each one of the centrioles that compose the centrosome duplicates to form two new pairs of centrioles that then function in mitotic spindle formation. The original centriole in each pair is referred to as the mother centriole and it is further distinguished from the daughter

centriole by the presence of accessory structures such as the distal appendages that allow the mother centriole to function as the basal body of the cilium. These distal appendages become the transition fibers when the basal body anchors to a membrane (described in more detail in Section IV, Fig. 1A) (Piel et al., 2000; Tanos et al., 2013). The use of the mother centriole as the base of the cilium explains why primary ciliogenesis is closely coordinated with the cell cycle, limiting construction and presence of primary cilia to cells in G1/G0 (Pugacheva et al., 2007; Rieder et al., 1979; Tucker et al., 1979; Wheatley et al., 1996).

After docking of the basal body, ciliogenesis proceeds by formation of the transition zone (TZ, discussed in more detail in Section IV) followed by axonemal outgrowth into the extracellular space (Fig. 1B & 1C). In non-polarized cells like fibroblasts and in smooth muscle cells, ciliogenesis begins with docking of a Golgi-derived vesicle on one end of the mother centriole as it is trafficking to the plasma membrane. In this pathway, the nascent axoneme begins to emerge before the mother centriole reaches the plasma membrane (Lu et al., 2015; Sorokin, 1962; Yee and Reiter, 2015). This intracellularly developing cilium eventually fuses with the plasma membrane that often creates what is referred to as the ciliary pocket, which is a deep invagination of the plasma membrane around the base of the cilium.

Axoneme assembly occurs through intraflagellar transport (IFT), a microtubule-motor-based trafficking system to move proteins within the cilium (Binder et al., 1975; Johnson and Rosenbaum, 1992; Pedersen et al., 2006; Pedersen and Rosenbaum, 2008; Rosenbaum and Child, 1967; Taschner et al., 2012; Witman, 1975). Though the motile flagella and primary cilia are functionally distinct, there are many parallels in the basic

structure and the intraciliary trafficking mechanism, IFT. Groundbreaking work on the flagella of the green alga *C. reinhardtii* has been a large contributor to the knowledge of the protein machinery and basic biology of IFT. IFT was first observed in *C. reinhardtii* using differential interference contrast (DIC) microscopy and described as the continuous bidirectional movement of granule-like particles along the flagella (Kozminski et al., 1993). This movement has also been described using GFP-tagged IFT proteins in the neuronal sensory cilia of *C. elegans* and the primary cilia of cultured kidney cell lines (Orozco, 1999; Qin et al., 2001; Signor, 1999; Tran, 2008). Follow-up studies using correlative light and electron microscopy demonstrated that these IFT particles were organized in linear arrays of structures connected to both the axonemal outer doublet microtubules and the flagellar membrane (Kozminski et al., 1995). Isolation of IFT particles from *C. reinhardtii* flagella revealed two large and biochemically distinct complexes termed IFT complex A and B (Cole, 1998; Piperno and Mead, 1997). Complex B IFT proteins and Kinesin-2 motors move cargo in the anterograde direction towards the distal tip along the axoneme while complex A proteins and dynein-2 motors return cargo in the retrograde direction back towards the cell body (Fig. 1C) (Kozminski et al., 1995; Kozminski et al., 1993; Pazour et al., 1999; Porter et al., 1999). Studies in *C. reinhardtii* with temperature-sensitive (ts) alleles of the gene *FLA10* (flagellar assembly, *fla*) revealed that not only was IFT important for flagella assembly but also important for flagella maintenance (Adams et al., 1982; Huang et al., 1977). *FLA10* is now known to encode a kinesin-2 motor subunit. When grown at the restrictive temperature, *fla10*^{ts} mutants are unable to form cilia indicating an essential role for kinesin-2 in flagella formation (Walther et al., 1994). In addition, when mutants grown at the permissive

temperature to form flagella were then shifted to the restrictive temperature, the flagella gradually shortened indicating that IFT was also essential for flagella maintenance (Huang et al., 1977; Kozminski et al., 1995). The restriction of protein synthesis to the cytoplasm makes elongation of the ciliary axoneme and turnover of ciliary components dependent on IFT and explains why disruption of this process results in human disease.

Though extensive study into the process of axoneme formation by IFT has significantly advanced the cilia field, our understanding of how the ciliary membrane that surrounds the axoneme develops and expands during the early stages of ciliogenesis remains limited (Pedersen and Rosenbaum, 2008; Taschner et al., 2012). One of the biggest questions comes from the idea that the cilium must account for one of the central problems of any organelle which is getting specific proteins delivered but has a unique problem in that it must keep certain proteins out because it is continuous with the plasma membrane. In the following section, I describe the current models on how the ciliary gate modulates the protein composition of the cilium.

Section IV. Mechanisms to control cilia composition: the ciliary gate

The most proximal region of the cilium is the ciliary gate, which is proposed to function in formation of the cilium as a distinct compartment, isolated from cellular cytoplasmic and plasma membrane proteins (Reiter et al., 2012). Early observations in transmission electron microscopy cross-sections identified this distinct region and suggested that formation of the gate region occurred at the early stages of ciliogenesis (Gilula and Satir, 1972; Sorokin, 1962). Work from Pazour *et al.* using the *C. reinhardtii* insertional mutant in the *IFT88* gene showed that *ift88*-1 cells lack flagella. Electron

microscopic analysis of these mutants reveals structurally normal basal bodies with clear transition zone (TZ) formation but no flagella assembly beyond the TZ (Pazour et al., 2000). These results have been interpreted to mean that formation of the ciliary gate represents one of the earliest steps in ciliogenesis, preceding IFT-dependent axoneme formation (Fig. 1B). The ciliary gate is divided into two subdomains, the transition fibers and TZ (Fig. 1D).

Section 4.1 The Transition Fibers

Anchoring the basal body to the base of the ciliary membrane are transition fibers, which extend from the distal end of the basal body and connect the basal body microtubules to the base of the ciliary membrane. Immunogold labeling for IFT-particle proteins in *C. reinhardtii* uncovered that IFT proteins localize at the membrane-associated ends of the transition fibers (Deane et al., 2001; Pedersen et al., 2006; Sloboda and Howard, 2007). Additionally, in *C. elegans*, IFT-associated proteins concentrate within this transition fiber region. Electron micrographs from various cell types indicate that the inter-fiber space is approximately 60 nm, too small to allow for the passage of vesicles and therefore defines the limit at which cilium-destined vesicles can fuse (Anderson, 1972; Nachury et al., 2010). The identification of IFT component localization at this region and the size limitations, led to the hypothesis that the transition fibers represent a loading zone for cilium-bound cargo to associate with IFT particles that then also interact with the proteins in the next region of the ciliary gate, the TZ.

Section 4.2 The Transition Zone (TZ)

Beyond the basal body, at the base of the cilium between where the basal body ends and the axoneme begins a specialized structure called the TZ forms that functions as a diffusion barrier to mediate the entry of specific cargoes in the cilium. In longitudinal sections of the TZ, the axonemal microtubules are linked to the ciliary membrane by Y-shaped connectors and form what is called the ciliary necklace that is believed to contribute to forming a membrane barrier (Fig. 1D) (Awata et al., 2014; Craige et al., 2010; Gilula and Satir, 1972; Horst et al., 1987). Septins, which are a family of ologomeric GTPases that form scaffolds to interact with membranes, also localize to this region and are thought to contribute to this membrane barrier. Septin 2 localizes at the base of the cilium and knockdown of septin 2 causes increased entry of ciliary transmembrane proteins (Hu et al., 2010). Studies using fluorescence recovery after photobleaching (FRAP) show that if a small section of the cilium is bleached, rapid recovery occurs within the cilium indicating movement of proteins within the cilium. However, if the entire cilium is bleached no recovery occurs consistent with the idea of a diffusion barrier between the plasma and ciliary membranes (Chih et al., 2012).

Rosenbaum and Witman (2002) proposed that the ciliary gate region was in certain ways homologous to the nuclear pore, controlling the entry of proteins into the cilium (Rosenbaum and Witman, 2002). The identification of importin-B1, importin-B2, and a gradient of RanGTP and RanGDP across the basal body is consistent with this hypothesis (Dishinger et al., 2010; Fan et al., 2011; Hurd et al., 2011). One of the influential experiments in support of this idea came from the identification of nuclear localization sequences on the IFT component, KIF17, the kinesin-2 motor (Dishinger et al., 2010). Removal of the C-terminal tail domain from KIF17 blocked ciliary

localization while expression of just the tail domain showed predominant localization to the nucleus. Mutational analysis revealed that the KRKK sequence in the KIF17 tail domain acts as the ciliary localization sequence and that this sequence interacts with importin-B2, which is necessary for KIF17 cilium import.

Though our understanding of ciliary gate formation and function is continually expanding, information into the regulatory mechanisms in place controlling the composition of the early emerging cilium remains limited (Garcia-Gonzalo and Reiter, 2012; Reiter et al., 2012). With the direct docking of the basal body to the apical plasma membrane, it seems as though some process of protein selection and exclusion would need to be in place at the plasma membrane before docking. Data I present in this dissertation details the formation of an apical ring of ANO1 along with key ciliary proteins and microtubules prior to cilium formation that we believe may function as a trafficking hub for proteins destined for the cilium and creating an area of protein exclusion to help regulate nascent ciliary protein composition. We have termed this ring the nimbus because of its resemblance to a halo. This idea of a future periciliary membrane with possible barrier functions has been documented and described before as an exclusionary area that forms prior to cilium formation at the apical membrane (Fig. 4) (Francis et al., 2011; He et al., 2012b; Kim et al., 2010; Kolb et al., 2004; Meder et al., 2005; Vieira et al., 2006; Wang et al., 2009). I will discuss the limited data and compare the various descriptions of this area and potential specialized membrane domain in the following sections.

Section V. The periciliary ring as a potential ciliary trafficking hub

In a series of reports from various labs, a unique circular organization and/or area of protein exclusion in polarized epithelial cell lines has been described, given different names and shown with different proteins (Fig. 4). These reports, along with the work presented in this dissertation suggest this site may act as a docking site for cilia-targeted vesicles and plays an early role in forming a membrane and cytoskeletal barrier to regulate protein and lipid composition of the early cilium. The purpose of this section is to consolidate the various reports and review the information for a more accurate and complete view of this specialized cellular domain related to early ciliogenesis.

Section 5.1 Ring-like structures related to the primary cilium

In 2004 Kolb *et al.* discovered a dense ring of microtubules at the apical portion of the cytoplasm in fixed mouse proximal tubule cells (mPT) that was under an area of the membrane devoid of wheat germ agglutinin (WGA) labeling (Kolb et al., 2004). In a highly polarized state, the mPT cells create a distinct ring structure of vesicles containing Angiotensin-1 (AT1) in the subapical region that they claim resembles the condensed apical recycling endosomes (CARE). This ring of AT1 and additionally identified component NHE3, an apical transporter, was adjacent to the primary cilium (Kolb et al., 2004). Disruption of the microtubules with nocodazole or stimulation of the cilium with fluid flow caused the ring of AT1 to disperse (Kolb et al., 2004). Similar to this area of specific protein enrichment, in 2006 Vieira described a "black hole" approx. 1.8 μm in diameter of a GPI-anchored fluorescent protein at the base of the cilium. Inside this excluded zone of the GPI anchored protein was a circular ring of galectin-3, a lectin implicated in regulation of glycoprotein apical trafficking in differentiated epithelial cells (Vieira et al., 2006).

In line with these descriptions, Wang *et al.* identified what they called a novel pericentriolar compartment at the base of the cilium. This compartment was a circular enrichment of the sphingolipid ceramide at the apical portion of MDCK cells. The cilium emerged off one edge of this approximately 1.5 μm ring of ceramide, which was also an area devoid of WGA labeling, like that described by Kolb *et al.* They conclude that this membranous compartment represents the de novo sphingolipid biosynthesis pathway involving ceramide transport from the ER to the *cis* Golgi (Wang et al., 2009). In a follow-up study, they further characterize this area and name it the Apical Ceramide Enriched Compartment (ACEC). Prior to cilium formation acetylated tubulin associates and emanates from the ACEC in MDCK cells. Later the procilium, a short stub at the cell surface labeled with acetylated tubulin, projects from this region. After cilium formation, the ring as detected by ceramide labeling is still present and the cilium projects from one edge of the ring. Of note, they identify a handful of proteins involved in or associated with pathways important in trafficking to the cilium including one of the BBSome components, BBS1, and aPKC linked through Cdc42 to exocyst complex recruitment (He et al., 2012b). Studies I present in Chapter 2 of this dissertation also localize components of these two trafficking pathways to the nimbus, which leads me to hypothesize *that the nimbus may function as an apical trafficking hub important in sorting proteins destined for the cilium from other apical membrane proteins.* In the following subsection I describe these two trafficking pathways and their linkage to the cilium.

Section 5.2 Ciliary trafficking mechanisms

In 2007 Nachury *et al.* identified a heptameric complex called the BBSome (BBS1, BBS2, BBS4, BBS5, BBS7, BBS8, BBS9) by tandem affinity purification of a

tagged BBS protein precipitated from ciliated mammalian cells followed by identification of associated proteins by mass spectrometry (Nachury, 2007). Mutations in BBS proteins cause the pleiotropic ciliopathy Bardet-Biedl Syndrome (BBS) characterized by obesity, mental retardation, cystic kidneys and retinal degeneration (Harville et al., 2010). The BBS proteins, together in the BBSome complex contain coat-like structural elements common to COP1 and COPII coated vesicles and are believed to be involved in vesicle transport from the Golgi to the basal body and cilia. Using detergent extraction, Nachury *et al*. demonstrated that the BBSome associates with membranous structures and more specifically associates with Rabin8, a guanine nucleotide exchange factor (GEF) for RAB8. GTP loading on Rab8 by Rabin8 promotes targeting of post-Golgi vesicles to polarized areas of the plasma membrane and more specifically, promotes docking and fusion of vesicles to the base of the ciliary membrane to promote ciliogenesis (Nachury, 2007). Consistent with the potential role for Rab8 in ciliogenesis, overexpression of Rab8 or expression of constitutively active Rab8 (Q76L) promotes elongation of the cilium, both in membrane and axoneme length, when compared to control (Yoshimura et al., 2007). Upstream of this interaction, post-Golgi trafficking of cilium destined vesicles involves Rab11 that regulates endosome recycling and recruits Rabin8 for transport to a pericentriolar compartment (Knodler et al., 2010).

The Rab11-Rabin8-Rab8 network connects to another key trafficking system critical for primary cilium formation by recruiting Cdc42 and exocyst proteins to the apical membrane of MDCK cells. The exocyst is a highly conserved tethering complex (Sec3, Sec5, Sec6, Sec8, Sec10, Sec15, Exo70 and Exo84) that in concert with SNARE and Rab proteins, facilitate the docking and fusion of vesicles with the target membrane

(Novick et al., 1980; TerBush et al., 1996). The exocyst localizes to areas of the plasma membrane involved in specialized cellular outgrowth or function like the yeast bud neck, the leading edge of motile cells, and in polarized epithelia areas of cell-cell contact to regulate delivery of cargo to these specific sites at the appropriate time. More recently, the exocyst has received attention because of its localization to the primary cilium and its role in ciliogenesis (Rogers et al., 2004). Knockdown of one of the exocyst components, Sec10, prevents ciliogenesis while overexpression promotes this process (Zuo et al., 2009). The exocyst has previously been shown to associate with Par3, a component of the Par polarity complex and more recently shown to associate with Cdc42 and is required for its localization to the primary cilium (Zuo et al., 2011a; Zuo et al., 2009). Expression of dominant negative Cdc42 in MDCK cells as well as knockdown of Cdc42 or the Cdc42 GEF Tuba inhibit ciliogenesis and prevent exocyst localization to the cilium (Zuo et al., 2011a). Consequently, because of the interaction of the exocyst with other ciliary proteins, specifically the cation channel PKD2 disrupted in the human disorder PKD, knockdown also prevented localization of PKD2 to the cilium.

In addition to localizing components of these two trafficking pathways including BBS1, Sec6, Sec8 and Cdc42 to the nimbus, I have identified association of the actin associated protein, moesin at the nimbus. Previously, our lab performed highly sensitive quantitative stable isotope labeling by amino acids in culture (SILAC) proteomic approach to obtain insights into stoichiometric protein networks associated with the ANO1 channel (Perez-Cornejo et al., 2012b). SILAC analysis revealed that ANO1 interacts at high stoichiometry with a network of notable proteins involved in cytoskeleton organization, membrane trafficking, and ciliogenesis including the small GTPases Rab8, Rab11 and

Cdc42 and among the proteins most highly enriched in association were the ERM (ezrin, radixin, moesin) proteins (Perez-Cornejo et al., 2012b). The ERM family of proteins coordinates processes at the plasma membrane to the reorganization of the actin cytoskeleton to form an organized actin network underlying the apical surface (Edwards et al., 1997; McCartney and Fehon, 1996; Saotome et al., 2004; Speck et al., 2003). The identification of moesin at the nimbus along with the discovery that the area demarcated by the nimbus is free of filamentous actin (F-actin) raises questions about the potential role of the actin cytoskeleton to cilium formation. Some clues about the involvement of the actin cytoskeleton to ciliogenesis and formation of this circular preciliary domain have been made in the literature and are discussed in the following section.

Section VI. The role of actin to preciliary domain formation

Section 6.1 Inhibition of actin polymerization promotes preciliary domain formation

One of the biggest clues into the potential role of actin in ciliogenesis came in 2010 when Kim *et al.*, using a high-throughput siRNA assay, evaluated the impact of over 7,700 genes on an *in vitro* ciliogenesis in htRPE cells. Using an EGFP-tagged Smoothened (Smo-EGFP) as a cilium marker for quantification purposes, they identified a handful of genes involved in regulating the actin cytoskeleton that significantly altered cilium length and conclude that branched F-actin plays an inhibitory role in cilium formation (Kim et al., 2010). They describe an area they call the pericentrosomal preciliary compartment (PPC), a ring approximately 2 μm in diameter of Smo-EGFP positive puncta around the centrosome prior to cilium formation. As the cilium begins to form at the ring, the PPC as seen by Smo-EGFP gradually attenuates until within just four

hours of serum starvation only 3% of cells still have a detectable PPC. If they deplete one of the major constituents of the ARP2/3 complex necessary for nucleating actin polymerization at filament branches, ACTR3 (Arp3), live cells maintain a pronounced PPC at the ciliary base much longer. Furthermore, an enhancement in cells with a clear PPC preceding ciliogenesis is seen when cells are treated with cytochalasin D, an inhibitor of actin polymerization. They conclude that the PPC may function as a temporary reservoir of membrane proteins and lipids destined for the cilia during the early stages of ciliogenesis and that blocking actin assembly may facilitate ciliogenesis by stabilizing this PPC. The PPC they described was also marked by recycling endosome marker Rab11. When they knockdown PTPN23, a protein involved in cargo sorting at early endocytic compartments, the Smo-EGFP constituting the PPC now accumulates in EEA1 positive vesicles and the PPC does not form. Taken together they believe a trafficking pathway connects recycling endocytic compartments to the PPC and that this pathway and structure are involved in cilium formation (Kim et al., 2010).

Section 6.2 Linkage to the actin cytoskeleton as a ciliary composition regulator

The possible link of the actin cytoskeleton to another PPC-like structure was also described by Meder *et al.* studying the apical marker gp135, which they identified as the dog orthologue of podocalyxin (Meder et al., 2005). Meder *et al.* noted an area approximately 1.8 μm in diameter at the apical membrane where gp135 was excluded and that corresponded to the site of outgrowth of the primary cilium. This special localization of gp135 was shared by a GFP tagged version of the cytoplasmic PDZ (PSD-95/Dlg/ZO-1) protein Na^+/H^+ exchanger regulatory factor (NHERF)-2. The C-terminal PDZ binding motif was already known to bind NHERF-2, which is a scaffold protein connecting

plasma membrane proteins with members of the ERM family to link them to the underlying actin cytoskeleton. In 2011, Francis *et al.* followed-up on this observation, and refer to the gp135 exclusion zone at the apical membrane as the ciliary membrane domain (CMD) (Francis et al., 2011). Along with gp135, Francis *et al.* show F-actin and NHERF-1, the predominant NHERF protein expressed in MDCK cells, exclusion from the CMD which they observe form prior to cilium formation. Within three days of seeding MDCK cells, the CMD develops and the centriole positions there, several days before detectable formation of the primary cilium. They hypothesize that disassembly of the dense subapical actin must occur to allow the centrosome to dock at the apical membrane.

Both Meder *et al.* and Francis *et al.* show that the formation of this exclusionary zone depends on linkage through the adapter NHERF to the ERM's. The ERM proteins provide a regulated link between membrane-associated proteins and the underlying actin cytoskeleton to organize the apical membrane and form an organized actin network underlying the apical surface (Edwards et al., 1997; McCartney and Fehon, 1996; Saotome et al., 2004; Speck et al., 2003). A growing body of evidence designates the function of the ERMs as upstream regulators of signaling mechanisms in epithelia. Coordination of the cytoskeleton and signaling pathways mediated by the ERM proteins at the apical membrane promote epithelial cell polarity and integrity (Atwood et al., 2007; Joberty et al., 2000; Martín-Belmonte et al., 2008; McCartney and Fehon, 1996; Saotome et al., 2004; Speck et al., 2003). In *Drosophila melanogaster* the loss of the single ERM orthologue Moesin presents in disruption to epithelial characteristics and acquisition of invasive migratory behavior, which correlates with the misregulation of ERM expression

associated with the metastatic abilities of cancer cells (McCartney and Fehon, 1996). Increasing evidence of a role for ERM proteins in tumor progression highlights the importance of proper ERM protein localization. In patients with oral squamous cell carcinoma, a cellular translocation of moesin from a membranous to a primarily cytoplasmic distribution is observed in metastatic cells.

The ERMs are characterized by the presence of a plasma membrane-associated FERM domain in the amino terminus and a C-terminal FERM-association domain with the ability to bind F-actin (Turunen et al., 1994). ERM proteins are conformationally regulated by an intramolecular interaction between the amino and carboxy-terminal domains (Gary and Bretscher, 1995). Activation through release of this domain interaction requires binding to phosphatidyl-inositol-4,5-biphosphate (PIP2) and phosphorylation of a conserved threonine in the actin binding site (Fievet et al., 2004; Nakamura et al., 1995; Yonemura et al., 2002). The FERM domain of activated ERMs can bind directly to the cytoplasmic tails of various membrane proteins or to related scaffolding proteins which mediate interaction with other membrane proteins such as ion channels and transporters (Reczek et al., 1997; Weinman et al., 2006; Yonemura et al., 1998). More recently, Solinet *et al.* demonstrated that the ERMs can bind to microtubules through a motif in their FERM domains and modulate microtubule dynamics (Solinet et al., 2013). Therefore, the ERM proteins provide a regulated link between membrane-associated proteins and the actin cytoskeleton to organize the apical membrane and may play important roles in mediating signaling between microtubules and actin.

Meder *et al.* and Francis *et al.* further characterized the potential mechanism of gp135 exclusion by assessing the importance of the C-terminal PDZ-binding motif of

gp135 (Francis et al., 2011; Meder et al., 2005). Both mutation and/or removal of the PDZ motif allow gp135 to enter the CMD and the primary cilium. Knockdown of NHERF-1 causes the same loss of gp135 segregation. They interpret this to mean that association with NHERF-1 retains gp135 and that NHERF-1 acts as an adapter linking interacting membrane proteins to the ERM proteins and the actin cytoskeleton to restrict lateral movement. When the ERM binding domain of NHERF-1 is added to Smoothened, a protein that can be trafficked laterally into the cilium, Smoothened was primarily restricted to the apical membrane in a pattern similar to the CMD with only a small amount in the cilium. They conclude that linkage of PDZ-containing membrane proteins to the actin cytoskeleton via interaction with NHERF-1 and the ERM proteins constitutes a retention matrix. This matrix prevents the passive diffusion of apical membrane proteins into the CMD and ciliary membrane. The conclusion by Francis *et al.* that a strict diffusion barrier at the base of the cilium does not exist because mutation of the PDZ domain of gp135 allows it to enter the cilium seems oversimplified. Gp135 arrives at the apical membrane early in polarization and prior to CMD formation and therefore before cilium formation. The timing of the proposed diffusion barrier development is unclear. If the mutated gp135 gains access to the CMD area prior to barrier formation and/or maturation, it is conceivable that it could then enter the cilium. Together though, it does suggest that a preapical membrane platform forms where transmembrane proteins are scaffolded by linkage to the cytoskeleton. This idea is consistent with my identification of ANO1, a transmembrane protein, and the ERM protein moesin at the nimbus and suggests that ANO1 retention at this region is mediated through its proposed interaction with moesin (Perez-Cornejo et al., 2012b).

Collectively, the assortment of ring-like structures described in sections 5 & 6 share overlapping similarities between themselves and to the nimbus (Fig. 4). All of the various rings, whether they are described as regions of specific protein localization or exclusion, form defined circular areas approximately 2 μm in diameter at the apical portion of the cell. The protein composition of the rings and/or areas of exclusion are primarily defined by apical (ie gp135), ciliary (ie Smoothened, Arl13b), and trafficking-associated proteins (ie Rab11), which is consistent with the composition of the nimbus. Additionally, the collective reports highlight distinct cytoskeletal associations with microtubule enrichment and F-actin clearance at the area defined by the ring, another likeness shared with the nimbus. The development of these structures appears to depend on the state of polarization, as they all form in polarized epithelial cells. These ring-like domains share a comparable spatiotemporal relationship to the formation and location of the primary cilium as they develop prior to and define the future location of cilium formation. On all accounts, the rings appear to be transient structures that diminish once cilium formation commences, which is consistent with our temporal characterization of the nimbus (described in more detail in Chapter 2). Overall, the similarities in protein composition, location, and timing of ring formation and attenuation suggest that a relationship exists among these descried ring structures and that the various reports have highlighted different but overlapping stages in the formation and/or maturation of the same structure. Taken together these results suggest that the ring-like structures define a specific hub for cellular trafficking that contributes to proper primary cilium formation and composition.

In the next chapter I present original work that contributes to this growing body of evidence that a trafficking platform, we call the nimbus, develops prior to ciliogenesis. Based on my detailed characterization of the nimbus described in Chapter 2, we hypothesize that the nimbus is involved in preparing an apical subdomain of the cell for primary cilium formation through localized cytoskeletal changes and collection of proteins needed for ciliogenesis. The analysis of the nimbus constitutes the first of two primary aims of this dissertation. The second aim stemmed from the identification of ANO1 associated with this specialized domain and ANO1 localization to the primary cilium. In Chapter 2, detailed assessment of the importance of ANO1 channel activity to primary cilium formation through pharmacological inhibition and ANO1 knockdown revealed that ANO1 perturbation compromises proper cilium formation leading to the hypothesis that ANO1 Cl^- channel activity regulates early ciliogenesis. These novel observations open new lines of investigation into the potential role of the nimbus and Cl^- channels in primary cilium biology.

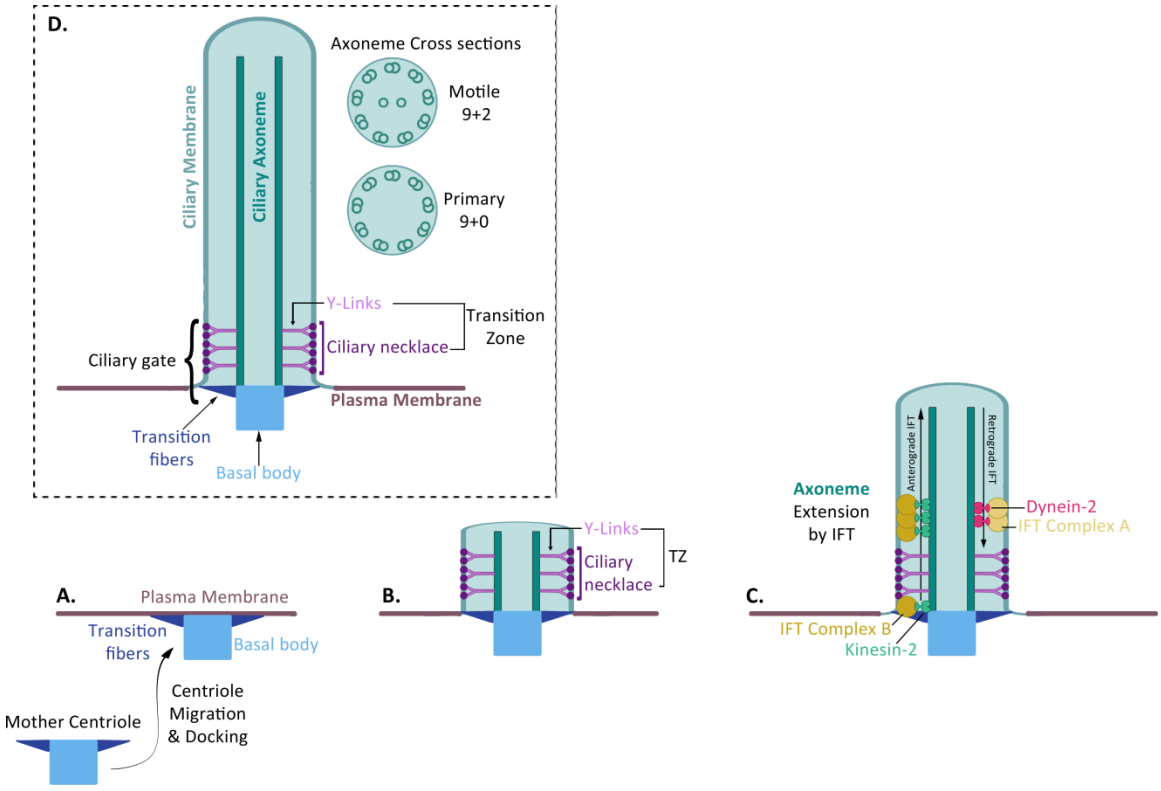

Figure 1. Diagram illustrating primary cilium structure and formation. A. In polarized epithelial cells, ciliogenesis begins with migration and docking of the mother centriole to the apical membrane to form the foundation of the primary cilium - the basal body. Transition fibers anchor the basal body to the base of the ciliary membrane. **B.** Ciliogenesis proceeds by formation of the TZ followed by **C.** axonemal outgrowth into the extracellular space. Axoneme extension occurs through intraflagellar transport (IFT), a microtubule-motor-based trafficking system to move proteins within the cilium. Complex B IFT proteins and Kinesin-2 motors move cargo in the anterograde direction towards the distal tip along the axoneme while complex A proteins and dynein-2 motors return cargo in the retrograde direction back towards the cell body. **D.** The primary cilium consists of a cylindrical array of nine doublet microtubules called the axoneme that extends from its foundation, the basal body. Surrounding the axoneme is the ciliary

membrane, which is continuous with the plasma membrane yet distinct in both protein and lipid composition. In motile cilia, the nine doublet microtubules surround a central pair of microtubules (9+2) while primary cilia lack this central pair (9+0). At the base of the cilium between where the basal body ends and the axoneme begins a specialized structure called the TZ forms that is proposed to function as a diffusion barrier to mediate the entry of specific cargoes in the cilium. In longitudinal sections of the TZ, the axonemal microtubules are linked to the ciliary membrane by Y-shaped connectors and form what is called the ciliary necklace. Together the transition fibers and TZ compose the ciliary gate.

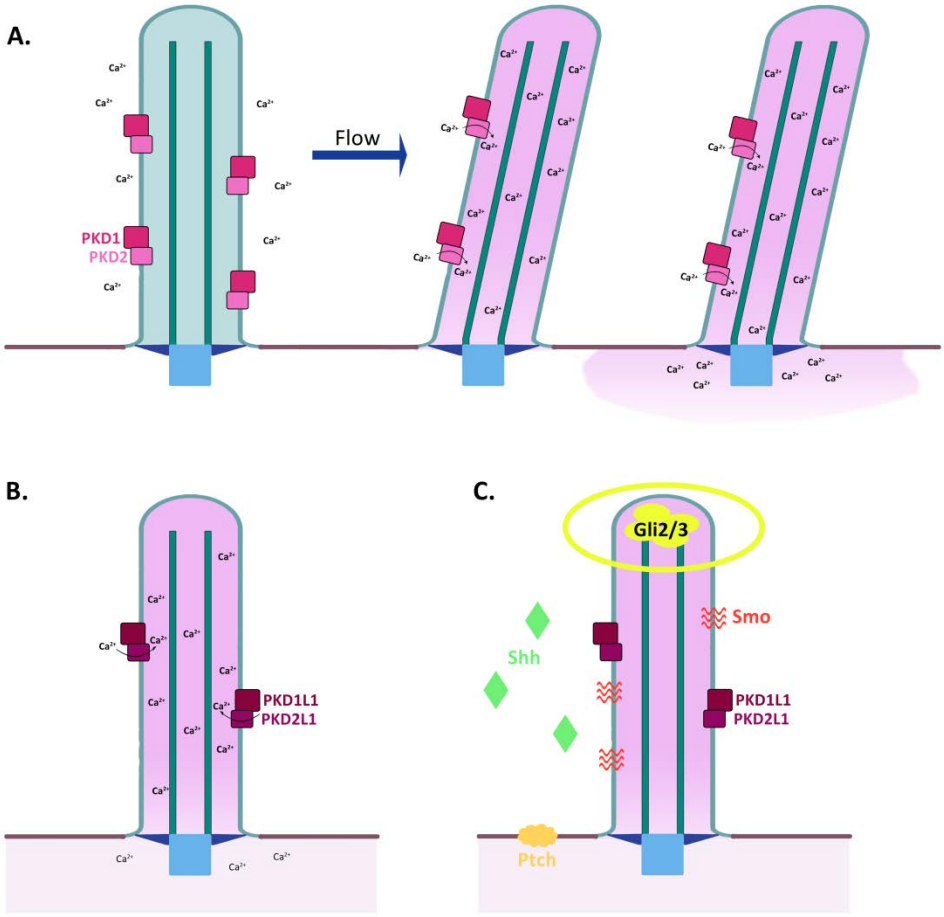

Figure 2. Two proposed mechanisms of Ca^{2+} signaling associated with the primary cilium. A. One of the prevailing hypotheses is that PKD1 and the cation channel PKD2 form a mechanosensory complex that localizes to the primary cilium to function as an extracellular sensor for mechanical force, such as urine flow. Upon flow induced ciliary bending, extracellular Ca^{2+} enters through PKD2 and leads to an eventual increase in intracellular Ca^{2+}. **B.** More recently, through quantitative Ca^{2+} measurements and whole-cilia patch clamping the cilium was found to contain Ca^{2+} levels 5X higher than the cytoplasm mediated through the PKD1L1-PKD2L1 channel. **C.** The high Ca^{2+} concentration in the cilium is proposed to mediate Sonic Hedgehog (Shh) signaling by

modulating the enrichment of Gli2/3 at the distal tip when the pathway is activated by the presence of Shh. The major components of the Shh pathway are dynamically localized to the cilia including Patched1 (Ptch1) a receptor for Hh ligands, Smoothened (Smo) and the Gli transcriptional effectors. In the presence of Shh, Ptch1 is removed from the cilium and Smo translocates to the cilium. Additionally, activation promotes the enrichment of Gli proteins within the cilium and blocks their processing into repressor forms and results in formation of Gli2/3 in active forms that leads to transcription of downstream target genes.

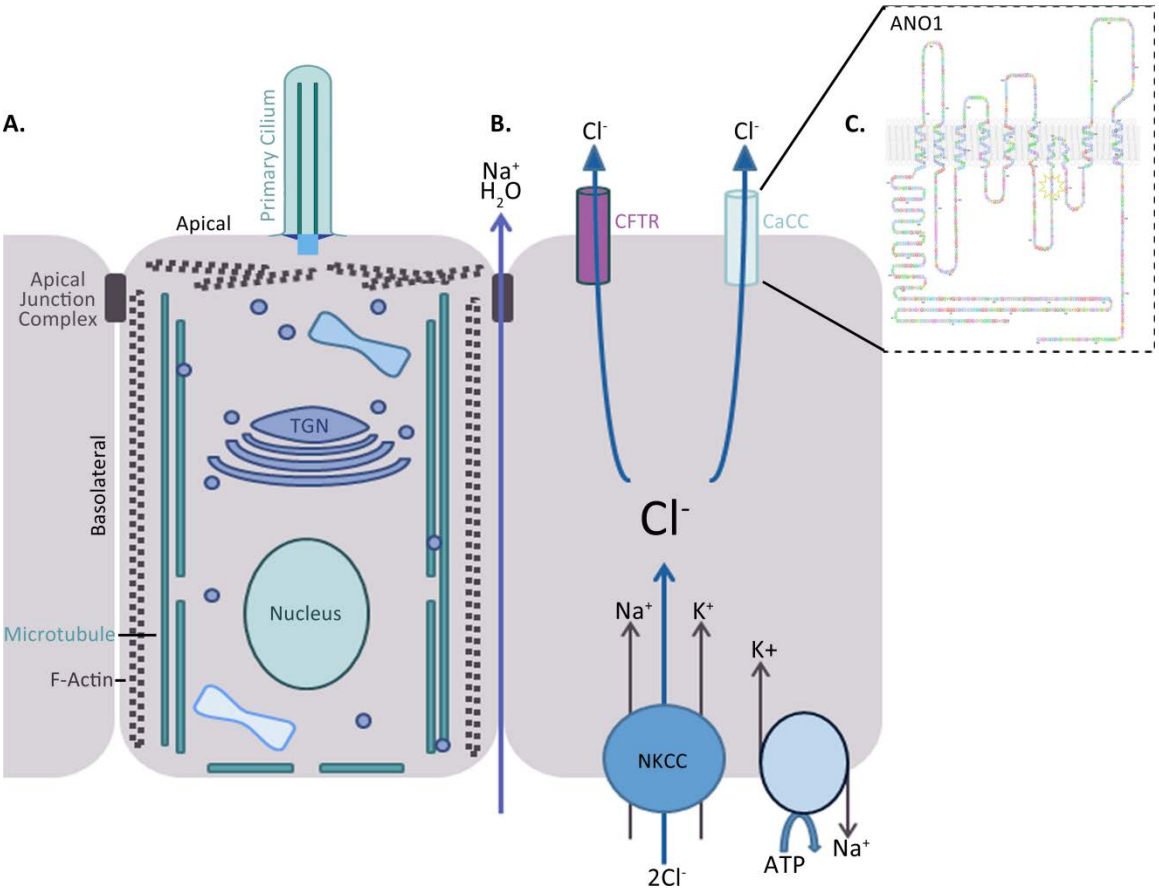

Figure 3. Polarized epithelial fluid secretion mediated by ANO1. A. Polarized epithelial cells have distinct apical and basolateral membranes separated by the apical junctional complex composed of tight and adherens junctions. The primary cilium emanates from the apical portion of the cell. **B.** In polarized epithelial cells Cl^- uptake across the basolateral membrane is mediated by the $Na^+/K^+/2Cl^-$ cotransporter while the Na^+/K^+ ATPase generates a large outward directed K^+ chemical gradient that works in concert to produce the K^+ and Cl^- electrochemical gradients necessary for secretion. Intracellular accumulation of Cl^- above its electrochemical gradient is followed by downhill Cl^- efflux into the lumen mediated by apical Cl^- channels that drive Na^+ ions across tight junctions and sets up a transepithelial osmotic gradient that drives the movement of water. **C.** Topology of the ANO1 channel that resides predominantly in the

apical membrane to provide a pathway for the transepithelial movement of Cl^- in Ca^{2+}-regulated epithelial fluid transport.

Name	Proteins	Cell type	Location	Notes	Reference
-	Microtubules, Angiotensin I & II, NHE3	mPT, highly differentiated	Adjacent to primary cilium	Devoid of WGA labeling	Kolb et al., 2004
-	Circular exclusion of gp135/podocalyxin, NHERF2	MDCK, terminally polarized	Site of primary cilium formation	-	Meder et al., 2005
-	GPI anchored protein (FP-GPI), Galectin-3	MDCK, polarized	Site of primary cilium formation	Base of cilium has highly condensed lipid staining	Vieira et al., 2006
Pericentriolar compartment	Ceramide, GM130, Cdc42, aPKC	MDCK, polarized	Base of cilium coming off edge of ring	Devoid of WGA labeling	Wang et al., 2009
Pericentrosomal preciliary compartment (PPC)	Smoothened-EGFP, Rab11, endocytosed transferrin	htRPE	Site of primary cilium formation, transition from PPC to cilium over course of hours	Blocking actin polymerization stabilies PPC when attenuates as the cilium forms	Kim et al., 2010
Ciliary membrane domain (CMD)	Exclusion of gp135, F-actin, NHERF1	MDCK, polarized	Base of cilium	CMD forms after centriole migration	Francis et al., 2011
Apical Ceramide Enriched Compartment (ACEC)	Acetylated tubulin, ceramide, sphingomyelin, Rab11, BBS1, HDAC6	MDCK, polarized	Site of primary cilium formation from edge of ring	Rab8 & Sec8 codistributed in center of ACEC with ceramide	He et al., 2012a
Nimbus	Microtubules, acetylated MTs, Arl13b, Cdc42, ANO1, EB1, Moesin, Rab11, Sec8, BBS1	IMCD3, $mpkCCD_{14}$, RPE	Site of primary cilium formation from edge of ring	Devoid of F-actin	Ruppersburg and Hartzell, 2014

Figure 4. Comparison of various ring-like apical structures. Protein abbreviations: wheat germ agglutinin (WGA), Na^+/H^+ exchanger type 3 (NHE3), Na^+/H^+ exchanger regulatory factor (NHERF), Glycosylphosphatidylinositol (GPI), cell division cycle 42 (Cdc42), atypical protein kinase C (aPKC), *cis* Golgi marker (GM130), histone deacetylase (HDAC), Anoctamin 1 (ANO1), end-binding protein 1 (EB1). **Cell type abbreviations:** mouse proximal tubule (mPT), Madin Darby Canine Kidney (MDCK), mouse intramedullary collecting duct (IMCD3), rat retinal pigmented epithelium (RPE), mouse cortical collecting duct ($mpkCCD_{14}$).

CHAPTER II

The Ca^{2+}-activated Cl^- channel ANO1 / TMEM16A regulates primary ciliogenesis.

Chelsey Chandler Ruppersburg and H. Criss Hartzell

The Department of Cell Biology, Emory University School of Medicine, Atlanta, GA 30322

Molecular Biology of the Cell

Vol. 11, 1793-1807, June 25, 2014

Abstract

Many cells possess a single, non-motile, primary cilium highly enriched in receptors and sensory transduction machinery that plays crucial roles in cellular morphogenesis. Although sensory transduction requires ion channels, relatively little is known about ion channels in the primary cilium (with the exception of TRPP2). Here we show that the Ca^{2+}-activated Cl^- channel ANO1 / TMEM16A is located in the primary cilium and that blocking its channel function pharmacologically or knocking it down with shRNA interferes with ciliogenesis. Prior to ciliogenesis, the channel becomes organized into a torus-shaped structure ("the nimbus") enriched in proteins required for ciliogenesis including the small GTPases Cdc42 and Arl13b and the exocyst complex component Sec6. The nimbus excludes F-actin and coincides with a ring of acetylated microtubules. The nimbus appears to form prior to, or independent of, apical docking of the mother centriole. Our data support a model where the nimbus provides a scaffold for staging of ciliary components for assembly very early in ciliogenesis and that chloride transport by ANO1 / TMEM16A is required for the genesis or maintenance of primary cilia.

Introduction

The ethos of chloride ions in biology has evolved dramatically over the past two decades from one in which passive Cl^- fluxes perform mundane tasks to one where Cl^- channels dynamically execute a myriad of cell biological functions including vesicular trafficking, cell cycle regulation, cell migration, and embryonic development and morphogenesis (Berend et al., 2012; Duran et al., 2010a; Hartzell, 2009; Stauber and Jentsch, 2013; Verkman and Galietta, 2009). One Cl^- channel that has recently received particular attention is Anoctamin-1 (ANO1, also known as TMEM16A) (Duran and Hartzell, 2011a; Ferrera et al., 2010; Hartzell et al., 2009b; Huang et al., 2012a; Kunzelmann et al., 2011b). The Anoctamin gene family was identified in 2003, before its Cl^- channel function was known, in a bioinformatic analysis of a region of chromosome 11 (11q13) that is amplified in many tumors (Espinosa et al., 2008; Hwang et al., 2011; Katoh, 2003; Katoh, 2005; Miettinen et al., 2009; Wilkerson and Reis-Filho, 2013). In 2008, ANO1 was shown to be a plasma membrane Ca^{2+}-activated Cl^- channel (CaCC) (Caputo et al., 2008b; Schroeder et al., 2008b; Yang et al., 2008c). CaCCs are present in the apical membranes of secretory epithelial cells where they are gated open by increases in cytosolic Ca^{2+} (Hartzell et al., 2005a). Cl^- efflux through the channel then drives fluid secretion as Na^+ and water follow to maintain charge neutrality and osmotic balance. As expected for a classical CaCC, ANO1 is expressed in the apical membranes of differentiated secretory epithelial cells such as salivary gland and pancreatic acinar cells (Perez-Cornejo et al., 2012a; Romanenko et al., 2010a; Yang et al., 2008c). Although CaCCs are best known for their role in transepithelial transport, novel functions for these channels in regulation of neuronal excitability, vascular tone, gastrointestinal motility,

and nociception have been uncovered as a result of identification of the ANO1 gene (Duran and Hartzell, 2011a; Ferrera et al., 2010; Huang et al., 2012a; Kunzelmann et al., 2011b).

Hints that ANO1 not only drives epithelial fluid secretion but also participates in cell biological functions were first provided by its link to poor prognosis in many cancers (reviewed in (Wilkerson and Reis-Filho, 2013)), but the awareness that ANO1 participates in cellular development and differentiation received a major boost from studies by Jason Rock and Brian Harfe who showed that ANO1 is highly expressed in the zone of polarizing activity (ZPA) of the mouse limb bud (Rock et al., 2007b). This anatomical region is involved in creating a gradient of the sonic hedgehog (SHH) morphogen that specifies the anterio-posterior axis of the limb. A role of ANO1 in embryonic development was then established by showing that disruption of the ANO1 gene in the mouse results in neonatal lethality as a result of developmental abnormalities including defects in morphogenesis of the trachea and gut (Rock et al., 2008).

Here we report a novel observation that is likely to open a new line of investigation into the role of ANO1 in the genesis of the primary cilium. The primary cilium is an apical appendage enriched in many signaling and morphogenetic networks including SHH (Berbari et al., 2009; Pazour and Witman, 2003; Seeley and Nachury, 2010). As cells withdraw from the cell cycle and develop apical-basal polarity, the centrosome, which in dividing cells functions to organize the mitotic spindle, migrates to the apical surface of the cell where it becomes a basal body to nucleate the primary cilium (Kobayashi and Dynlacht, 2011). Defects in ciliogenesis are linked to mutations in a number of genes that produce a pleomorphic spectrum of diseases typified by defective

tissue morphogenesis (Davis and Katsanis, 2012; Hildebrandt et al., 2011; Valente et al., 2014; Veland et al., 2009). Here we show that ANO1 forms a unique structure at the apical surface of polarizing epithelial cells prior to the formation of the primary cilium and that ANO1 enters the cilium at early stages of ciliogenesis. This apical ANO1-containing structure is likely a hub for ciliary components that are trafficked into the cilium during early stages of ciliogenesis. We have shown previously that ANO1 interacts at high stoichiometry with proteins involved in membrane-cytoskeletal organization and primary cilia (Perez-Cornejo et al., 2012a), suggesting that ANO1 may serve as a component of a scaffold in this organization. Consistent with a role for ANO1 in ciliogenesis, we find that interference with ANO1 channel function or expression disrupts normal ciliogenesis.

Results

Concentration of ANO1 in an Apical Annular Structure

While investigating the role of the Ca^{2+}-activated Cl^- channel (CaCC) ANO1 in transepithelial transport, we immunolabeled various epithelial cell lines grown on permeable supports to determine the apical-basal distribution of ANO1. We initially concentrated on a widely-used murine immortalized cortical collecting duct cell line ($mpkCCD_{14}$) whose ion transport functions have been well studied (Chassin et al., 2007; Rajagopal et al., 2012). Surprisingly, we found that when cells were cultured under conditions that disfavored formation of primary cilia, ANO1 was concentrated at the apical surface in a sharply-defined annulus ~3 μm in diameter composed of smaller discrete puncta (Fig. 1A). We refer to this structure including other associated proteins as

the *nimbus*, because of its resemblance to a halo. The vast majority of cells have only one nimbus per cell. The ring of ANO1 staining circumscribes an area covering ~6% of the apical aspect of each cell: the average area demarcated by the ring was 9.5 ± 1.2 μm^2 (n=798) compared to an average total apical membrane area of 156.9 ± 3.8 μm^2. The average ANO1 nimbus was elliptically shaped with major and minor axial radii of 2.0 and 1.4 μm. Nimbus sizes were distributed exponentially rather than in a Gaussian fashion (Fig. 1E), suggesting the possibility that the nimbus is a dynamic structure.

The nimbus is not unique to the mpkCCD_{14} cell line but rather appears to be a common feature of several epithelial cells we examined. Well-defined nimbi were observed in the rat retinal pigmented epithelium cell line RPE-J (Fig. 1B) and the mouse intramedullary collecting duct cell line IMCD3 (Fig. 1C). In IMCD3 cells the nimbus was often less clearly demarcated than in mpkCCD_{14} or RPE-J cells: In IMCD3 cells, ANO1 nimbi were regularly observed, although frequently ANO1 was concentrated at the apical surface in an amorphous patch without an annulus (Fig. 1C). Nimbi were also observed in HEK cells transfected with ANO1-EGFP (Fig. 1D).

The specificity of our antibody is demonstrated by experiments showing that the antibody does not label cells in which ANO1 has been knocked down with shRNA (Fig. 1F), that the antibody recognizes a band of the expected molecular weight in western blots that is absent in $ANO1^{-/-}$ mice (Fig. 1G), and co-localizes with ANO1-EGFP in transfected HEK cells (Fig. 1D).

Structures that we believe are related to the nimbus have been described previously in the literature and are thought to be areas where ciliary membrane is

organized for assembly into the primary cilium (see Discussion). The organization of a CaCC into a structure of such unusual and conspicuous appearance raised questions regarding its potential role in orchestrating apical membrane function. We therefore set out to characterize this structure in more detail.

The Nimbus is an Antecedent of Ciliogenesis

The exponential distribution of nimbi sizes observed (Fig. 1E) suggests (but by no means proves) that the nimbus is a dynamic structure, because the probability of finding a certain size nimbus would be expected to be exponentially distributed if its size were determined by kinetic processes of aggregation and disaggregation of subunits (Moffitt et al., 2010). We investigated the temporal aspects of ANO1 localization and nimbus formation in mpkCCD$_{14}$ cells that were fixed and labeled at different time points after plating onto permeable supports. Before the cells reach confluency (~2 days after plating), ANO1 is widely distributed (Fig. 2A), but after the cells become confluent (>3 days after plating), ANO1 becomes progressively concentrated into an apical patch (Fig. 2B-C). The nimbus is most clearly defined after the cells reach confluence but before they develop cilia (Fig. 2D). As the cells continue to polarize, ANO1 becomes localized to a highly compact apical spot that correlates with a concentration of acetylated tubulin, a marker of the primary cilium (Fig. 2E).

To investigate the relationship of the ANO1 nimbus to the primary cilium, we varied culture conditions (serum concentration, cell plating density, and days in culture) and quantified the fraction of cells positive for a nimbus, a primary cilium, or both. In cultures in which most cells lacked a primary cilium (4 days in culture), nearly all cells

had an ANO1 nimbus (Fig. 3A,C), but in cultures where the cells had a cilium labeled with acetylated tubulin (10 days in culture), very few cells exhibited a nimbus (Fig. 3B,C). When both a cilium and a nimbus were present in the same cell, the emerging cilium emanated from one side of the ANO1 nimbus 74% of the time (Fig. 3D, n = 34 randomly selected cells having both nimbi and cilia). The emerging cilium labeled positive for ANO1 as well as acetylated tubulin and always sprouted from one side of the nimbus. The spatial proximity of the nimbus to the primary cilium in these cases and the temporal progression from nimbiated to ciliated cells supports the idea that the nimbus may be involved in organization of ciliary components prior to or early in ciliogenesis. We also observe full-length primary cilia that label for ANO1, acetylated tubulin, and the ciliary protein Arl13b (Fig. 3E).

Ciliary proteins in the nimbus

The identification of ANO1 as a component of both the nimbus and the cilium led us to test whether the nimbus contained other ciliary proteins. Assembly of primary cilia is a concerted process that involves trafficking of post-Golgi vesicles to the base of the cilium, their exocytosis by a process engineered by the exocyst complex, and transport of ciliary components by intraflagellar transport (IFT) (Ishikawa and Marshall, 2011; Nachury et al., 2010; Pedersen and Rosenbaum, 2008). By immunofluorescence we detect the exocyst complex protein Sec6 associated with the ANO1 nimbus (Fig. 4A), consistent with the idea that the nimbus is associated with the establishment of a ciliary membrane compartment (Das and Guo, 2011; Nachury et al., 2010; Zuo et al., 2011b). Furthermore, the ciliary protein Arl13b is also found in the nimbus at a stage in the nimbus life cycle (Fig. 4B). Arl13b is a small GTPase required for proper primary cilium

structure (Cantagrel et al., 2008; Caspary et al., 2007; Larkins et al., 2011) and Arl13b mutations are linked to Joubert Syndrome, a human ciliopathy (Cantagrel et al., 2008). The ANO1 puncta in Arl13b-positive nimbi seemed more indistinctly-defined than in Arl13b-negative nimbi. One interpretation is that Arl13b associates with nimbi that are disassembling or reorganizing at a stage just prior to ciliogenesis. At a later stage, some cells possessed a bleb at the apical surface that was positive for both ANO1 and Arl13b (Fig. 4C). These blebs presumably are nascent procilia at an early stage of emergence from the cell. The association of ANO1 and Arl13b with the nimbus and the procilium is shown in Fig. 4C where the left cell has a fuzzy ANO1 ring associated with Arl13b puncta while the right cell has a bleb that is positive for ANO1 and Arl13b that emanates from Arl13b puncta.

The nimbus also labels positive for Cdc42 (Fig. 4D), a small GTPase that is essential for ciliogenesis (Choi et al., 2013; Zuo et al., 2011b) and a principal determinant in establishing correct cell polarity with respect to the external environment by controlling cytoskeletal dynamics and stabilizing appropriate cellular asymmetry (de Curtis and Meldolesi, 2012; Etienne-Manneville and Hall, 2002). ANO1 and Cdc42 occupy approximately the same contour in the nimbus and in many cases the two proteins are co-localized (Fig. 4D). In addition, blebs of Cdc42 and ANO1 were seen in some cells (Fig. 4E). The Cdc42 blebs are surrounded by puncta of ANO1 and are presumably nascent procilia.

Relationship of the Nimbus to the Centrosome

To investigate further the connection between the nimbus and the primary cilium, we examined the relationship of the centrosome to the nimbus. In dividing cells, centrosomes coordinate the formation of the microtubule spindle during mitosis, whereas in interphase cells the centrosome undergoes an incompletely-understood functional transition as it migrates to the cell surface. There, the mother centriole becomes a basal body that nucleates the axoneme of the primary cilium (Kobayashi and Dynlacht, 2011). Consistent with this model, we observe that each primary cilium is invariably anchored to a basal body as visualized by γ-tubulin staining. However, we believe that the nimbus forms prior to migration of the basal body to the apical surface, because only about half of the nimbi are associated with a basal body (Fig. 5A,B). In one typical culture, 33% of nimbi (292/870) had at least one clearly-identified basal body within its perimeter (Fig. 5A, white arrow) and an additional 24% of nimbi (210/870) had a basal body <1.2 μm away (Fig. 5B). In the remaining 43% of the cells, the nimbus and the centrioles were clearly separated by >1.2 μm (Fig. 5A, square, Fig. 5C). However, a careful examination of z-stacks of these centriole-estranged nimbi revealed significant accumulations of γ-tubulin within the nimbi, even though discrete centrioles were present at a remote location in the cell (Fig. 5C,D). Although live-cell imaging will be required to resolve this issue definitively, these data are consistent with a scenario where nimbus formation occurs prior to migration of the centriole to the apical membrane. (Joo et al., 2013; Sorokin, 1962)

The Nimbus is an Interface between the Microtubule and Actin Cytoskeletons

Following docking of the mother centriole to the apical membrane, there is extension of the ciliary axoneme, a microtubule based structure. To explore the spatial

relationships of microtubules to the ANO1 nimbus, z-stacks of confocal images labeled for ANO1, acetylated tubulin, and α-tubulin were deconvolved and isosurfaces were reconstructed (Fig. 6A). This processing revealed that microtubules describe a torus ~3 μm diameter that coincides with the ring of ANO1 puncta. The torus is composed of both acetylated and non-acetylated microtubules that intermingle with puncta of ANO1. The microtubule plus-end tracking protein (+TIP), end-binding protein-1 (EB1), is also associated with the nimbus (Fig. 6B). Microtubule +TIPs play an integral role in attaching and stabilizing microtubule ends at the cell cortex and EB1 specifically has been shown to be essential for ciliogenesis in mouse fibroblasts (Gouveia and Akhmanova, 2010; Schroder et al., 2011).

Recently, data has emerged that branched F-actin is a negative regulator of ciliogenesis (Kim et al., 2010; Yan and Zhu, 2013a). Consistent with our hypothesis that the nimbus represents a staging area for ciliogenesis, F-actin was largely excluded from the center of the nimbus as visualized by labeling with fluorescent phalloidin (Fig. 7A). The average pixel intensity of fluorescent phalloidin at the center of the ring was an average 11.9-fold less than in the adjacent cytoplasm (Fig. 7D). The ERM (ezrin, radixin, moesin) proteins link the underlying actin cytoskeleton to the plasma membrane (Fehon et al., 2010) and are the most highly enriched proteins in the ANO1 proteome (Perez-Cornejo et al., 2012a). Labeling mpkCCD$_{14}$ cells for moesin revealed that moesin is highly concentrated at the interface of the F-actin-free and F-actin-rich zones co-incident with ANO1 (Fig. 7A-C). Plots of moesin and F-actin intensities revealed that the peak moesin intensity was located exactly midway between the cytoplasm and the F-actin-free zone (Fig. 7D). The nimbus contained overlapping rings of moesin and ANO1 by

confocal microscopy (Fig. 7B) while structured illumination microscopy (SIM) revealed that both the ANO1 and the moesin rings were each comprised of 8-12 puncta (Fig. 7C). Typically, the puncta of moesin and ANO1 occupy sporadically overlapping and alternating positions in the nimbus. Although moesin is best known in the context of the actin cytoskeleton, moesin also binds and stabilizes microtubules at the cell cortex (Solinet et al., 2013). This location of moesin at the interface of actin-rich and tubulin-rich zones places it in a prime location to coordinate the actin and microtubule cytoskeletons.

Effects of Block of ANO1 Cl^- Currents on Ciliogenesis

To test whether ANO1 plays a role in ciliogenesis, we measured the effects of inhibitors of ANO1 Cl^- current on cilium length and percentage of ciliated cells. Although Cl^- channel blockers are notoriously non-specific (Hartzell et al., 2005a), a number of selective ANO1 inhibitors have recently been described including $T16A_{inh}$-A01 (Namkung et al., 2011), dichlorophen (Huang et al., 2012b), benzbromarone (Huang et al., 2012b), and MONNA (Oh et al., 2013). We tested the effect of these drugs on $mpkCCD_{14}$ cells grown on permeable supports. Cells were grown on permeable supports until a monolayer was formed (transepithelial resistance > 250 Ω/cm^2), then switched to serum-free media to promote ciliogenesis and simultaneously exposed to ANO1 blockers for 24 - 48 hours. Cells were labeled with acetylated tubulin antibody to visualize cilia, phalloidin to assess overall cell and monolayer morphology, and ANO1 antibody (Fig. 8A). Benzbromarone had the most severe effect: epithelial morphology was disrupted and no ciliated cells were observed after 24 hours of treatment with drug. The effect of dichlorophen was less severe, but also dramatic: it decreased the percentage of ciliated

cells by 50% and the length of cilia by 28 % (Fig. 8A). The ANO1 inhibitors $T16A_{inh}$-A01 and MONNA did not affect the percentage of ciliated cells, but consistently decreased the length of cilia by 28 – 42 % (Fig. 8A). Of the ANO1 blockers, the selectivity of MONNA has been most thoroughly examined (Oh et al., 2013). MONNA does not inhibit several other Cl^- channels including CFTR and members of the CLC and Bestrophin family. In two independent experiments, MONNA decreased cilium length a similar amount. In contrast to the effects of ANO1 inhibitors, the CFTR inhibitor, GlyH-101, which has no effect on ANO1 currents, has no effect on cilium length. Incubation of cells in any of the ANO1 blockers for more than several days inevitably disrupted epithelial polarity and integrity as evidenced by large decreases in transepithelial resistance and loss of cell-cell contacts visualized by microscopy.

To be certain that the effects of ANO1 blockers were not limited to $mpkCCD_{14}$ cells, we repeated these experiments on IMCD3 cells (Fig. 8B,C). IMCD cells on average have longer cilia than $mpkCCD_{14}$ cells. Nevertheless, both $T16A_{inh}$-A01 and MONNA caused a ~50% decrease in average cilium length, while the CFTR inhibitor GlyH-101 had no effect (Fig. 8B). Although overall cilia length was decreased in MONNA treated cells, localization of the somatostatin receptor 3 tagged with EGFP (SSTR3-EGFP) to the primary cilium was not affected (Fig. 8C).

The effect of ANO1 channel blockers on cilium length could be explained by an effect on the assembly of the cilium or an effect on the processes that maintain the length of an already assembled cilium. To test for an effect on maintenance, IMCD3 cells stably expressing the SSTR3-EGFP were induced to ciliate by serum starvation for 24 hours and then exposed to either T16A-inh or MONNA for 6 hours. Under these conditions, the

inhibitor had little effect on cilium length as measured by SSTR3-EGFP fluorescence (Fig. 8D,E). This observation suggests that once the cilia have formed, their length is not dependent upon ANO1 function. In contrast, ANO1 function is important when cilia are initially forming.

As another approach to testing the role of ANO1 in ciliogenesis, we transduced mpkCCD$_{14}$ cells with lentiviral particles harboring sequences encoding shRNA against ANO1. Control cells were infected with non-silencing negative control lentiviral particles or lentivirus having shRNA against GAPDH. Western blot showed that ANO1 shRNA reduced the level of ANO1 expression by >70 % (Fig. 9A). Knockdown of ANO1 caused a significant reduction in both the percentage of ciliated cells and in the length of the cilia measured by acetylated tubulin labeling (Fig. 9B-D). The percentage of ciliated cells was reduced by 50% (Fig. 9D) and the length of the cilia was reduced by 45% (Fig. 9C).

The observation that cilium length is shortened by knockdown or inhibition of ANO1 raises the question whether ANO1 knockdown affects the structure of the nimbus or alters cell polarity. Although we have not investigated these issues in depth, we find that ANO1 knockdown does not affect the formation of the F-Actin free area or the nimbus as visualized by Cdc42 labeling (Fig. 9E,F). Furthermore, ANO1 knockdown does not appear to affect overall cell polarity as visualized by β-catenin labeling (Fig. 9G,H).

Discussion

We describe a transient organelle, the “nimbus,” that is temporally and spatially related to the primary cilium. The nimbus is a torus-shaped structure comprised of the

Ca^{2+}-activated Cl^- channel ANO1 and other proteins involved in ciliogenesis including Cdc42,Arl13b, the exocyst complex component Sec6, and acetylated tubulin (Choi et al., 2013; Das and Guo, 2011; Larkins et al., 2011; Zhang et al.; Zuo et al., 2011b). The nimbus is located at an interface between the actin and microtubule cytoskeletons demarcated by moesin, a protein that interacts stoichiometrically with ANO1 (Perez-Cornejo et al., 2012a). The relationship of ANO1 to the primary cilium is strengthened by the composition of the ANO1 proteome (Perez-Cornejo et al., 2012a), which is highly enriched in proteins known to participate in ciliogenesis and cell polarity (Hattula et al., 2002; Hehnly et al., 2012; Nachury et al., 2007; Westlake et al., 2011; Yoshimura et al., 2007) including Rab8 (SILAC enrichment ratio = 6.7), Rab11 (6.0), TRAPPC3 (3.4), and Cdc42 (4.0). 62% of ANO1-interacting proteins are represented in the Cilia Proteome Database (v3.ciliaproteome.org; (Albertson, 2006)) and the highest-ranking ANO1-interacting proteins have experimentally-verified functions of organization of the cytoskeleton, membrane-cytoskeletal interactions, and membrane trafficking. This suggests that ANO1 is part of a signaling network that organizes the membrane and cytoskeleton in the process of ciliogenesis.

The nimbus shares similarities to the pericentrosomal preciliary compartment (PPC) described by others (Kim et al., 2010). Although the nimbus, unlike the PPC, does not label for early endosomal markers, it seems likely that the PPC and nimbus perform related or sequential functions. The nimbus also resembles a compartment highly enriched in ceramide sphingolipids that may be involved in tubulin acetylation during ciliogenesis (He et al., 2012a). Another structure that one might equate with the nimbus is the ciliary pocket, an invagination of plasma membrane around the cilium (Benmerah,

2013). The ciliary pocket might be a nimbus remnant, but is smaller and collars the cilium, whereas the nimbus lies adjacent to the cilium. The ciliary vesicle that assembles at the distal end of the mother centriole (Joo et al., 2013; Sorokin, 1962) apparently forms after the nimbus, because many (43%) nimbi are not adjacent to centrioles.

The central question raised here is the role of Cl^- channels in ciliogenesis. Blocking ANO1 Cl^- currents or knocking down ANO1 expression results in shortened cilia, suggesting that ANO1 may participate in cilium length control. Changes in cilium length are also caused by defects in Arl13b and IFT proteins that cause polycystic kidney disease (Caspary et al., 2007; Ong, 2013; Pazour et al., 2000). Mechanisms controlling ciliary length are poorly understood but involve precursor molecule availability, intraflagellar transport, cytoskeletal dynamics, and turnover of components at the ciliary tip (Avasthi and Marshall, 2012; Ishikawa and Marshall, 2011).

The finding that ANO1 knockout in mice produces a lethal developmental phenotype supports the assertion that ANO1 is involved in cilium assembly or maintenance (Rock et al., 2008). Although $ANO1^{-/-}$ mice have not been reported to exhibit hallmarks of classical ciliopathies (cystic disease, polydactyly, or situs inversus) (Badano et al., 2006b), few $ANO^{-/-}$ studies have been published. It is likely that disruption of Cl^- transport would have different phenotypic consequences than disruption of the BBsome or intraflagellar transport (Bettencourt-Dias et al., 2011; Cardenas-Rodriguez and Badano, 2009; Hildebrandt et al., 2011).

We propose three testable hypotheses for a role of ANO1 Cl^- currents in ciliogenesis (Fig. 10).

(1) ANO1 could regulate apical membrane potential (V_m). This could affect other ciliogenic processes such as Ca^{2+} signaling. The TRP ion channel polycystin-2 (PKD2, TRPP2) is a Ca^{2+}-permeable channel responsible for the ciliopathy autosomal dominant polycystic kidney disease (Chapin and Caplan, 2010) and left-right asymmetry in the embryo (McGrath et al., 2003; Takao et al., 2013; Yoshiba et al., 2012). Ca^{2+} influx through PKD2, or other Ca^{2+} channels, could activate ANO1, which could provide feedback control on Ca^{2+} influx by altering V_m. Changes in V_m could affect both the driving force for Ca^{2+} influx and the open probability of voltage-gated channels.

(2) ANO1 may create hydrodynamic and osmotic forces that encourage ciliary extension. In this model, membrane trafficking and cytoskeletal assembly alone are insufficient to erect a normal cilium; osmotic pressure would assist by producing a cellular bleb (Duran et al., 2010a; Hoffmann et al., 2009; Nilius et al., 1997) into which ciliary components could traffic and assemble. This idea is attractive because it seems consistent with membrane blebs such as those in Fig. 4C,E.

(3) The Cl^- ion may function as a regulator of protein function (Duran et al., 2010a). Over 1500 human proteins in the Protein Data Bank, including Rab11A and SHH, have Cl^- as a ligand. In these structures, Cl^- is frequently located at protein interfaces, hinting that anions could participate in protein-protein interaction. The observation that the enzymatic activities of many proteins including certain G-proteins and protein kinases are affected by Cl^- in the physiological range supports a regulatory role for Cl^- (Duran et al., 2010a; Lo Nostro and Ninham, 2012; Nakajima et al., 1992; Pacheco-Alvarez and Gamba, 2011; Szalontai et al., 2013). Because intracellular Cl^- is spatially and temporally dynamic (Berglund et al., 2008; Duebel et al., 2006; Kuner and

Augustine, 2000), gradients of intracellular Cl^- in the periciliary region could locally regulate protein function. For example, tubulin polymerization is affected by the species and concentration of anion (Ray et al., 1984; Suzaki et al., 1978; Wolff et al., 1996). Alternatively, Cl^- concentration in intracellular vesicular compartments might alter vesicular trafficking (Faundez and Hartzell, 2004a; Stauber and Jentsch, 2013).

The ciliary membranes differ from the plasma membrane in both protein and lipid composition (Conduit et al., 2012; Emmer et al., 2010; He et al., 2012a; Maric et al., 2010). Intriguingly, some members of the ANO family are required for phospholipid scrambling (Malvezzi et al., 2013; Suzuki et al., 2013; Suzuki et al., 2010; Yang et al., 2012). Although there is no evidence that ANO1 has lipid scramblase activity, the high sequence conservation among ANO's suggests that ANO1 may have important interactions with lipids (Hartzell and Ruppersburg, 2013).

Hopefully, the association of ANO1 with the primary cilium will shed light on the relationship of ANO1 to cancer (Wilkerson and Reis-Filho, 2013). Ciliary signaling has an important role in the control of cell division because of the dichotomous role of the centrosome in nucleating the cilium and in organizing the mitotic spindle. Crosstalk between ciliogenesis and mitosis is evident from observations that defective cell division results in abnormal ciliogenesis and that defective ciliogenesis alters the cell cycle. For example, proliferative transformed cells typically lack a primary cilium (Wheatley, 1995) and cells having defective primary cilia can undergo inappropriate cell division as occurs in cystic disease (Sharma et al., 2013). ANO1 is overexpressed in several cancer cell lines and knockdown or interference with ANO1 expression or function has been reported to suppress proliferation (Britschgi et al., 2013; Duvvuri et al., 2012a; Mazzone

et al., 2012; Stanich et al., 2011b), although results are inconsistent (Ayoub et al., 2010; Kamentsky et al., 2011; Ruiz et al., 2012; Simon et al., 2013).

In summary, we have identified for the first time an anion channel that both localizes to the primary cilium and at some level appears to contribute to primary cilium formation. We believe that this novel finding will open new lines of investigation into the role of Cl^- channels in primary cilium biology.

Materials and Methods

Cell Culture. mpkCCD$_{14}$ cells were maintained in modified medium (DMEM:Ham's F12 1:1 + GlutaMax; 20 μg/ml sodium selenite, 5 μg/ml apo-transferrin, 1 nM triiodothyronine, 12 mM D-glucose, 2% fetal bovine serum (FBS), and 15 mM HEPES [pH 7.4]) at 37°C in a 5% CO_2 / 95% air humidified atmosphere. Cells were seeded on semipermeable filters (Millicell, 0.4 μm pore size; Millipore) for experiments. For cell staging experiments mpkCCD$_{14}$ cells were seeded at starting concentration of $2.25x10^5$ onto permeable supports (Millipore Millicell filters) and samples taken every 24 hours for six days. IMCD3 cells were maintained in DMEM:F12 supplemented with 10% FBS. IMCD3 cells stably expressing SSTR3-EGFP were a generous gift from Greg Pazour (Pazour, 2008). RPE-J cells were cultured in DMEM medium with 10% FBS.

Immunofluorescence and Image Analysis. Cells grown on permeable supports filters were fixed in 4% paraformaldehyde overnight at 4°C, washed in phosphate-buffered saline (PBS), incubated in a blocking solution of PBS containing 0.15% Triton X-100 and 2% cold water fish gelatin at room temperature, and subsequently incubated with primary antibodies. Primary antibodies were used against the following antigens:

ANO1 1:1000 (SDIX Custom rabbit polyclonal Genomic Antibody G3 directed against mAno1 amino acids 878-960 and G2 directed against amino acids 54-126 provided identical results), anti-moesin mouse monoclonal 1:1000 (Abcam; A50007), anti-acetylated tubulin mouse monoclonal 1:1000 (subtype IgG2b, Sigma-Aldrich; 6-11B-1), anti-Cdc42 mouse monoclonal 1:500 (Santa Cruz Biotechnology sc-8401), anti-α-tubulin mouse monoclonal 1:500 (subtype IgG1, Sigma-Aldrich T9026), anti-γ-tubulin monoclonal 1:2000 (subtype IgG1, Sigma-Aldrich T6557), anti-EB1 monoclonal 1:1000 (subtype IgG1, BD Biosciences 610534), anti-Arl13b mouse monoclonal clone N295B 1:10 (subtype IgG2a, UC Davis/NIH NeuroMab Facility 73-287), anti-β-catenin mouse 1:200 (BD Transduction Lab 610153, gift of Dr. Michael Koval) and anti-Sec6 mouse monoclonal 1:5 (9H5, Dr. Charles Yeaman, University of Iowa (Andersen and Yeaman, 2010)). The cells were then washed and incubated in secondary antibodies (1:1000): Alexa Fluor 488–labeled goat anti–rabbit or anti–mouse IgG (Invitrogen), Daylight 549-labeled goat anti-rabbit IgG (Jackson Immunochemicals), Alexa Fluor 555–labeled goat anti–mouse IgG1 (Invitrogen), Alexa Fluor 633–labeled goat anti–mouse IgG2b (Invitrogen). Actin filaments were stained with phalloidin conjugated to Alexa Fluor 633 (Invitrogen). The filters were mounted in ProLong Gold (Invitrogen). Confocal images were acquired at room temperature using a Zeiss LSM-510 microscope and ZEN software. Objectives used were 63x 1.4 NA and 100x 1.4 NA Plan-Apochromat oil objectives. Z-stacks were deconvolved using Huygens Essential 3.7 deconvolution software with a signal:noise ratio of 15, quality 0.1 and automatic bleaching correction. Resulting images were processed using ZEN and Imaris software. Three-dimensional

structured illumination microscopy (3D-SIM) was performed on an inverted Nikon microscope running NIS Elements with a 100x oil objective, NA 1.49.

Measurements of ANO1 nimbus size were performed using Cell Profiler. Maximum intensity projections (MIPs) were made of z-stacks taken through the ANO1 ring using Zeiss Zen software. The MIPs were then thresholded using robust background subtraction in Cell Profiler (Carpenter et al., 2006; Kamentsky et al., 2011).The algorithm trims the brightest and dimmest 5% of pixel intensities over the image, then calculates the mean and standard deviation of the remaining pixels and calculates the threshold as the mean plus two times the standard deviation. The dimensions (area and axes) of the resulting thresholded structures were then automatically measured by Cell Profiler. Approximately 800 rings were identified and measured. Distances between nimbi and centrioles were also determined using Cell Profiler after identifying the structures by a similar thresholding procedure.

Cells used to assess the percentage of ciliated cells and cilium lengths were processed for immunofluorescence microscopy by staining with anti-acetylated tubulin. The number of ciliated cells and total number of cells were counted in random fields to determine the percentage of ciliated cells for each condition. Cilia lengths were measured using confocal z-stacks analyzed in ZEN software. Only cilia which projected from the apical portion of the cell were measured.

ANO1 Inhibitor Treatment. mpkCCD$_{14}$ cells were seeded at 5.0x10^5 and grown on permeable supports until the transepithelial resistance increased to >5-times background (>500 Ohms), usually several days. The cells were the treated with the

indicated inhibitors by replacing both the apical and basal medium with serum free medium with or without inhibitors. The inhibitors used were: $T16A_{inh}$-A01 (2-[(5-Ethyl-1,6-dihydro-4-methyl-6-oxo-2-pyrimidinyl)thio]-*N*-[4-(4-methoxyphenyl)-2-thiazolyl]acetamide) (Namkung et al., 2011) (a generous gift from Alan Verkman, UCSF), dichlorophen ((4-chloro-2-[(5-chloro-2-hydroxyphenyl)methyl]phenol) (Huang et al., 2012b) (Sigma-Aldrich), benzbromarone ((3,5-dibromo-4-hydroxyphenyl)-(2-ethyl-1-benzofuran-3-yl)methanone) (Huang et al., 2012b) (Sigma-Aldrich), MONNA (*N*-((4-methoxy)-2-naphthyl)-5-nitroanthranilic acid) (Oh, in press) (a generous gift from Justin Lee, Korean Institute of Science and Technology), and GlyH-101 (N-(2-Naphthalenyl)-((3,5-dibromo-2,4-dihydroxyphenyl)methylene)glycine hydrazide (Muanprasat et al., 2004) (EMD Millipore). IMCD3 cells were grown to confluency on glass bottom dishes in the presence of serum after which they were simultaneously switched to serum-free medium and exposed to the various inhibitors for 24 hours.

The ANO1 inhibitor MONNA was used at a final concentration of 10μM and 1% DMSO, $T16A_{inh}$-A01 at 10 μM and 0.1% DMSO, dichlorophen at 20 μM and 0.1% DMSO, and benzbromarone at 50 μM and 0.1% DMSO. The CFTR channel inhibitor GlyH-101 was used at a final concentration of 2.5μm and 0.1% DMSO. Cells were treated with the indicated concentrations of inhibitors or matching percentage of DMSO in serum free medium for either 24 or 48 hours prior to fixation. Cells were labeled with an antibody against acetylated tubulin to label primary cilia. Individual cilia lengths and the percentage of ciliated cells were measured using Zeiss ZEN software.

For experiments to test the effects ANO1 inhibitors on cilia maintenance, IMCD3 cells were cultured as described above, serum starved for 24 hours then exposed to inhibitors, still in serum free medium, for 6 hours before fixation.

Lentivirus Transduction. GIPZ lentiviral shRNA particles were obtained from Thermo Fisher Scientific and targeted to mANO1 (V2LMM_92063), GAPDH (RHS4372) or negative non-silencing control (RHS4348). For lentiviral transduction, mpkCCD$_{14}$ cells were plated at 8x10^5 cells per plate in 60 mm dishes and allowed to grow overnight. After 24 hours cells were switched to serum-free medium with lentiviral particles. At 24 hours after transduction, infected cells were selected by the addition of 1.5 μg/mL puromycin in serum-containing medium. At 7 days after selection, cells were plated at 5x10^5 cells per filter in serum-containing medium. After 48 hours cells were switched to serum-free medium for an additional 48 hours before fixation. Only cells identified as positively transduced by expression of TurboGFP were counted in the analysis of the percentage of ciliated cells and measurements of cilia lengths.

Acknowledgements

We thank Bonnie Blazer-Yost and Stephanie Flaig for mpkCCD$_{14}$ cells and advice on their culture, Alexa Mattheyses at the Integrated Cellular Imaging Core for advice and training in microscopy, Greg Pazour, Tamara Caspary, Joseph Besharse, and Victor Faundez for helpful advice and reagents, Alan Verkman, Justin Lee, Charles Yeaman, and Daniel Billadeau for reagents. This work was supported by NIH grants GM60448 and EY11482 and a pilot grant from the Emory Center for Cystic Fibrosis Research of Children's Healthcare of Atlanta. Chelsey Chandler Ruppersburg was

supported by NIH Training Grant 5T32GM008367. This research project was supported in part by the Emory University Integrated Cellular Imaging Microscopy Core and a SIM pilot grant from the Core.

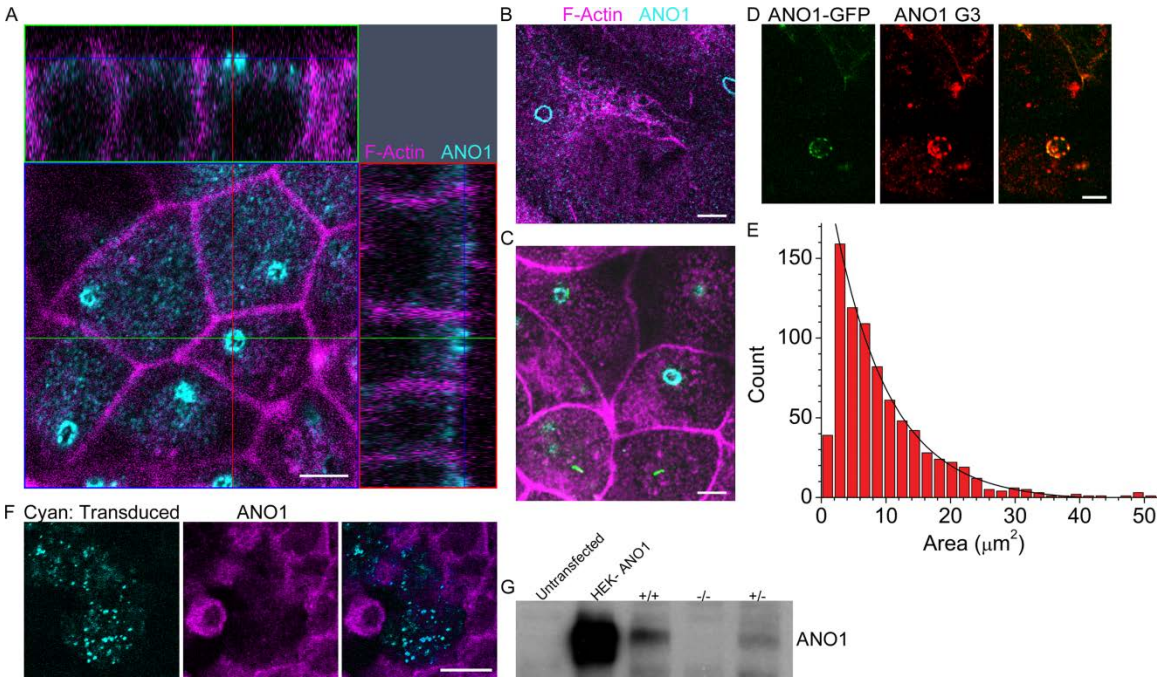

Figure 1. An annulus of ANO1 is located at the apical aspect of cultured epithelial cells. A. Confocal image of mpkCCD$_{14}$ cells grown on permeable supports in the presence of serum. The XY plane is an optical section taken near the apical surface (faint blue line in the z-sections) showing ANO1 (cyan) concentrated in an annular structure. The YZ plane (upper panel, green line in XY image) and XZ plane (right panel, red line in XY image) show that the nimbus is located at the apical surface of the cell. Fluorescent phalloidin was used to label F-actin (magenta). **B.** ANO1 (cyan) nimbus in RPE-J cells grown on glass coverslips. Acetylated tubulin (magenta). **C.** ANO1 (cyan) nimbi in IMCD3 cells grown on permeable supports. Maximum intensity projection of a z-stack. Acetylated tubulin (magenta). IMCD3 cells were stably transfected with SSTR3-EGFP and some cells in the lower part of image have short cilia (green). Scale bars A-C = 5μm. **D.** HEK cells were transfected with ANO1-EGFP (green) and stained with ANO1 antibody (red). Signal from the mANO1-EGFP overlaps with G3 antibody labeling. Scale bar = 10μm. **E.** Size distribution of ANO1 rings. Maximum intensity projections (MIPs)

were made from z-stacks using Zeiss Zen software. The MIPs were then thresholded using robust background subtraction in Cell Profiler (see Methods, (Jiang et al., 2012; Wang et al., 2012)). The size distribution histogram was fitted to an exponential (black line, Count = $223e^{Area/8.9}$). For the fit, the smallest size bin was ignored because the thresholding procedure discarded the smallest ANO1 clusters. **F.** Specificity of ANO1 antibody. Representative image of mpkCCD$_{14}$ cells before nimbus formation (see Fig. 2) treated with lentivirus encoding ANO1 shRNA and EGFP (see Fig. 9A). Lentivirus infected cells are identified by EGFP expression (cyan). ANO1 G3 antibody (magenta) shows a decrease in labeling in shRNA transduced cells. Scale bar = 10 μm. **G.** Western blot showing the level of ANO1 in untransfected HEK cells, ANO1-transfected HEK cells, embryo lysate from wild type (+/+), ANO1 knockout (-/-) and heterozygous (+/-) mice.

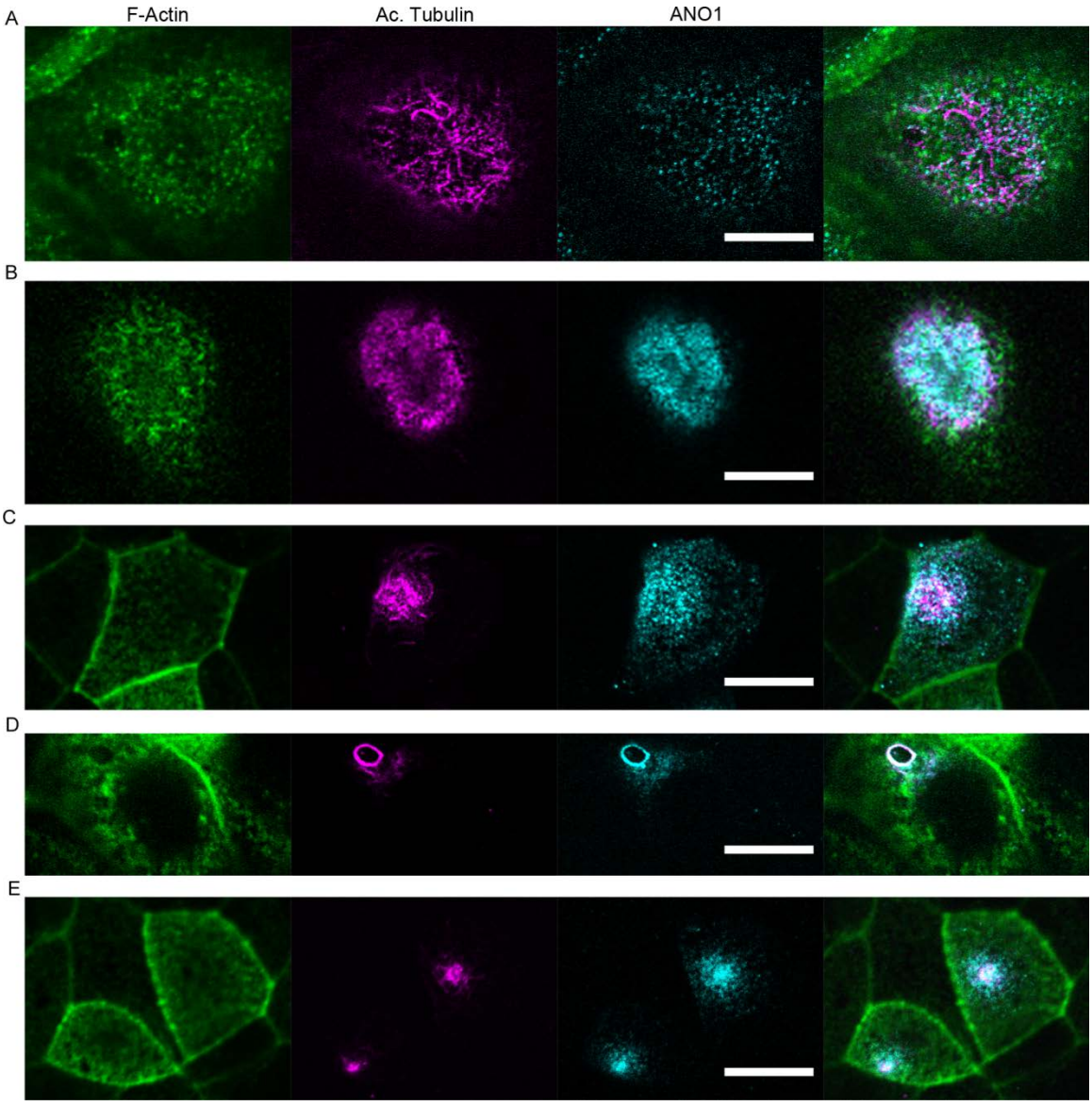

Figure 2. ANO1 localization and nimbus formation prior to formation of the primary cilium. mpkCCD$_{14}$ cells were plated onto permeable supports, fixed at various times after plating, and stained with fluorescent phalloidin for F-actin (green) and antibodies against acetylated tubulin (magenta) and ANO1 (cyan). In this and subsequent figures, the rightmost panel is a merged image of the panels to the left. **A.** 24 hours after seeding, cells are spread out and ANO1 is visualized as puncta throughout the cell. Acetylated tubulin is found as microtubules distributed throughout the cell. **B.** 2 days and

C. 3 days after seeding. ANO1 and acetylated tubulin become concentrated in a patch at the apical membrane. **D.** 4 days after seeding, ANO1 and acetylated tubulin are visualized in the ring structure we term the nimbus. **E.** 5 days after seeding, as cells continue to polarize and form primary cilia, ANO1 and acetylated tubulin are localized to a discrete spot at the apical portion of the cell. Scale bars A-E = 10μm.

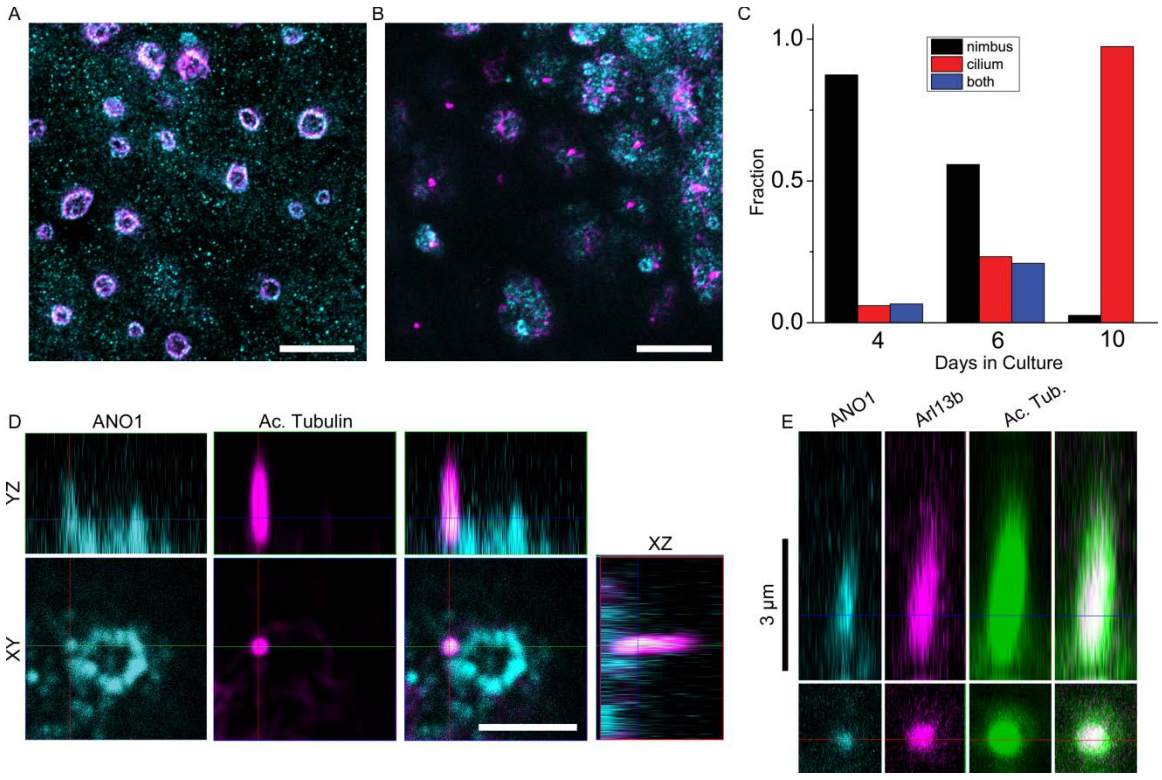

Figure 3. The ANO1 nimbus precedes primary cilium formation and localization of ANO1 in the nascent cilium. A. Maximum intensity projection of mpkCCD$_{14}$ cells grown under conditions (high serum, 4 days in culture) where few cells develop cilia. Under these conditions most cells have a nimbus composed of both ANO1 (cyan) and acetylated tubulin (magenta). **B.** Maximum intensity projection of cells grown under conditions (10 days in culture) where most cells have cilia, labeled by acetylated tubulin (magenta), but very few nimbi (ANO1, cyan). **C.** Quantification of the number of cells with well-define nimbi (black), cilia (red), or both (blue) as a function of days in culture shows that ciliated cells rarely have a well-defined nimbus. Nimbi were defined as annular ANO1-staining structures 2 – 4 µm in diameter. Cilia were defined as acetylated tubulin-staining projections > 2 µm in length. N = 325. **D.** The primary cilium (magenta) develops as a projection from the side of a nimbus (cyan). In the few cells that have both

a nimbus and a cilium, the cilium usually (74% of the time) projects from the side of the nimbus. Bottom row, XY plane. Top row YZ-plane. **E.** Primary cilium labeled with ANO1 (cyan), Arl13b (magenta), and acetylated tubulin (green). Scale bars A,B = 10µm; D = 2.5µm; E = 3µm.

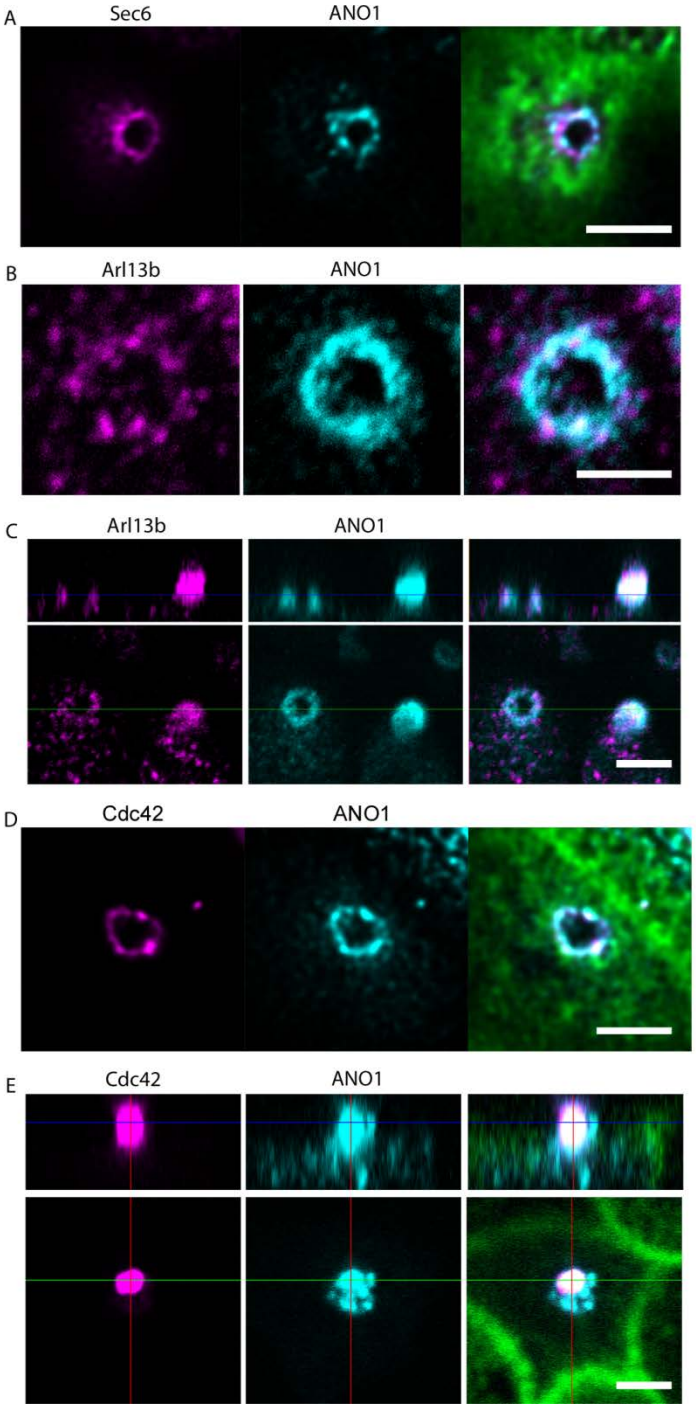

Figure 4. Location of key ciliary proteins in the nimbus. mpkCCD$_{14}$ cells were grown on permeable supports to a nimbiated stage and labeled with the indicated antibodies. **A.** Sec6 (magenta), ANO1 (cyan), and F-actin (green) labeled with Alexa Fluor 633 conjugated phalloidin. **B.** Intense puncta of Arl13b (magenta) co-localize with ANO1

(cyan) in the nimbus. **C.** Bottom row, XY plane. Top row YZ-plane. The left cell has a nimbus containing both ANO1 (cyan) and Arl13b (magenta). The right cell contains a bleb that labels for both ANO1 and Arl13b. **D.** Cdc42 (magenta), ANO1 (cyan); F-actin (green). **E.** Bottom row, XY plane. Top row YZ-plane. A bleb of Cdc42 (magenta) also labels positive for ANO1 (cyan) is presumably a nascent cilium. F-actin (green). Scale bars A-E = 2.5µm.

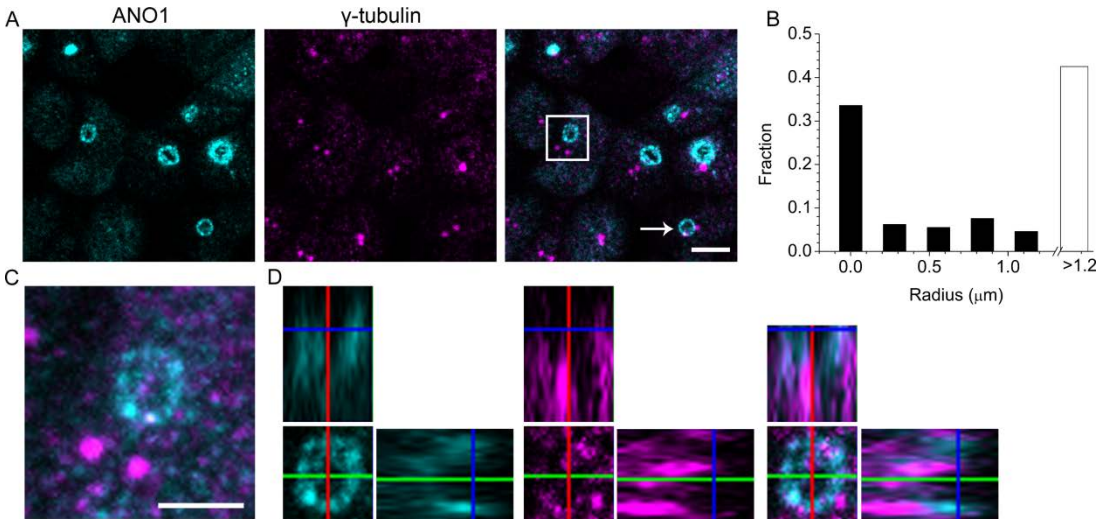

Figure 5. Relationship of the centriole to the ANO1 nimbus. A. A maximum-intensity projection of a z-stack of confocal images of mpkCCD$_{14}$ cells, showing that the spatial relationship of nimbi (ANO1, cyan) to centrioles (γ-tubulin, magenta) is variable. A portion of nimbi have centrioles within their boundary (white arrow), while others do not (white box). **B.** Quantification of the distance of centrioles from ANO1 nimbi. ANO1 nimbi and centrioles were identified by thresholding using Cell Profiler. The left-most bar indicates the fraction of ANO1 nimbi having at least one centriole completely contained within the perimeter in the maximum intensity projection (33%). Another 24% of the ANO1 nimbi had centrioles within <1.2 μm. 43% of rings did not have a centriole within 1.2 μm. **C.** A high magnification image of the nimbus boxed in **A**. Puncta of γ-tubulin (magenta) are evident in the nimbus (ANO1, cyan), despite the remote location of the centrioles to the nimbus. **D.** Individual ortho slices through the nimbus show that γ-tubulin in the nimbus partially overlaps with ANO1. Scale bar A = 5μm; C = 2.5μm.

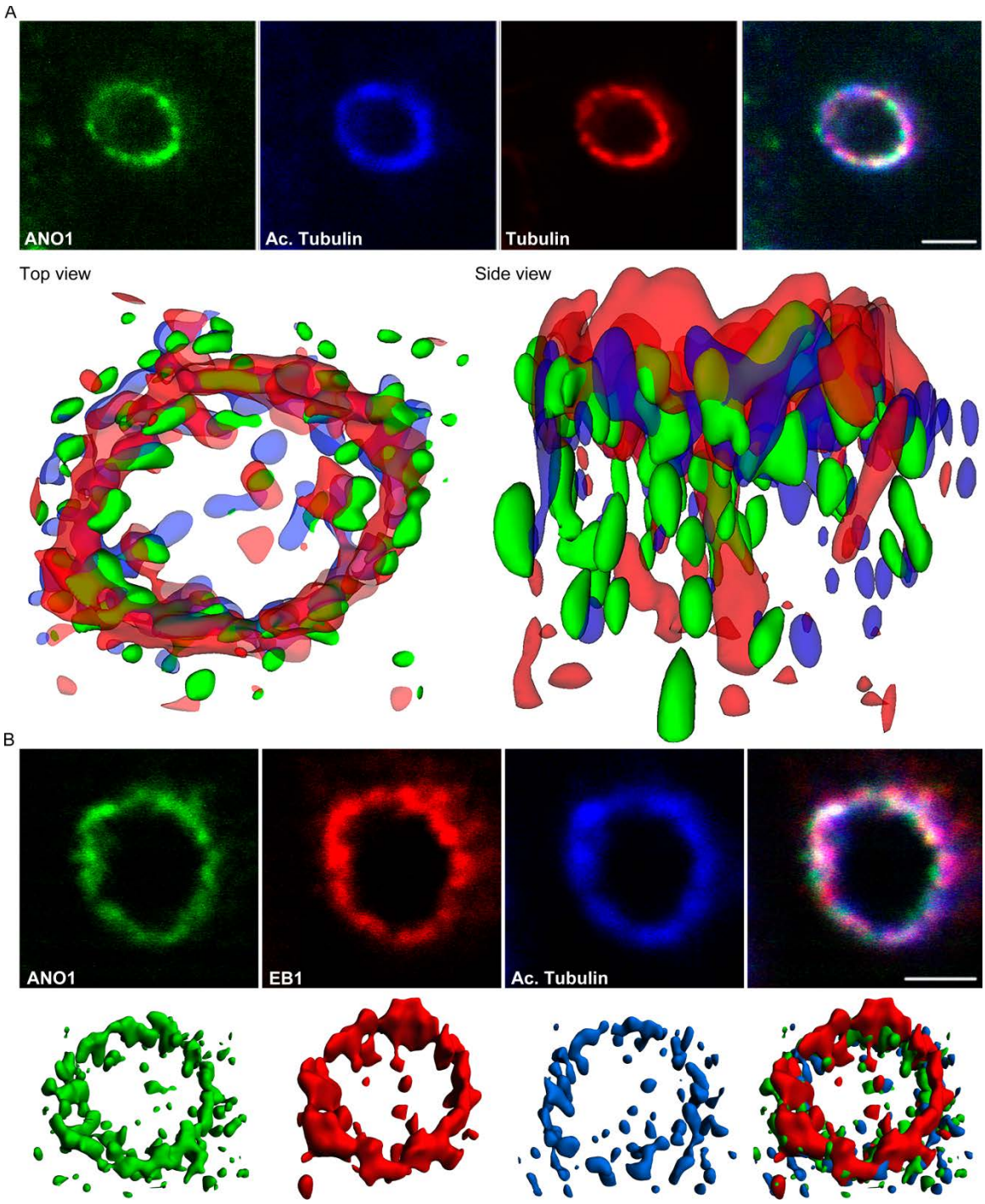

Figure 6. The nimbus is a hub of the microtubule cytoskeleton. A. The ANO1 (green) nimbus contains both acetylated (blue) and non-acetylated (red) α-tubulin. Top row of panels: Representative confocal XY planes of a z-stack of a nimbus that was subjected to deconvolution. Bottom panels: The z-stack was deconvolved using Huygens Essential

software and isosurfaces were then constructed from the deconvolved image using Imaris software. *Top view*: viewed from the apical surface of the cell. *Side view*: viewed from a plane near the apical surface. **B.** EB1 (red) is located at the tips of the microtubules (blue) in the nimbus and comingles with ANO1 (green). Top row of panels: representative confocal XY plane images of a z-stack used for deconvolution. Bottom row of panels: Isosurfaces were constructed from deconvolved images. Scale bars A,B = 2.5μm.

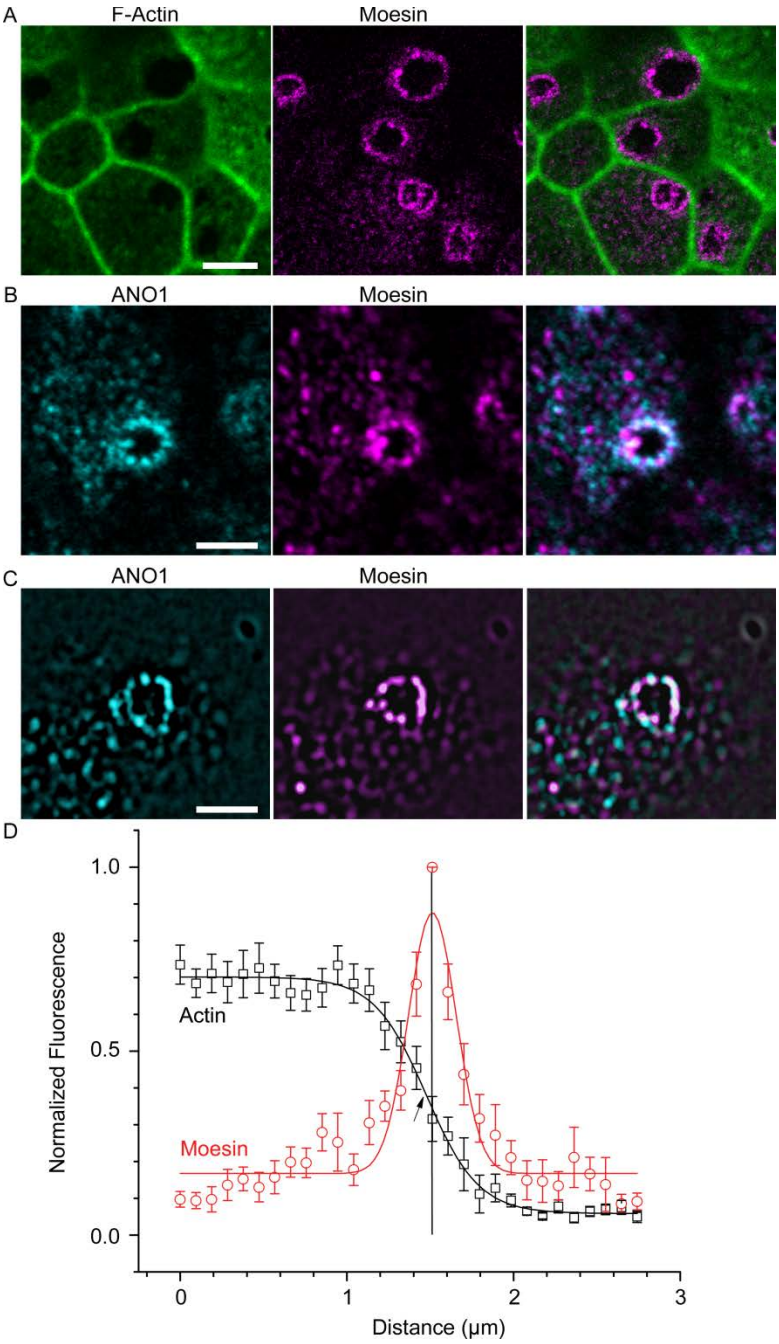

Figure 7. Moesin marks the boundary of an F-actin-free zone that coincides with the ANO1 nimbus. A. F-actin (green) concentration is lower in the center of the nimbus and the interface between F-actin-free and F-actin-rich zones is defined by moesin (magenta) labeling. **B.** Confocal image of mpkCCD$_{14}$ cell nimbus showing that ANO1 (cyan) and moesin (magenta) occupy overlapping locations in the nimbus. **C.** Structured illumination

microscopy of ANO1 (cyan) and moesin (magenta) show that the ANO1 and moesin rings are comprised of distinct puncta that are irregularly superimposed. **D.** Quantification of moesin distribution relative to F-actin. To measure the relationship between moesin and F-actin labeling, pixel intensities along a line starting near the center of the cell and ending at the approximate center of a nimbus were recorded and normalized to the highest intensity in each channel. These measurements for 12 nimbi were then aligned on the x-axis to the moesin pixel with the highest intensity (vertical line, = 1) and the actin (black data points) and moesin (red data points) intensities averaged at each position on the x-axis. The moesin data were fitted to a Gaussian function (red line) and the actin was fitted to a Boltzman equation (black line). Because the moesin channels were aligned to the highest moesin pixel intensity in order to calculate the average of multiple nimbi, the peak moesin intensity = 1, whereas variation in actin intensities around each nimbus resulted in a maximum intensity < 1. Scale bar A = 5µm. Scale bars B,C = 2.5µm.

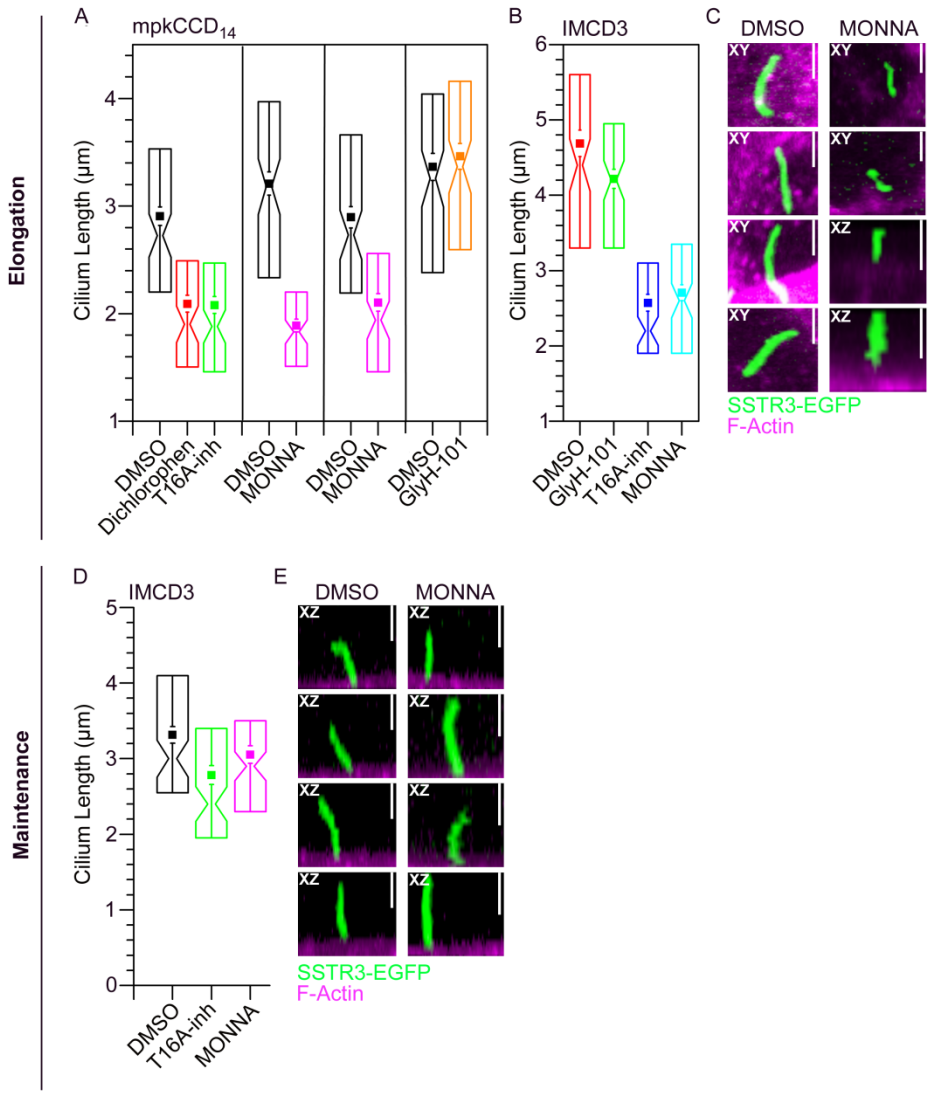

Figure 8. Inhibitors of ANO1 channel activity have a negative effect on cilium length. A. Quantification of the effect of ANO1 inhibitors on ciliary length in mpkCCD$_{14}$ cells. **B.** Quantification of the effect of ANO1 inhibitors on ciliary length in IMCD3 cells. Solid squares: mean. Whiskers: one S.E.M. Box: 25th and 75th percentiles. Notch: median and 1% - 99% confidence intervals of the median. Asterisks: $P < 0.001$ by two-tailed t-test compared to the matched DMSO control. Each data point is the mean of 84 to 110 cilia measured in randomly selected fields. **C.** Representative images of DMSO (control) and MONNA-treated IMCD3 cells labeled for F-Actin (magenta) and expressing EGFP-

tagged somatostatin receptor 3 (SSTR3-EGFP, green). In **C**, MONNA was added to the medium at the same time serum starvation was initiated. This protocol tested the effect of ANO1 inhibitors on cilium formation, elongation, and maintenance (labeled "elongation"). **D.** Quantification of the effect of ANO1 inhibitors added for 6 hours after 24 hours of serum starvation. This protocol tested the potential effect of ANO1 inhibitors on maintenance of ciliary length (labelled "maintenance"). **E.** Representative image of DMSO (control) and MONNA-treated IMCD3 cells labeled for F-Actin (magenta) and expressing EGFP-tagged somatostatin receptor 3 (SSTR3-EGFP, green). Under both conditions of ANO1 inhibitor exposure (**C,E**) the somatostatin receptor continues to localize to the primary cilium. Vertical scale bars in C and E = 2.5μm.

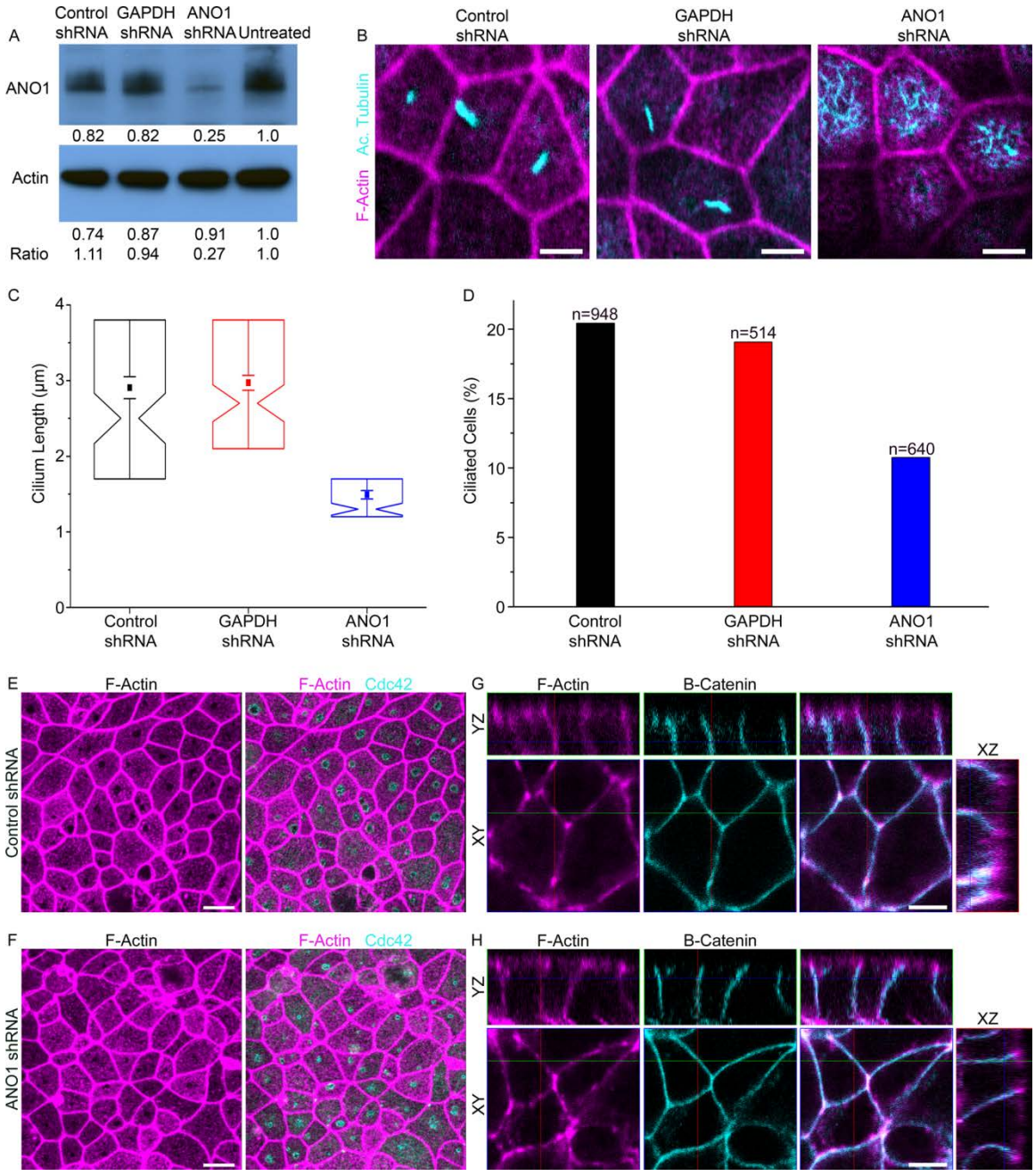

Figure 9. Effects of shRNA knockdown of ANO1. A. Western blot showing the level of ANO1 and β-actin in untreated mpkCCD$_{14}$ cells and cells treated with lentiviral particles encoding shRNA against ANO1 or GAPDH or a non-silencing control sequence as indicated. The numbers below the lanes represent the densitometric measurement of the respective bands. The row of numbers labelled "ratio" is the ratio of the ANO1 band to

the β-actin band normalized to the untreated control. **B.** Representative images of ciliated mpkCCD$_{14}$ cells that were treated with lentivirus encoding ANO1 or GAPDH shRNA or a non-silencing control shRNA. Cyan: acetylated tubulin. Magenta: phalloidin. Scale bars = 5 μm. **C.** Cilium length in cells treated with shRNA as indicated. Box plot as in Fig. 8. **D.** Percentage of ciliated cells. **E-F.** Nimbi of Cdc42 (cyan) are observed in cultures treated with either (**E**) control shRNA or (**F**) ANO1 shRNA. Magenta: F-actin labelled with phalloidin. Scale bars = 10μm. **G-H.** Overall cell polarity appears unperturbed and similar in cells treated with (**G**) control shRNA (**H**) and ANO1 shRNA as assessed by β-catenin (cyan) and F-Actin (magenta) organization. Scale bars = 5μm.

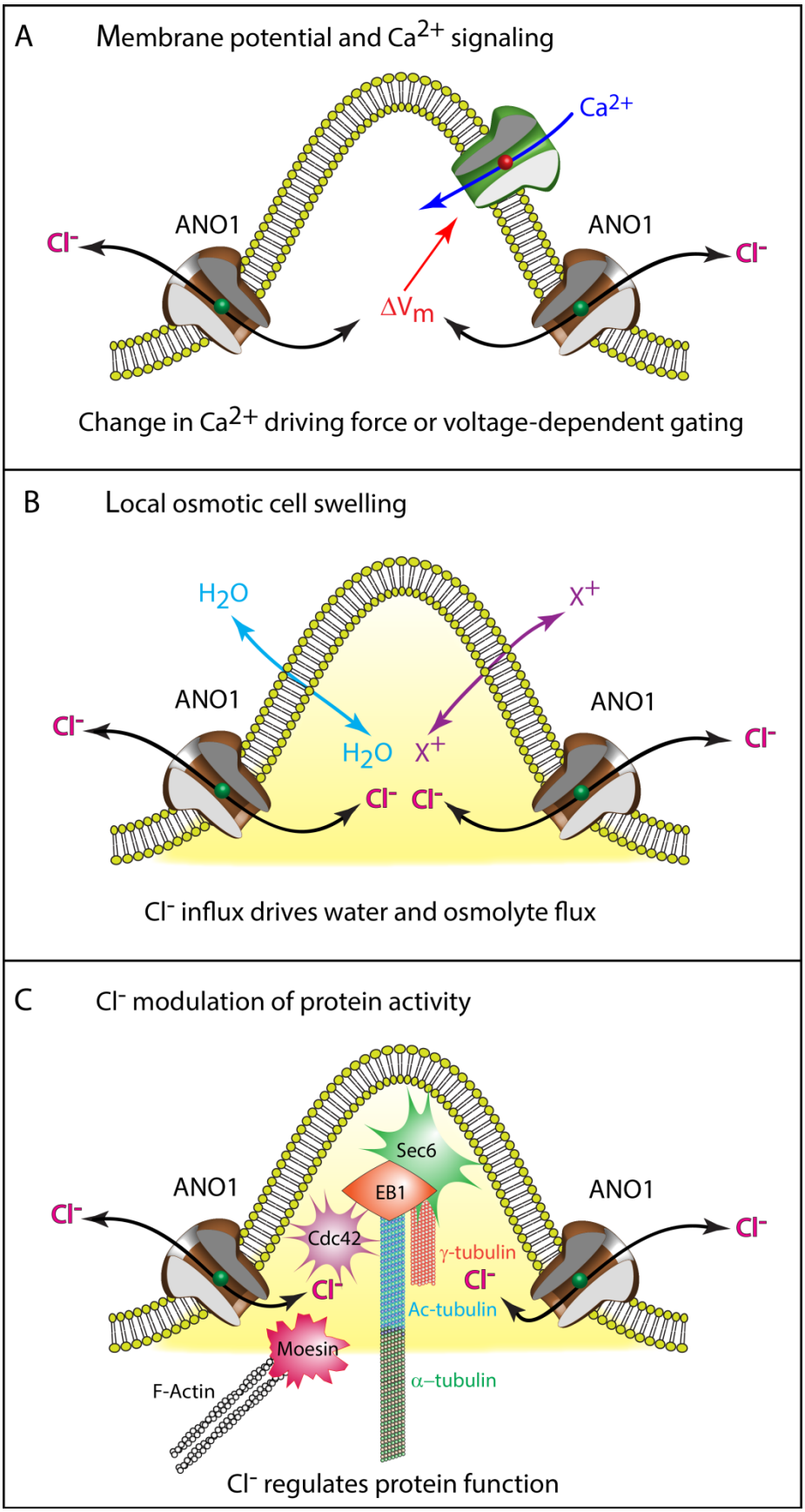
A
Membrane potential and Ca2+ signaling
Ca2+
ANO1
ANO1
Cl-
Cl-
ΔVm
Change in Ca2+ driving force or voltage-dependent gating
B
Local osmotic cell swelling
H2O
X+
ANO1
ANO1
Cl-
Cl-
H2O
X+
Cl-
Cl-
Cl- influx drives water and osmolyte flux
C
Cl- modulation of protein activity
Sec6
EB1
ANO1
ANO1
Cl-
Cl-
Cdc42
γ-tubulin
Cl-
Cl-
Ac-tubulin
Moesin
F-Actin
α–tubulin
Cl- regulates protein function

Figure 10. Cartoon depicting possible mechanisms of ANO1 function in ciliogenesis. See Discussion for more information. Although the figure depicts ANO1 in the plasma membrane at the base of a nascent cilium as suggested by Fig. 3E, we have no firm evidence that ANO1 is located in the plasma membrane. Also, the proximity of Sec6, EB1, Cdc42, moesin, tubulin, and actin in the illustration is not meant to imply they form a complex.

CHAPTER 3

Conclusions & New Questions

Overview

Although regulation of primary cilium formation is essential for normal development and tissue homeostasis, our understanding of the process of ciliogenesis is limited. Ciliogenesis research generally focuses on the events impacting basal body maturation and axoneme extension by intraflagellar transport (IFT) with little attention paid to processes that occur at the plasma membrane before cilia outgrowth. Additionally, though significant advancements have been made in our understanding of the cilium as a unique Ca^{2+} compartment and regulator of Ca^{2+} signaling relatively little is known about ion channels in the primary cilium with the exception of the Ca^{2+} permeable channel polycystin-2 (PC-2, PKD2, TRPP2) (Kottgen et al., 2008; Nauli et al., 2003) (Kottgen et al., 2008; Nauli et al., 2003) (Kottgen et al., 2008; Nauli et al., 2003) (Kottgen et al., 2008; Nauli et al., 2003) (Kottgen et al., 2008; Nauli et al., 2003). The work presented in this dissertation furthers our understanding of primary cilium formation through two main avenues. The first focuses on the characterization of a novel cellular structure we termed the nimbus. The second comes from identifying a new player in ciliogenesis, the Cl^- channel ANO1 and the potential role of Cl^- transport in cilium formation. These novel observations raise unprecedented questions about the role of the nimbus and ANO1 in primary cilium biology, as the potential contribution of Cl^- channels in regulating cilium dynamics is a new and unidentified function. In my dissertation I hypothesized that *the nimbus provides a scaffold for staging of ciliary components for assembly very early in ciliogenesis and that Cl^- transport by ANO1 is required for the genesis or maintenance of primary cilia*. The primary findings that provide support for this are as follows:

1. Characterization of the nimbus including identification of trafficking and cilium-associated proteins along with microtubules and an underlying F-actin free area.

2. Defining the spatiotemporal relationship that exists between the nimbus and cilium in that the nimbus precedes cilium outgrowth and nascent cilia develop from the edge of the ring.

3. Identification of the Ca^{2+}-activated Cl^- channel ANO1 concentrated in the nimbus and later localized to the primary cilium.

4. Blocking ANO1 channel function pharmacologically or ANO1 knockdown with shRNA interferes with primary cilium development.

In this chapter I will briefly summarize the findings of this dissertation, along with the inclusion of a subset of relevant unpublished data that supports the hypothesis. I will discuss their significance for understanding primary cilium biology and future directions.

What role does the nimbus play in primary cilium biology?

As discussed in Chapter 1, the current model for cilium formation involves migration and docking of the mother centriole to the apical membrane, formation of the ciliary gate, and axoneme extension by IFT (Chapter 1, Fig. 1). Despite the advances in understanding these steps, we know little about what happens at the apical plasma membrane in preparation for cilium formation. Given that the ciliary membrane is

continuous with the plasma membrane but must establish a distinct protein and lipid composition, it is imperative that the mechanisms controlling the early establishment of this segregation are defined. My findings provide evidence of a mechanism governing primary cilium formation that involves establishment of a circular organization of key ciliary proteins and a network of tubulin at the apical portion of polarized epithelial cells prior to ciliogenesis termed the nimbus. The identification and characterization of this area of protein segregation provide insight into possible mechanisms of early cilium composition selectivity.

Recent experimental advancements in nimbus studies

Before I discuss the significance and future directions associated with this section, I would like to address a piece of important data recently obtained. The majority of the work presented in Chapter 2 characterizing the nimbus utilizes cultured epithelial cells that were fixed prior to use. The use of fixed cells raises concerns about the whether this ring structure exists in live cells or if it is a product of the fixation process. Additionally, fixation hinders our ability to understand some basic aspects of the nimbus including ring dynamics and correlation of nimbus changes to key cellular events. Recently, in collaboration with the Bassell lab (Emory University, Cell Biology) working with Paul Donlin-Asp, we have made significant strides forward in addressing these concerns and questions. With the use of SiR-tubulin, a fluorescent and cell permeable microtubule stain, we can visualize formation of microtubules into the nimbus in live cells (Fig. 1) (Lukinavicius et al., 2014). In live cells nimbus associated microtubules develop over the course of one hour from a concentration of microtubules to a distinct ring. In these initial trials, only one focal plane near the apical surface was imaged but the early success using

this probe in live-cell studies opens up a range of experimental possibilities that will provide significant insight into the basic questions about the nimbus. Going forward, we can answer questions about the dynamics of the ring and understand the formation, maturation and disassembly of is this structure.

What is the defined spatiotemporal relationship between the nimbus and primary cilium?

One of the major questions we have yet to resolve centers on when in the process of ciliogenesis the nimbus forms and determining if it is the dedicated site of future cilium formation. My results from Chapter 2 provide evidence that the nimbus develops prior to cilium formation and that the nascent cilium begins to form off one edge of the nimbus leading to the hypothesis *that the nimbus represents an early stage of cilium formation and future site of primary ciliogenesis*. By expanding our live-cell microtubule imaging studies to include imaging in the Z-dimension, we hope to follow the formation of the nimbus and the transition from nimbus to cilium to clearly define the spatiotemporal relationship between the nimbus and primary cilium formation.

Another major question surrounding this potential relationship is the timing between centriole migration and nimbus formation. Migration of the centrosome to the apical surface, where the mother centriole docks and matures to form the basal body is one of the earliest described steps in ciliogenesis (Sorokin, 1962). Data collected from our lab on fixed cells at different stages prior to and during cilia development suggests that the nimbus forms prior to apical docking of the mother centriole and that in the majority of cells the centriole localizes at or immediately adjacent to the nimbus before the primary cilium forms (Chapter 2, Fig. 5; Chapter 3, Fig. 4)). Live-cell imaging of mother centriole

migration, for example using a Centrin1-EGFP expressing cell line in conjunction with the use of the SiR-tubulin, would provide answers to where in the path of ciliogenesis the nimbus develops by determining if the ring forms in response to centriole migration or if nimbus formation occurs upstream of basal body migration. These studies could be expanded to compare the loss of the nimbus to other key ciliogenesis steps including transition zone and axoneme formation to determine if a distinct correlation exists between these events (Fig. 4).

Are nimbus-associated proteins trafficked exclusively to the developing primary cilium?

One of the important connections linking the nimbus to cilium is the concentration of key ciliary proteins involved in membrane trafficking including the exocyst complex components Sec6 and Sec8, the small GTPases Arl13b, Cdc42 and Rab11, and the BBsome component BBS1 (Chapter 2, Fig. 4; Chapter 3, Fig. 2 includes the additional proteins identified since the MBoC paper) at the nimbus. The concentration of this particular collection of proteins along with the mutually exclusive relationship between the nimbus and primary cilium leads me to hypothesize *that the nimbus is a hub for the staging of ciliary components that are trafficked into the cilium during early stages of ciliogenesis* (Fig. 4). Increasing our understanding of the basic mechanisms that control protein targeting and trafficking to the cilium has the potential to further our knowledge of human diseases caused by ciliary defects such as polycystic kidney disease.

To test the hypothesis that the nimbus is a unique storage area for ciliary proteins, we need insight into the trafficking of nimbus components in relation to cilium development. One of the key pieces of data that would help in our understanding of this

would be to determine if nimbus-associated proteins are trafficked into the cilium or to other areas of the cell. The established role of ANO1 as an apical membrane protein and now a ciliary protein makes this channel a good candidate to follow. A photoconvertible fluorescent protein fused to ANO1 would allow for continuous tracking of a subpopulation of tagged protein. Photoconversion of nimbus-associated ANO1 followed by examination of photoconverted ANO1 localization over time would provide insight into the mobility of ANO1 in the nimbus and determine if nimbus-associated proteins are trafficked from the nimbus to the developing cilium. Though the primary hypothesis is that the nimbus selectively sequesters cilium-bound proteins, it is possible the nimbus serves a broader role than collecting proteins necessary for cilium formation and could serve as a modulator of apical membrane organization by sorting proteins destined for the apical membrane. The experiments described above would provide some insight into both possibilities and is central to elucidating the functionality of the nimbus. If nimbus-associated proteins are selectively retained for trafficking to the developing cilium, it could be a mechanism of controlling early cilium composition even before formation of the transition zone.

Is the nimbus an obligate antecedent to the primary cilium?

One of the main questions still remaining between the nimbus and cilium is if the nimbus is an obligate step in cilium formation and what are the consequences of nimbus perturbation? In Chapter 2, I tested the effects of ANO1 knockdown on nimbus formation but could not detect any defects in formation of the nimbus, though cilium formation was impaired (discussed in more detail below) (Chapter 2, Fig. 9). One potential way to determine the functional relationship between the two would be to disrupt the associated cytoskeleton components. Along with the unique protein composition, the nimbus

displays distinct cytoskeletal associations. In Chapter 2, I describe that the nimbus-associated microtubules form an interface with the actin cytoskeleton so that F-actin, visualized with a fluorescently conjugated phalloidin, is excluded from the center of the nimbus (Chapter 2, Fig. 7; Chapter 3, Fig. 4). The use of microtubule modifying drugs like nocodazole would disrupt the ring and allow us to assess which proteins are no longer localized to the ring or if the actin cytoskeleton exclusion is altered but would not allow for assessment of the effects of ring perturbation on cilium formation because the cilium is a microtubule-based structure sensitive to the effects of these agents. In addition, the use of actin disrupting agents also impact proper cilium formation and therefore presents another limitation (Kim et al., 2010; Sharma et al., 2011). Though the use of these drugs would limit the assessment of nimbus impact on cilium formation, they would provide useful information to the role of the cytoskeleton in formation of the ring and potential trafficking of components to the nimbus. Interestingly, a surge of studies looking at the relationship of the actin cytoskeleton to ciliogenesis suggest that inhibition of actin polymerization promotes ciliogenesis (Kim et al., 2010; Sharma et al., 2011; Yan and Zhu, 2013b). The identification of the nimbus as an area free of F-actin where the primary cilium is proposed to form illuminates opportunities to discover new insights into the paradoxical role of actin in ciliogenesis. This area free of F-actin at the nimbus is reminiscent of the changes in actin organization in the developing immune synapse that forms at the interface of a T-cell and an antigen presenting cell. The clearance of actin from this region makes it an easier target for vesicular trafficking. One possibility is that the nimbus is an area of high traffic and needs the clearance of F-actin to facilitate delivery of these vesicles to the apical plasma membrane (Fig. 4). Additionally, the F-actin clearance from underneath the

membrane makes this portion of the membrane more conducive to bleb formation that may function as a vessel for early cilium extension (discussed in more detail below) (Fig. 4).

A correlative avenue to explore that may circumvent these described issues of using cytoskeletal disrupting drugs is to perturb nimbus-associated proteins that may be involved in regulating the cytoskeletal features or protein retention at the nimbus. One of the most promising candidates comes from the observation that the ERM protein moesin demarcates this interface between the enrichment of microtubules that compose the nimbus and the F-actin free area. The ERM proteins mediate interaction of membrane proteins with the underlying actin network and more recently were shown to bind to and stabilize microtubules (Solinet et al., 2013). Additionally, quantitative SILAC proteomic analysis revealed that ANO1 interacts at high stoichiometry with a network of notable proteins involved in actin organization and among the proteins most highly enriched from the SILAC experiment were the ERM's (Perez-Cornejo et al., 2012b). The established role of moesin in membrane organization through the regulated linkage of membrane proteins to the underlying actin network along with new connections to the microtubule cytoskeleton, leads me to hypothesize *that moesin is involved in retaining and organizing ANO1 in the nimbus prior to ciliogenesis by regulated linkage to the underlying cytoskeleton and that loss of functional moesin will cause altered nimbus morphology and composition*. One mechanism of moesin regulation and activation involves phosphorylation on Thr558 in the F-actin binding site (Fievet et al., 2004; Gautreau et al., 2000). Expression of moesin-T558D, a phosphomimetic form and moesin-T558A a form that cannot be phosphorylated, would allow for investigation into whether the active form of moesin is important for nimbus formation by assessing the association of identified components, morphology, and

cytoskeletal associations. If my hypothesis that expression of the inactive form of moesin leads to loss of ANO1 localization to the nimbus and altered cytoskeletal associations with the nimbus then use of these mutants would provide a tool to explore the effects of nimbus perturbation on primary cilium formation. Additionally, the constitutively active form of moesin could cause stabilization of the nimbus and provide valuable insight into whether dissolution of the nimbus is required for proper cilium formation.

Is the nimbus more than a site for protein localization?

The primary cilium is an area of specialized cellular outgrowth that on a broader scale shares similarities with other polarized structures including developing neuronal growth cones or the growing bud of yeast cells. One of the overarching themes relating these structures is the need to control protein composition, as they all show distinct protein segregation from the rest of the cell. One efficient way to create these functional and structural asymmetries is through the localization of mRNA's to specific sites to allow for the spatial segregation of protein synthesis (Jansen, 2001; Martin and Ephrussi, 2009). Compartmentalization of mRNA's to subcellular sites provides a means for cells to alter the composition of that region in response to physiological stimuli like the localized translation of β-actin mRNA to the leading edge of migrating fibroblasts (Shestakova et al., 2001). Additionally, mRNA localization may also be involved in sorting membrane proteins to specific subdomains of the plasma membrane. Work from Takizawa *et al.* identified localization of mRNA encoding a proposed ion channel and yeast Anoctamin homolog, Ist2, to the developing yeast bud. At the developing bud *IST2* mRNA is translated and inserted into the bud plasma membrane to generate distinct levels of Ist2 in the developing bud from the mother cell (Takizawa et al., 2000). These

results suggest that mRNA localization can contribute to the generation or maintenance of membrane subdomains. This idea led me to hypothesize *that the nimbus, as a proposed specialized domain, is also an area of mRNA localization.*

In collaboration with the Bassell Lab at Emory University (Dept. of Cell Biology) and work done with Paul Donlin-Asp, we tested by RNA fluorescence in situ hybridization (FISH) whether the nimbus contained concentrated levels of poly(A) RNA. mpkCCD$_{14}$ cells labeled by oligo d(T) FISH show a ring of concentrated poly(A) RNA that correlate with the nimbus visualized by α-tubulin (Fig. 3A). In control samples, oligo d(A) FISH shows a lack of signal correlating with the nimbus. In addition, we detect the mRNA binding protein (RBP) PAPBC1 at the ring, whereas in the negative control sample the predominantly nuclear PABPN1 is not (Fig. 3B). Together these results suggest that the nimbus is a specific area of mRNA localization, which opens up an entirely new avenue in the cilia field, as the role of mRNA localization in primary cilium biology has not been explored. These observations directly lead to the question of why mRNA enriched at the nimbus. Two primary possibilities considered were that nimbus localized mRNA 1) is held at the nimbus to be trafficked into the developing cilium or 2) actively translated into proteins needed for nimbus and/or cilium formation. Given that protein translation is excluded from the cilium, we hypothesized *that active translation of nimbus associated mRNA's contributes to the distinct composition of the nimbus and may support primary cilium formation by locally synthesizing ciliary proteins.*

To test if the nimbus is a site of active translation, we performed a puromycin incorporation experiment in live cells. Puromycin is a structural analog of an amino-acyl tRNA molecule, which enters ribosomes actively engaged in translation. The puromycin

becomes covalently attached to the carboxy terminus of nascent proteins through a peptide bond. By performing a quick thirty second exposure and then fixing and labeling the cells for puromycin and ANO1, we can determine if translation occurs at the nimbus. The short time of puromycin exposure minimizes the possibility that nascent peptides labeled with the puromycin elsewhere in the cell are trafficked to the nimbus. The preliminary results show that in mpkCCD$_{14}$ cells an enrichment of puromycin correlates with ANO1 labeling at the nimbus (Fig. 3C), which suggests that the mRNA's detected at the nimbus by FISH are also translated at the nimbus.

Identifying the nimbus as an area of protein synthesis further supports the idea that the nimbus functions as a specialized cellular domain and opens the possibility that formation of the nimbus, as an area of structural asymmetry from the rest of the cell, is in part mediated by localized translation. Furthermore, these results suggest that mRNA localization and translation at the nimbus may contribute to early cilium development. Given that primary cilium formation and function depend on tight control of protein composition at the cilium, it is possible that both the established regulation of ciliary protein trafficking as well as mRNA localization and localized protein synthesis at the nimbus contribute to modulating early cilium formation and/or composition. Going forward, it will be crucial to determine the role of mRNA localization and local protein synthesis in nimbus development and function as well as in primary cilium formation. Local protein synthesis at the site of cilium formation could provide an additional layer of ciliary composition control. Understanding this potential role could be vital to elucidating the mechanisms controlling ciliogenesis and furthering our comprehension of how defects in cilium formation contribute to human disease.

What is the role of Cl^- channel activity in primary cilium formation?

The second major discovery embodied in this dissertation is the identification of the Cl^- channel, Anoctamin 1 (ANO1/TMEM16A), in the primary cilium, and that blocking its channel function pharmacologically or knocking it down with shRNA interferes with cilium development as there are fewer ciliated cells and the cilia are shorter (Chapter 2, Figs. 8&9). These novel observations raise unprecedented questions about the role of ANO1 in primary cilium biology, as the potential contribution of Cl^- channels in regulating cilium dynamics is a new and unidentified function. In Chapter 2, I propose three models to address the potential role of ANO1 in primary cilium formation (Chapter 2, Fig. 10). In the following sections, I will discuss these possibilities in light of recent advances in the field and describe potential avenues of investigation related to these ideas.

Does ANO1-mediated Cl^- regulation modulate ciliary protein function and/or trafficking?

One idea is that Cl^- ions could regulate protein function or trafficking so that changes in intracellular Cl^- could conceivably alter the function and/or trafficking of proteins involved in ciliogenesis. One of the better known examples of Cl^- modulation of protein functions comes from a report from Nakajima *et al.* who demonstrated that the level of Cl^- present in solution modulates the GTPase activity of tubulin and stimulates *in vitro* tubulin polymerization (Nakajima et al., 2012). Given that the nimbus is concentrated in microtubules and that the primary cilium is a microtubule-based structure, it is possible that ANO1 regulation of local Cl^- concentration affects microtubule formation and dynamics important in either nimbus formation and stability or axoneme development.

Many of the ciliary proteins identified at the nimbus are trafficking-associated proteins and defects in Arl13b and IFT proteins have been linked to aberrations in cilia length, similar to the defects caused by ANO1 perturbation (Larkins et al., 2011; Pazour et al., 2000). Though the mechanisms controlling ciliary length are poorly understood, contributing factors include IFT, precursor molecule availability, cytoskeletal dynamics, and turnover of components at the ciliary tip (Avasthi and Marshall, 2012; Hilton et al., 2013; Pan and Snell, 2014). Given that ciliary trafficking is a key component in cilia length regulation and that regulation of Cl^- levels in vesicles is important for intracellular trafficking, the defect in cilia length observed in the ANO1 knockdown and inhibitor treated cells opens the possibility that ANO1 is involved in ciliary trafficking (Faundez and Hartzell, 2004b). Future studies utilizing ANO1 perturbation should assess potential defects in IFT to assess intracilliary trafficking and any disruption to the localization of trafficking mechanisms to the cilium including the BBsome and exocyst complex in ANO1 knockdown cells. Additionally, these experiments could be expanded to compare defects in ANO1 knockdown cells with those expressing conduction and gating mutant ANO1 channels like the C836S mutation that allows for normal trafficking of the channel but renders it incapable of generating Cl^- currents. Given the vital role of vesicle luminal acidification in the secretory and endocytic pathways and the use of Cl^- as the counterion current for charge compensation, the possibility that ANO1 Cl^- channel activity contributes to the trafficking of proteins to the cilium by modulating vesicle pH warrants exploration (Faundez and Hartzell, 2004b; Stauber and Jentsch, 2013).

Are osmotic forces generated by ANO1 Cl^- flux needed in early cilium extension?

Another possibility is that ANO1 participates in creating local osmotic forces that contributes to ciliary extension by generating a cellular bleb. In this model, IFT alone is not sufficient to produce a normal cilium. In addition osmotic pressure, driven by ionic and water fluxes in part mediated by ANO1, would be needed to assist in locally remodeling cell shape at the membrane to produce a cellular bleb that becomes the nascent primary cilium (Fig. 4B). The absence of detectable F-actin within the nimbus along with the concentration of ANO1 surrounding this F-actin free area suggests that ANO1 could be poised to regulate Cl^- and hence water fluxes that would favor inflation of a membrane bleb at the nimbus, essentially creating a vestibule for axoneme assembly. In Chapter 2, I describe cellular blebs containing ANO1, Cdc42, and Arl13b that are consistent with this possibility (Chapter 2, Fig. 4). In the history of cilia research, IFT has received a significant portion of the attention but for the axoneme to continue to grow, the ciliary membrane surrounding it must also grow as well meriting investigation into the mechanisms controlling this process. Furthermore, after docking of the mother centriole to the apical membrane, there must be a mechanism that creates something like a cellular bleb to provide room for the developing transition zone and then axoneme. Live-cell experiments following ciliogenesis in the presence of ANO1 and aquaporin blockers would provide useful insight into the potential requirement for local ion and water fluxes in this process. If early cilium extension requires membrane bleb formation, then the use of these blockers should result in either no detectable cilium extension or formation or short cilia.

Does ANO1 or ANO1 channel activity contribute to the distinct ciliary Ca^{2+} levels?

The last proposed model hypothesizes that ANO1 could locally regulate apical membrane potential that affects other processes like the driving force for Ca^{2+} or the open

probability of voltage-gated channels. The recent developments into the concept of the primary cilium as a unique Ca^{2+} compartment functionally distinct from the cytoplasm (discussed in Chapter 1, Section 1.3), leads me to the question if ANO1 contributes to generating or maintaining the cilium as a high Ca^{2+} compartment (DeCaen et al., 2013; Delling et al., 2013)? Given that the diffusion barrier at the base of the cilium allows proteins under 40kDa to freely diffuse into the cilium, it is surprising that the cilium has a distinct resting Ca^{2+} concentration from the cytoplasm (Delling et al., 2013). One important question to answer that would provide significant insight into the process of ciliogenesis would be to determine the timing at which the ciliary Ca^{2+} levels are set. It is unknown whether the higher Ca^{2+} levels are established from the beginning in the nascent cilium or if this Ca^{2+} gradient is established after the cilium reaches a steady state level. Localization of ANO1 to developing and fully formed cilia positions ANO1, a CaCC, to act as a sensor and responder to this ciliary Ca^{2+} signaling early on.

Though further work is required to determine the presence of a Ca^{2+} buffering mechanism, results from the Clapham lab (described in Chapter 1) suggest that Ca^{2+} binding proteins may play a role in creating this Ca^{2+} concentration (Delling et al., 2013). Recently data from Terashima *et al.* demonstrate that mutagenesis of two glutamates, that had previously been determined by our lab as crucial for Ca^{2+} sensing, greatly reduce the Ca^{2+} signaling (Brunner et al., 2014; Terashima, 2013; Yu et al., 2012a). These results strengthen the suggestions that Ca^{2+} directly binds to ANO1 and opens the possibility that ANO1 may contribute to generating this high concentration of Ca^{2+} in the cilium. Utilizing the genetically encoded Ca^{2+} sensors described in Chapter 1 in ANO1 knockdown cells would provide insight into this possibility by allowing researchers to quantitatively

compare the level of Ca^{2+} in the absence of ANO1. Furthermore, use of the ANO1 E702/705Q mutant that has >1000 fold reduced sensitivity to activation by Ca^{2+} in these studies could prove useful insight into whether direct binding of Ca^{2+} to ANO1 in the cilium contributes to the high levels of ciliary Ca^{2+}. A separate possibility is that ANO1-mediated regulation of Cl^- levels in the cilium contributes to the establishment and/or maintenance of the high Ca^{2+} levels. Following the effects of ANO1 channel inhibition in live-cells expressing the genetically encoded Ca^{2+} sensors could elucidate this possibility. Furthermore, the unique Ca^{2+} concentration in the cilium prompts investigation into the concentration of other ions, like Cl^- in the cilium compared to the rest of the cell.

Could ANO1 play a role in cilia-related cancer progression and polycystic kidney disease (PKD)?

Clues that ANO1 performs cell biological functions first came from studies in cancer biology that discovered amplification of the *Ano1* locus in both oral and head and neck squamous cell carcinoma and that expression of ANO1 is significantly increased in patients with a propensity to develop metastases (Ayoub et al., 2010; Carles et al., 2005; Duvvuri et al., 2012b; Huang et al., 2006; Ruiz et al., 2012). These observations prompted investigation into the contribution of ANO1 to cell proliferation and migration that went on to demonstrate that knockdown of ANO1 in tumor cells leads to a decrease in colony size and tumor volume (Britschgi et al., 2013; Duvvuri et al., 2012b; Shiwarski et al., 2014; Stanich et al., 2011a). Interestingly, links between the presence of primary cilia and cancer development are growing (Christensen et al., 2007; Han and Alvarez-Buylla, 2010; Seeger-Nukpezah et al., 2013). The presence of the primary cilium is tightly coordinated with the cell cycle so that primary cilia are limited to non-proliferating cells because of the use of

the mother centriole as the basal body (Rieder et al., 1979; Tucker et al., 1979; Wheatley et al., 1996). These associations have led to the hypothesis that the cilium controls cell proliferation and that ciliary abnormalities could disrupt the control of proliferation and contribute to the formation and/or progression of disorders like cancer and the human ciliopathy polycystic kidney disease (PKD) (Pan et al., 2013).

In autosomal polycystic kidney disease (ADPKD) renal cysts begin to form due to increases in epithelial cell proliferation and eventually separate from their parent tubule (Osathanondh and Potter, 1964; Wilson, 2004). These cysts enlarge due to transepithelial Cl^- secretion driving fluid accumulation in the lumen (Grantham et al., 1995; Mangoo-Karim et al., 1995; Wallace et al., 1996; Wilson et al., 1991). The formation of fluid-filled cysts in the kidney and liver is a hallmark of the ciliopathies (Brown and Witman, 2014; Chapin and Caplan, 2010; Harris and Torres, 2009; Oh and Katsanis, 2012; Zhou, 2009). The Cl^- channel CFTR has been the primary candidate proposed in this cyst expansion but data has shown that some cysts do not express CFTR (Brill et al., 1996; Davidow et al., 1996; Hanaoka et al., 1996). Given the canonical role of ANO1 in regulating fluid secretion and the speculative role of ANO1 in cell proliferation, along with my discovery of ANO1 as a ciliary localized Cl^- channel, leads me to question if ANO plays a role in the progression of the ciliopathy PKD? Mutations in PKD1 and PKD2 cause ADPKD presumably due to defects in cilium-regulated Ca^{2+} signaling (Hanaoka et al., 2000; Harris et al., 1995a; Harris et al., 1995b; Hughes et al., 1995; Kuo et al., 2014; Mochizuki et al., 1996). However, how this defective signaling leads to over proliferation and eventual formation of the fluid-filled cysts is unclear. Therefore, determining if ANO1 activity is altered in ADPKD and if that altered activity contributes to the initial defects in cell

proliferation or driving the fluid accumulation in these cysts, would be a significant advancement in our understanding of this disease. Though the original ANO1 knockout mouse strain did not present characteristics of classical ciliopathies the mice died shortly after birth, severely limiting the ability to study the role of ANO1 in this progressive kidney disease. Generation of a kidney-specific ANO1 knockout mouse would be a key element in studying this potential connection. Additionally, close examination of ANO1 up and/or down regulation and localization in PKD mouse models could provide critical new evidence into the pathology of PKD. Recent work by Buchholz *et al.* provides initial evidence to suggest that ANO1 could contribute to ADPKD pathology (Buchholz et al., 2014). Disrupting ANO1 activity either by knockdown or pharmacological inhibition reduced cyst growth and enlargement in an embryonic kidney cyst model (Buchholz et al., 2014). These results provide a strong base to support detailed investigation into the mechanism of ANO1 Cl^- channel activity in ADPKD.

Summary

Identifying the mechanisms regulating cilium development is vital to understanding tissue homeostasis and the progression of the growing number of human diseases associated with cilia dysfunction. My work exploring 1) the nimbus and 2) a role for ANO1 Cl^- channel activity in cilium development provides seminal insight into the complex biological process of ciliogenesis. A model combining the ideas related to the potential contribution of the nimbus and ANO1 Cl^- channel activity to primary cilium formation are summarized in Fig. 4. Overall, I hypothesize that the nimbus develops as F-actin is cleared and microtubules, ciliary (ie Arl13b) & scaffolding proteins (ie moesin), and mRNA become enriched into this circular region of high vesicular trafficking and localized

translation at the apical membrane prior to ciliary outgrowth (Fig. 4A). As the nimbus forms, the mother centriole migrates to this area where the basal body will dock (Fig. 4B). Based on the ANO1 knockdown studies (Chapter 2, Fig. 9), I propose that ANO1 Cl^- channel activity is not essential in nimbus formation but rather plays a role in early cilium extension by three proposed mechanisms described in detail in the previous section (Fig. 4C). As the ciliary transition zone develops and the cilium extends, the nimbus attenuates as nimbus-associated ciliary proteins are trafficked into the nascent cilium (Fig. 4D).

As a key contributor to proper development and cellular physiology it is vital that we investigate the potential involvement of the nimbus and ANO1 in the complex cellular pathway of primary ciliogenesis. Understanding the role of ANO1 in cilium development may provide a mechanistic foundation for interpreting the roles of ANO1 in development and provide novel insight into the progression of the growing number of human diseases linked to primary cilium defects, including polycystic kidney disease. Establishing these connections could spur investigation into ANO1 as a novel target for therapeutic intervention. Although much is being learned about the biophysics of ANO1 as a Cl^- channel, the regulatory networks associated with ANO1 remain largely unexplored. To fill this gap of knowledge and to provide vital insight into the contribution of ANO1 to normal cell function and different disease states will require extensive investigation into the physiological significance of nimbus and ciliary associated ANO1.

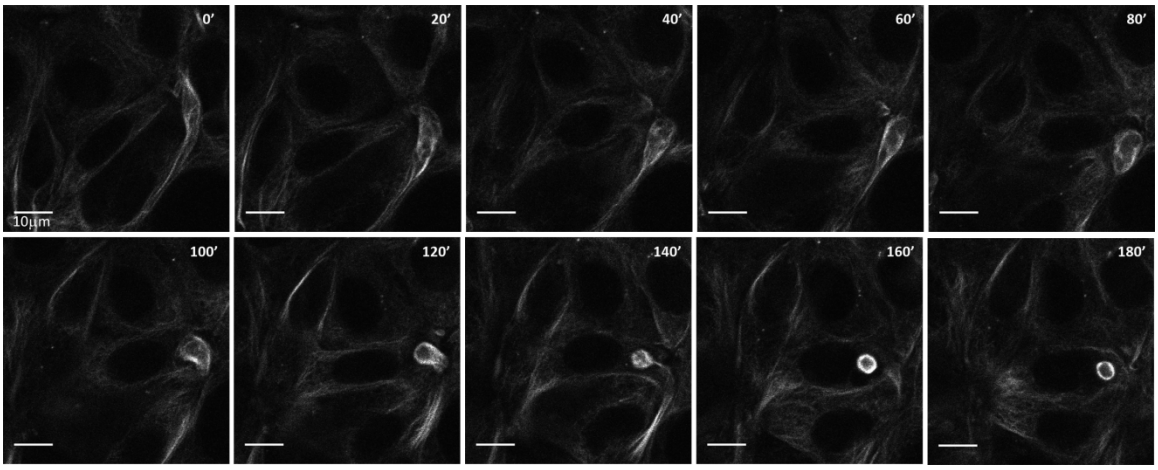

Figure 1. Live-cell imaging of nimbus formation. Live mpkCCD$_{14}$ cells pre-stained for one hour with SiR-tubulin were imaged every twenty minutes for three hours at one focal plane near the apical portion of the cell. The nimbus progresses from a developing concentration of microtubules into a distinct ring over the course of one hour.

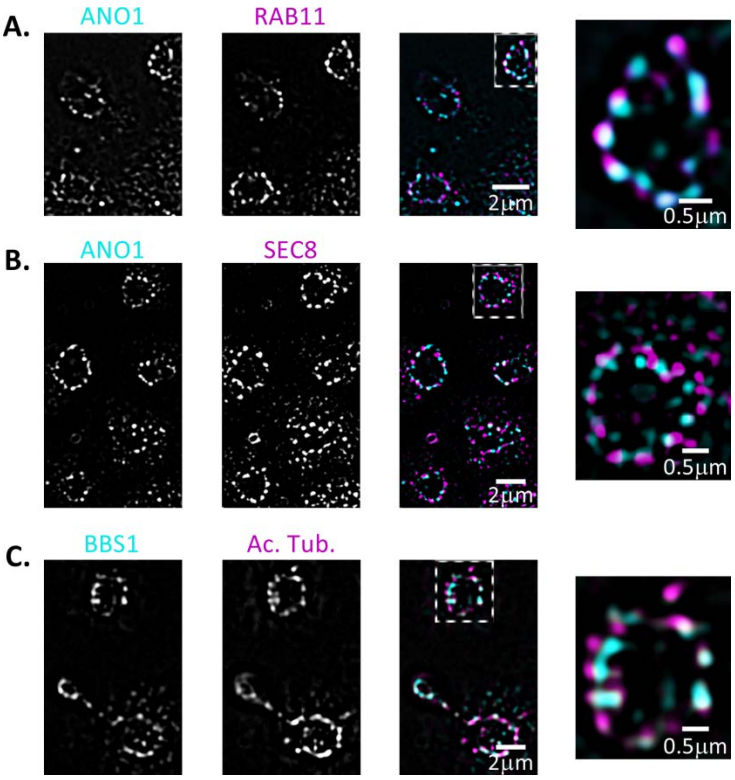

Figure 2. Additional nimbus components imaged using structured illumination microscopy (SIM). The white boxes indicate the area of the image expanded in the following panel. All samples of mpkCCD$_{14}$ cells grown on Transwell filters. **A.** The small GTPase Rab11 (magenta) at the nimbus labeled with ANO1 (cyan). **B.** The exocyst complex component Sec8 (magenta) with ANO1 (cyan) in the nimbus. **C.** The BBSome component BBS1 (cyan) in the nimbus labeled with acetylated tubulin (magenta).

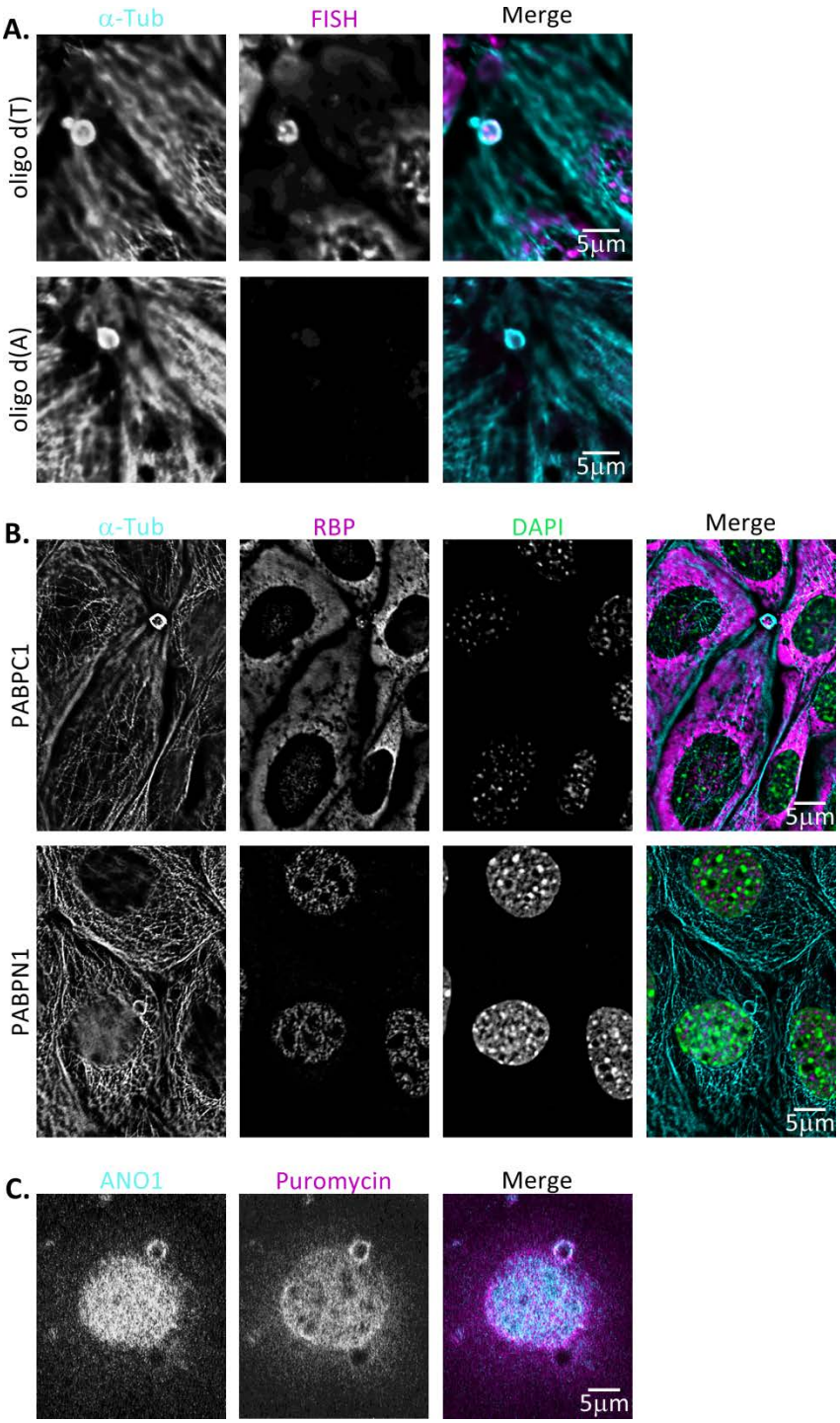

Figure 3. Association of poly(A) RNA and RNA binding protein (RBP) with the nimbus. A. In mpkCCD$_{14}$ cells grown to confluence on glass coverslips, poly(A) mRNA (magenta), as detected by oligo d(T) fluorescence *in situ* hybridization (FISH), is

enriched at the nimbus labeled with α-tubulin (cyan). The negative control using an oligo d(A) probe shows no signal enrichment. **B.** The mRNA binding protein (RBP) PABPC1 (magenta) is found at the ring labeled with α-tubulin (cyan), whereas the predominately nuclear PABPN1 is not found associated with the nimbus. DAPI staining (green) used to visualize the nucleus. **C.** To determine if the nimbus is an area of active translation, 30 sec puromycin labeling was performed on live mpkCCD$_{14}$ cells. Puromycin is a structural analog of an amino-acyl tRNA molecule, enters ribosomes actively engaged in translation, and becomes covalently attached to the carboxy terminus of nascent proteins through a peptide bond. Samples were then fixed and labeled for ANO1 (cyan) and puromycin (magenta).

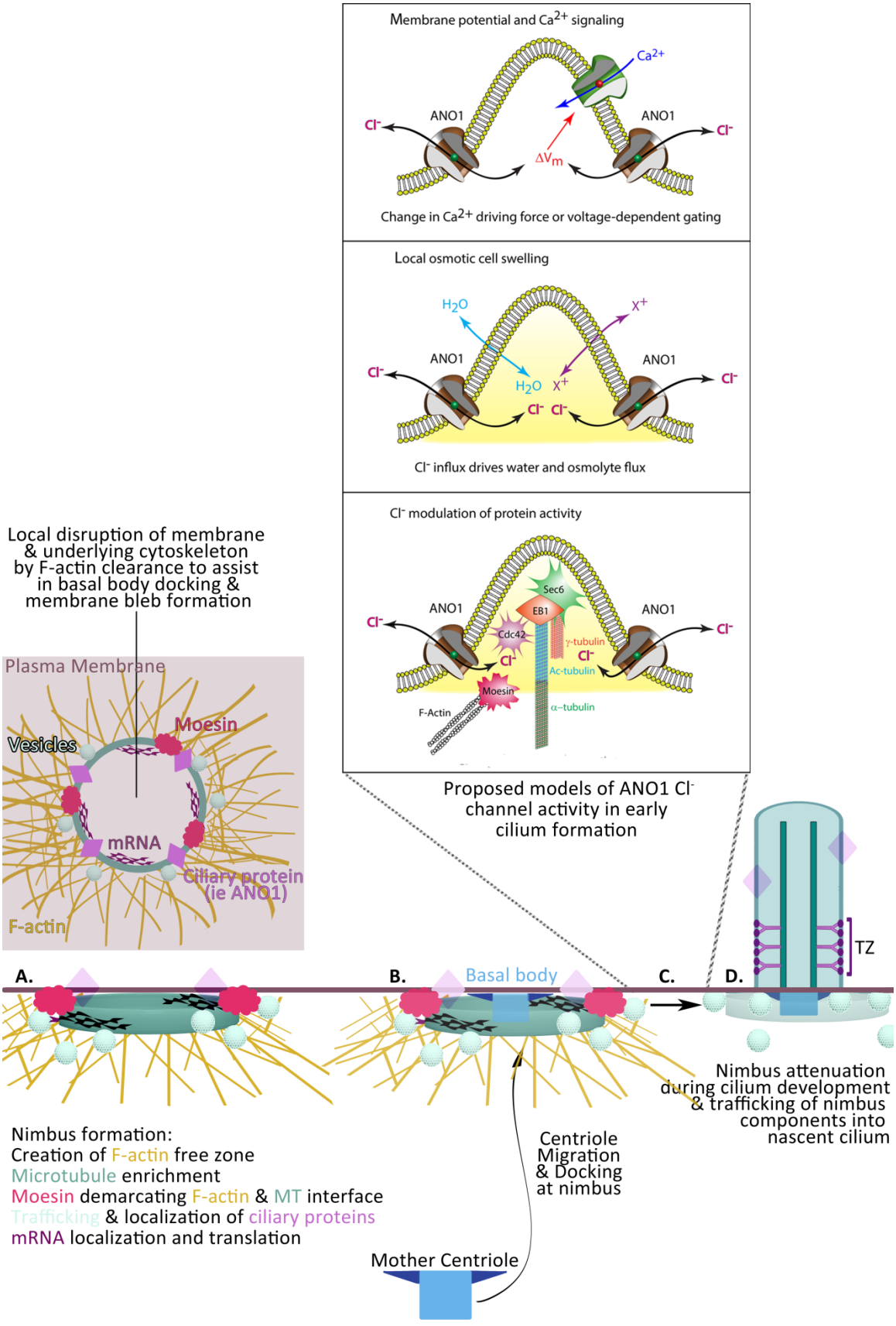
Membrane potential and Ca2+ signaling
Ca2+
ANO1
ANO1
Cl-
Cl-
ΔVm
Change in Ca2+ driving force or voltage-dependent gating
Local osmotic cell swelling
H2O
X+
ANO1
ANO1
Cl-
Cl-
H2O
X+
Cl- Cl-
Cl- influx drives water and osmolyte flux
Cl- modulation of protein activity
Sec6
EB1
ANO1
ANO1
Cl-
Cl-
Cdc42
γ-tubulin
Cl-
Cl-
Ac-tubulin
Moesin
F-Actin
α-tubulin
Proposed models of ANO1 Cl- channel activity in early cilium formation
Local disruption of membrane & underlying cytoskeleton by F-actin clearance to assist in basal body docking & membrane bleb formation
Plasma Membrane
Moesin
Vesicles
mRNA
Ciliary protein (ie ANO1)
F-actin
TZ
A.
B.
Basal body
C.
D.
Nimbus attenuation during cilium development & trafficking of nimbus components into nascent cilium
Nimbus formation:
Creation of F-actin free zone
Microtubule enrichment
Moesin demarcating F-actin & MT interface
Trafficking & localization of ciliary proteins
mRNA localization and translation
Centriole Migration & Docking at nimbus
Mother Centriole

Figure 4. Model of nimbus formation and ANO1 Cl^- channel activity in stages of primary cilium formation. Prior to cilium formation, most likely concomitant with centriole migration, the nimbus forms at the apical plasma membrane. Formation of the nimbus involves generating a zone free of F-actin (yellow lines) directly underneath the membrane (brown line) demarcated by the ERM protein moesin (hot pink shape) and enriched in microtubules (teal ring). Proteins destined for the primary cilium will be trafficked to the nimbus (cyan vesicles) where they will either be anchored to the plasma membrane or kept in vesicles directly underneath the membrane. The ciliary proteins I have identified at the nimbus include Arl13b, Cdc42, EB1, ANO1, and BBsome & exocyst complex components (purple triangles). mRNA enrichment (dark purple twisted lines) at the nimbus allows for the spatial segregation of protein synthesis that contributes to the generation of this specific membrane subdomain. **B.** The nimbus marks the site of basal body docking. After docking, I propose the ANO1 activity contributes to early cilium formation by three potential mechanisms (**C**). The generation of the F-actin free area directly underneath the membrane marked by the nimbus allows for separation of the membrane from the cytoskeleton which is conducive to membrane bleb formation. Cl^- flux in part mediated by ANO1 then generates enough osmotic force to bleb out the membrane, creating a small vestibule for initial transition zone (TZ) formation and axoneme extension. **D.** As the cilium extends nimbus-localized ciliary proteins, including ANO1, are trafficked into the cilium and the nimbus gradually dissipates.

Materials & Methods

Live-Cell Imaging. mpkCCD$_{14}$ cells were grown to confluence on glass coverslips then incubated with 2 μM SiR-tubulin probe in growth medium for one hour then washed before imaging. Silicon-rhodamine (SiR) tubulin is a cell permeable microtubule stain. Imaging was performed every twenty minutes for three hours using confocal microscopy (A1R, Nikon) using NIS-Elements software. Cells were maintained at 37°C and 5% CO_2 throughout the experiment. For these experiments the cells were maintained and samples generated by me. Paul Donlin-Asp performed the imaging.

Fluorescence *in situ* hybridization (FISH). mpkCCD$_{14}$ cells were fixed in 4% paraformaldehyde for 15 minutes at room temperature then rinsed in PBS containing 5mM $MgCl_2$, and equilibrated in 15% formamide, 1X SSC for 5 minutes before pre-incubation with hybridization buffer alone (10% dextran sulfate, 4 mg/ml bovine serum albumin, 2 X SSC, 20 mM ribonucleoside vanadyl complex, 10 mM sodium phosphate buffer) for 1.5 hours at 37°C then incubated in hybridization buffer in the presence of biotinylated oligonucleotide probe (10 ng per coverslip) for 3 hours at 37°C. After stringent washes with 15% formamide/1X SSC then 1X SSC alone, the biotinylated probe is then detected with Streptavidin-Cy3. FISH images were visualized using a 60X/1.4 Plan Apo (Nikon) objective on a Nikon Eclipse Ti inverted microscope and acquired using NIS-Elements software. FISH images were deconvolved using AutoQuant X2 (Media Cybernetics) and analyzed using the Imaris software (Bitplane). For these experiments samples were prepared by myself and Paul Donlin-Asp and imaged by Paul Donlin-Asp.

Puromycin Labeling. mpkCCD$_{14}$ cells were grown to confluence on glass coverslips then incubated with 50 μM. puromycin added to the cell culture media for 30 seconds. Puromycin is a structural analog of an amino-acyl tRNA molecule, enters ribosomes actively engaged in translation, and becomes covalently attached to the carboxy terminus of nascent proteins through a peptide bond. After 30 seconds, the samples are washed to remove any unincorporated puromycin then fixed and labeled for puromycin and ANO1 to visualize the nimbus.

Immunofluorescence. Immunofluorescence and imaging were performed as described in Chapter 2. Antibodies used include: ANO1 1:1000 (SDIX Custom rabbit polyclonal Genomic Antibody G3 directed against mAno1 amino acids 878-960 and G2 directed against amino acids 54-126 provided identical results), anti-acetylated tubulin mouse monoclonal 1:1000 (subtype IgG2b, Sigma-Aldrich; 6-11B-1), anti-Rab11 mouse monoclonal 1:50 (Abcam), anti-Sec8 mouse monoclonal 1:100 (Enzo), anti-BBS1 rabbit polyclonal 1:100 (Santa Cruz), anti-α-tubulin rat 1:1000 (Abcam), anti-PABPC1 rabbit monoclonal 1:100 (Abcam) and anti-PABN1 rabbit monoclonal 1:100 (Abcam).

CHAPTER 4

REFERENCES

Adams, G.M.W., B. Huang, and D.J.L. Luck. 1982. Temperature-sensitive, assembly-defective flagella mutants of Chlamydomonas reinhardtii. *Genetics*. 100:579-586.

Albertson, D.G. 2006. Gene amplification in cancer. *Trends in genetics : TIG*. 22:447-455.

Andersen, N.J., and C. Yeaman. 2010. Sec3-containing Exocyst Complex Is Required for Desmosome Assembly in Mammalian Epithelial Cells. *Molecular Biology of the Cell*. 21:152-164.

Anderson, R.G. 1972. The three-dimensional structure of the basal body from the rhesus monkey oviduct. *J Cell Biol*. 54:246-265.

Arreola, J., J.E. Melvin, and T. Begenisich. 1995. Inhibition of Ca 2+ -dependent Cl - channels from secretory epithelial cells by low internal pH. *Journal of Membrane Biology*. 147:95-104.

Atwood, S.X., C. Chabu, R.R. Penkert, C.Q. Doe, and K.E. Prehoda. 2007. Cdc42 acts downstream of Bazooka to regulate neuroblast polarity through Par-6–aPKC. *Journal of Cell Science*. 120:3200-3206.

Avasthi, P., and W.F. Marshall. 2012. Stages of ciliogenesis and regulation of ciliary length. *Differentiation*. 83:S30-42.

Awata, J., S. Takada, C. Standley, K.F. Lechtreck, K.D. Bellvé, G.J. Pazour, K.E. Fogarty, and G.B. Witman. 2014. NPHP4 controls ciliary trafficking of membrane proteins and large soluble proteins at the transition zone. *J Cell Sci*. 127:4714-4727.

Ayoub, C., C. Wasylyk, Y. Li, E. Thomas, L. Marisa, A. Robe, M. Roux, J. Abecassis, A. de Reynies, and B. Wasylyk. 2010. ANO1 amplification and expression in HNSCC with a high propensity for future distant metastasis and its functions in HNSCC cell lines. *Br J Cancer*. 103:715-726.

Bacallao, R., C. Antony, C. Dotti, E. Karsenti, E.H. Stelzer, and K. Simons. 1989. The subcellular organization of Madin-Darby canine kidney cells during the formation of a polarized epithelium. *J Cell Biol*. 109:2817-2832.

Badano, J.L., N. Mitsuma, P.L. Beales, and N. Katsanis. 2006a. The ciliopathies: an emerging class of human genetic disorders. *Annu. Rev. Genomics Hum. Genet.* 7:125-148.

Badano, J.L., N. Mitsuma, P.L. Beales, and N. Katsanis. 2006b. The ciliopathies: an emerging class of human genetic disorders. *Annual review of genomics and human genetics*. 7:125-148.

Bae, K.T., F. Zhu, A.B. Chapman, V.E. Torres, J.J. Grantham, L.M. Guay-Woodford, D.A. Baumgarten, B.F. King, Jr., L.H. Wetzel, P.J. Kenney, M.E. Brummer, W.M. Bennett, S. Klahr, C.M. Meyers, X. Zhang, P.A. Thompson, J.P. Miller, and D. Consortium for Radiologic Imaging Studies of Polycystic Kidney. 2006. Magnetic resonance imaging evaluation of hepatic cysts in early autosomal-dominant polycystic kidney disease: the Consortium for Radiologic Imaging Studies of Polycystic Kidney Disease cohort. *Clinical journal of the American Society of Nephrology : CJASN*. 1:64-69.

Barr, M.M., and P.W. Sternberg. 1999. A polycystic kidney-disease gene homologue required for male mating behaviour in C. elegans. *Nature*. 401:386-389.

Basu, B., and M. Brueckner. 2008. Chapter Six Cilia: Multifunctional Organelles at the Center of Vertebrate Left–Right Asymmetry. *In* Current topics in developmental biology. Vol. Volume 85. K.Y. Bradley, editor. Academic Press. 151-174.

Benmerah, A. 2013. The ciliary pocket. *Current opinion in cell biology*. 25:78-84.

Berbari, N.F., A.K. O'Connor, C.J. Haycraft, and B.K. Yoder. 2009. The primary cilium as a complex signaling center. *Curr Biol*. 19:R526-535.

Berend, K., L.H. van Hulsteijn, and R.O.B. Gans. 2012. Chloride: The queen of electrolytes? *European Journal of Internal Medicine*. 23:203-211.

Berglund, K., W. Schleich, P. Krieger, L.S. Loo, D. Wang, N.B. Cant, G. Feng, G.J. Augustine, and T. Kuner. 2008. Imaging synaptic inhibition in transgenic mice expressing the chloride indicator, Clomeleon. *Brain Cell Biol*. 35:207-228.

Bettencourt-Dias, M., and D.M. Glover. 2007. Centrosome biogenesis and function: centrosomics brings new understanding. *Nat Rev Mol Cell Biol*. 8:451-463.

Bettencourt-Dias, M., F. Hildebrandt, D. Pellman, G. Woods, and S.A. Godinho. 2011. Centrosomes and cilia in human disease. *Trends in Genetics*. 27:307-315.

Bilder, D., M. Li, and N. Perrimon. 2000. Cooperative regulation of cell polarity and growth by Drosophila tumor suppressors. *Science*. 289:113-116.

Bilder, D., M. Schober, and N. Perrimon. 2003. Integrated activity of PDZ protein complexes regulates epithelial polarity. *Nature cell biology*. 5:53-58.

Binder, L.I., W.L. Dentler, and J.L. Rosenbaum. 1975. Assembly of chick brain tubulin onto flagellar microtubules from Chlamydomonas and sea urchin sperm. *Proc. Natl Acad. Sci. USA*. 72:1122-1126.

Brailov, I., M. Bancila, M.J. Brisorgueil, M.C. Miquel, M. Hamon, and D. Verge. 2000. Localization of 5-HT(6) receptors at the plasma membrane of neuronal cilia in the rat brain. *Brain research*. 872:271-275.

Brill, S.R., K.E. Ross, C.J. Davidow, M. Ye, J.J. Grantham, and M.J. Caplan. 1996. Immunolocalization of ion transport proteins in human autosomal dominant polycystic kidney epithelial cells. *Proc Natl Acad Sci U S A*. 93:10206-10211.

Britschgi, A., A. Bill, H. Brinkhaus, C. Rothwell, I. Clay, S. Duss, M. Rebhan, P. Raman, C.T. Guy, K. Wetzel, E. George, M.O. Popa, S. Lilley, H. Choudhury, M. Gosling, L. Wang, S. Fitzgerald, J. Borawski, J. Baffoe, M. Labow, L.A. Gaither, and M. Bentires-Alj. 2013. Calcium-activated chloride channel ANO1 promotes breast cancer progression by activating EGFR and CAMK signaling. *Proc Natl Acad Sci U S A*. 110:E1026-1034.

Brookes, Z.L., L. Ruff, V.S. Upadhyay, L. Huang, S. Prasad, T. Solanky, S.M. Nauli, and A.C. Ong. 2013. Pkd2 mesenteric vessels exhibit a primary defect in endothelium-dependent vasodilatation restored by rosiglitazone. *American journal of physiology. Heart and circulatory physiology*. 304:H33-41.

Brown, J.M., and G.B. Witman. 2014. Cilia and Diseases. *Bioscience*. 64:1126-1137.

Brunner, J.D., N.K. Lim, S. Schenck, A. Duerst, and R. Dutzler. 2014. X-ray structure of a calcium-activated TMEM16 lipid scramblase. *Nature*. 516:207-212.

Buchholz, B., D. Faria, G. Schley, R. Schreiber, K.-U. Eckardt, and K. Kunzelmann. 2014. Anoctamin 1 induces calcium-activated chloride secretion and proliferation of renal cyst-forming epithelial cells. *Kidney Int*. 85:1058-1067.

Cantagrel, V., J.L. Silhavy, S.L. Bielas, D. Swistun, S.E. Marsh, J.Y. Bertrand, S. Audollent, T. Attie-Bitach, K.R. Holden, W.B. Dobyns, D. Traver, L. Al-Gazali, B.R. Ali, T.H. Lindner, T. Caspary, E.A. Otto, F. Hildebrandt, I.A. Glass, C.V. Logan, C.A. Johnson, C. Bennett, F. Brancati, G. International Joubert Syndrome Related Disorders Study, E.M. Valente, C.G. Woods, and J.G. Gleeson. 2008. Mutations in the cilia gene ARL13B lead to the classical form of Joubert syndrome. *Am J Hum Genet*. 83:170-179.

Caputo, A., E. Caci, L. Ferrera, N. Pedemonte, C. Barsanti, E. Sondo, U. Pfeffer, R. Ravazzolo, O. Zegarra-Moran, and L.J.V. Galietta. 2008a. TMEM16A, A Membrane Protein Associated with Calcium-Dependent Chloride Channel Activity. *Science*. 322:590-594.

Caputo, A., E. Caci, L. Ferrera, N. Pedemonte, C. Barsanti, E. Sondo, U. Pfeffer, R. Ravazzolo, O. Zegarra-Moran, and L.J.V. Galietta. 2008b. TMEM16A, A Membrane Protein Associated With Calcium-Dependent Chloride Channel Activity. *Science*. 322:590-594.

Cardenas-Rodriguez, M., and J.L. Badano. 2009. Ciliary biology: understanding the cellular and genetic basis of human ciliopathies. *American journal of medical genetics. Part C, Seminars in medical genetics*. 151C:263-280.

Carles, A., R. Millon, A. Cromer, G. Ganguli, F. Lemaire, J. Young, C. Wasylyk, D. Muller, I. Schultz, Y. Rabouel, D. Dembele, C. Zhao, P. Marchal, C. Ducray, L. Bracco, J. Abecassis, O. Poch, and B. Wasylyk. 2005. Head and neck squamous cell carcinoma transcriptome analysis by comprehensive validated differential display. *Oncogene*. 25:1821-1831.

Carpenter, A.E., T.R. Jones, M.R. Lamprecht, C. Clarke, I.H. Kang, O. Friman, D.A. Guertin, J.H. Chang, R.A. Lindquist, J. Moffat, P. Golland, and D.M. Sabatini. 2006. CellProfiler: image analysis software for identifying and quantifying cell phenotypes. *Genome biology*. 7:R100.

Caspary, T., C.E. Larkins, and K.V. Anderson. 2007. The graded response to Sonic Hedgehog depends on cilia architecture. *Developmental cell*. 12:767-778.

Chapin, H.C., and M.J. Caplan. 2010. The cell biology of polycystic kidney disease. *J Cell Biol*. 191:701-710.

Chassin, C., M. Bens, and A. Vandewalle. 2007. Transimmortalized proximal tubule and collecting duct cell lines derived from the kidneys of transgenic mice. *Cell biology and toxicology*. 23:257-266.

Chih, B., P. Liu, Y. Chinn, C. Chalouni, L.G. Komuves, P.E. Hass, W. Sandoval, and A.S. Peterson. 2012. A ciliopathy complex at the transition zone protects the cilia as a privileged membrane domain. *Nature cell biology*. 14:61-72.

Choi, S.Y., M.F. Chacon-Heszele, L. Huang, S. McKenna, F.P. Wilson, X. Zuo, and J.H. Lipschutz. 2013. Cdc42 Deficiency Causes Ciliary Abnormalities and Cystic Kidneys. *Journal of the American Society of Nephrology : JASN*. 24:1435-1450.

Christensen, S.T., L.B. Pedersen, L. Schneider, and P. Satir. 2007. Sensory cilia and integration of signal transduction in human health and disease. *Traffic*. 8:97-109.

Cole, D.G. 1998. Chlamydomonas kinesin-II-dependent intraflagellar transport (IFT): IFT particles contain proteins required for ciliary assembly in Caenorhabditis elegans sensory neurons. *J. Cell Biol.* 141:993-1008.

Conduit, S.E., J.M. Dyson, and C.A. Mitchell. 2012. Inositol polyphosphate 5-phosphatases; new players in the regulation of cilia and ciliopathies. *FEBS letters*. 586:2846-2857.

Corbit, K.C., P. Aanstad, V. Singla, A.R. Norman, D.Y. Stainier, and J.F. Reiter. 2005. Vertebrate Smoothened functions at the primary cilium. *Nature*. 437:1018-1021.

Craige, B., C.-C. Tsao, D.R. Diener, Y. Hou, K.-F. Lechtreck, J.L. Rosenbaum, and G.B. Witman. 2010. CEP290 tethers flagellar transition zone microtubules to the membrane and regulates flagellar protein content. *J Cell Biol*. 190:927-940.

Damerla, R.R., C. Cui, G.C. Gabriel, X. Liu, B. Craige, B.C. Gibbs, R. Francis, Y. Li, B. Chatterjee, J.T. San Agustin, T. Eguether, R. Subramanian, G.B. Witman, J.L. Michaud, G.J. Pazour, and C.W. Lo. 2015. Novel Jbts17 mutant mouse model of Joubert syndrome with cilia transition zone defects and cerebellar and other ciliopathy related anomalies. *Hum Mol Genet*. 24:3994-4005.

Das, A., and W. Guo. 2011. Rabs and the exocyst in ciliogenesis, tubulogenesis and beyond. *Trends Cell Biol*. 21:383-386.

Davidow, C.J., R.L. Maser, L.A. Rome, J.P. Calvet, and J.J. Grantham. 1996. The cystic fibrosis transmembrane conductance regulator mediates transepithelial fluid secretion by human autosomal dominant polycystic kidney disease epithelium in vitro. *Kidney Int*. 50:208-218.

Davis, E.E., and N. Katsanis. 2012. The ciliopathies: a transitional model into systems biology of human genetic disease. *Current opinion in genetics & development*. 22:290-303.

de Curtis, I., and J. Meldolesi. 2012. Cell surface dynamics - how Rho GTPases orchestrate the interplay between the plasma membrane and the cortical cytoskeleton. *J Cell Sci*. 125:4435-4444.

Deane, J.A., D.G. Cole, E.S. Seeley, D.R. Diener, and J.L. Rosenbaum. 2001. Localization of intraflagellar transport protein IFT52 identifies basal body transitional fibers as the docking site for IFT particles. *Curr. Biol.* 11:1586-1590.

DeCaen, P.G., M. Delling, T.N. Vien, and D.E. Clapham. 2013. Direct recording and molecular identification of the calcium channel of primary cilia. *Nature*. 504:315-318.

Delling, M., P.G. DeCaen, J.F. Doerner, S. Febvay, and D.E. Clapham. 2013. Primary cilia are specialized calcium signalling organelles. *Nature*. 504:311-314.

Dishinger, J.F., H.L. Kee, P.M. Jenkins, S. Fan, T.W. Hurd, J.W. Hammond, Y.N. Truong, B. Margolis, J.R. Martens, and K.J. Verhey. 2010. Ciliary entry of the kinesin-2 motor KIF17 is regulated by importin-beta2 and RanGTP. *Nature cell biology*. 12:703-710.

Drummond, I.A. 2012. Cilia functions in development. *Current opinion in cell biology*. 24:24-30.

Duan, D. 2009. Phenomics of cardiac chloride channels: the systematic study of chloride channel function in the heart. *J Physiol*. 587:2163-2177.

Duebel, J., S. Haverkamp, W. Schleich, G. Feng, G.J. Augustine, T. Kuner, and T. Euler. 2006. Two-photon imaging reveals somatodendritic chloride gradient in retinal ON-type bipolar cells expressing the biosensor Clomeleon. *Neuron*. 49:81-94.

Duran, C., and H.C. Hartzell. 2011a. Physiological roles and diseases of TMEM16/anoctamin proteins: are they all chloride channels? *Acta Pharmacol Sin*. 32:685-692.

Duran, C., and H.C. Hartzell. 2011b. Physiological roles and diseases of tmem16/anoctamin proteins: are they all chloride channels? *Acta Pharmacol Sin*. 32:685-692.

Duran, C., C.H. Thompson, Q. Xiao, and H.C. Hartzell. 2010a. Chloride channels: often enigmatic, rarely predictable. *Annu Rev Physiol*. 72:95-121.

Duran, C., C.H. Thompson, Q. Xiao, and H.C. Hartzell. 2010b. Chloride Channels: Often Enigmatic, Rarely Predictable. *Annual Review of Physiology*. 72:95-121.

Duvvuri, U., D.J. Shiwarski, D. Xiao, C. Bertrand, X. Huang, R.S. Edinger, J.R. Rock, B.D. Harfe, B.J. Henson, K. Kunzelmann, R. Schreiber, R.S. Seethala, A.M. Egloff, X. Chen, V.W. Lui, J.R. Grandis, and S.M. Gollin. 2012a. TMEM16A induces MAPK and contributes directly to tumorigenesis and cancer progression. *Cancer Res*. 72:3270-3281.

Duvvuri, U., D.J. Shiwarski, D. Xiao, C. Bertrand, X. Huang, R.S. Edinger, J.R. Rock, B.D. Harfe, B.J. Henson, K. Kunzelmann, R. Schreiber, R.S. Seethala, A.M. Egloff, X. Chen, V.W. Lui, J.R. Grandis, and S.M. Gollin. 2012b. TMEM16A Induces MAPK and Contributes Directly to Tumorigenesis and Cancer Progression. *Cancer Research*. 72:3270-3281.

Edwards, K.A., M. Demsky, R.A. Montague, N. Weymouth, and D.P. Kiehart. 1997. GFP-moesin illuminates actin cytoskeleton dynamics in living tissue and

demonstrates cell shape changes during morphogenesis in Drosophila. *Dev Biol*. 191:103-117.

Emmer, B.T., D. Maric, and D.M. Engman. 2010. Molecular mechanisms of protein and lipid targeting to ciliary membranes. *Journal of Cell Science*. 123:529-536.

Endoh-Yamagami, S. 2009. The mammalian Cos2 homolog Kif7 plays an essential role in modulating Hh signal transduction during development. *Curr. Biol*. 19:1320-1326.

Espinosa, I., C.H. Lee, M.K. Kim, B.T. Rouse, S. Subramanian, K. Montgomery, S. Varma, C.L. Corless, M.C. Heinrich, K.S. Smith, Z. Wang, B. Rubin, T.O. Nielsen, R.S. Seitz, D.T. Ross, R.B. West, M.L. Cleary, and R.M. van de. 2008. A novel monoclonal antibody against DOG1 is a sensitive and specific marker for gastrointestinal stromal tumors. *Am.J Surg.Pathol*. 32:210-218.

Etienne-Manneville, S., and A. Hall. 2002. Rho GTPases in cell biology. *Nature*. 420:629-635.

Fan, S., E.L. Whiteman, T.W. Hurd, J.C. McIntyre, J.F. Dishinger, C.J. Liu, J.R. Martens, K.J. Verhey, U. Sajjan, and B. Margolis. 2011. Induction of Ran GTP drives ciliogenesis. *Mol Biol Cell*. 22:4539-4548.

Faundez, V., and H.C. Hartzell. 2004a. Intracellular Chloride Channels: Determinants of Function in the Endosomal Pathway. *Science's Stke [Electronic Resource]: Signal Transduction Knowledge Environment*. 2004:re8.

Faundez, V., and H.C. Hartzell. 2004b. Intracellular chloride channels: determinants of function in the endosomal pathway. *Science's STKE : signal transduction knowledge environment*. 2004:re8.

Fehon, R.G., A.I. McClatchey, and A. Bretscher. 2010. Organizing the cell cortex: the role of ERM proteins. *Nat Rev Mol Cell Biol*. 11:276-287.

Ferrera, L., A. Caputo, and L.J. Galietta. 2010. TMEM16A protein: a new identity for Ca^{2+}-dependent Cl channels. *Physiology (Bethesda)*. 25:357-363.

Fievet, B.T., A. Gautreau, C. Roy, L. Del Maestro, P. Mangeat, D. Louvard, and M. Arpin. 2004. Phosphoinositide binding and phosphorylation act sequentially in the activation mechanism of ezrin. *The Journal of Cell Biology*. 164:653-659.

Fliegauf, M., T. Benzing, and H. Omran. 2007. When cilia go bad: cilia defects and ciliopathies. *Nat Rev Mol Cell Biol*. 8:880-893.

Francis, S.S., J. Sfakianos, B. Lo, and I. Mellman. 2011. A hierarchy of signals regulates entry of membrane proteins into the ciliary membrane domain in epithelial cells. *J Cell Biol*. 193:219-233.

Garcia-Gonzalo, F.R., and J.F. Reiter. 2012. Scoring a backstage pass: Mechanisms of ciliogenesis and ciliary access. *The Journal of Cell Biology*. 197:697-709.

Gary, R., and A. Bretscher. 1995. Ezrin self-association involves binding of an N-terminal domain to a normally masked C-terminal domain that includes the F-actin binding site. *Molecular Biology of the Cell*. 6:1061-1075.

Gautreau, A., D. Louvard, and M. Arpin. 2000. Morphogenic Effects of Ezrin Require a Phosphorylation-Induced Transition from Oligomers to Monomers at the Plasma Membrane. *The Journal of Cell Biology*. 150:193-204.

Gerdes, J., E.E. Davis, and N. Katsanis. 2009a. The vertebrate primary cilium in development, homeostasis, and disease. *Cell*. 137:32-45.

Gerdes, J.M., E.E. Davis, and N. Katsanis. 2009b. The Vertebrate Primary Cilium in Development, Homeostasis, and Disease. *Cell*. 137:32-45.

Gilula, N.B., and P. Satir. 1972. The ciliary necklace. A ciliary membrane specialization. *J Cell Biol*. 53:494-509.

Goetz, S.C., and K.V. Anderson. 2010. The primary cilium: a signalling centre during vertebrate development. *Nat Rev Genet*. 11:331-344.

Gouveia, S.M., and A. Akhmanova. 2010. Cell and molecular biology of microtubule plus end tracking proteins: end binding proteins and their partners. *International review of cell and molecular biology*. 285:1-74.

Grantham, J.J., V.E. Torres, A.B. Chapman, L.M. Guay-Woodford, K.T. Bae, B.F. King, Jr., L.H. Wetzel, D.A. Baumgarten, P.J. Kenney, P.C. Harris, S. Klahr, W.M. Bennett, G.N. Hirschman, C.M. Meyers, X. Zhang, F. Zhu, J.P. Miller, and C. Investigators. 2006. Volume progression in polycystic kidney disease. *The New England journal of medicine*. 354:2122-2130.

Grantham, J.J., M. Ye, V.H. Gattone, 2nd, and L.P. Sullivan. 1995. In vitro fluid secretion by epithelium from polycystic kidneys. *J Clin Invest*. 95:195-202.

Han, Y.-G., and A. Alvarez-Buylla. 2010. Role of primary cilia in brain development and cancer. *Current Opinion in Neurobiology*. 20:58-67.

Hanaoka, K., O. Devuyst, E.M. Schwiebert, P.D. Wilson, and W.B. Guggino. 1996. A role for CFTR in human autosomal dominant polycystic kidney disease. *Am J Physiol*. 270:C389-399.

Hanaoka, K., F. Qian, A. Boletta, A.K. Bhunia, K. Piontek, L. Tsiokas, V.P. Sukhatme, W.B. Guggino, and G.G. Germino. 2000. Co-assembly of polycystin-1 and -2 produces unique cation-permeable currents. *Nature*. 408:990-994.

Handel, M. 1999. Selective targeting of somatostatin receptor 3 to neuronal cilia. *Neuroscience*. 89:909-926.

Harris, P.C., and V.E. Torres. 2009. Polycystic kidney disease. *Annu. Rev. Med.* 60:321-337.

Harris, P.C., C.J. Ward, B. Peral, and J. Hughes. 1995a. Autosomal dominant polycystic kidney disease: molecular analysis. *Hum Mol Genet*. 4 Spec No:1745-1749.

Harris, P.C., C.J. Ward, B. Peral, and J. Hughes. 1995b. Polycystic kidney disease. 1: Identification and analysis of the primary defect. *Journal of the American Society of Nephrology : JASN*. 6:1125-1133.

Hartzell, C., I. Putzier, and J. Arreola. 2005a. Calcium-activated chloride channels. *Annu.Rev.Physiol*. 67:719-758.

Hartzell, C., I. Putzier, and J. Arreola. 2005b. CALCIUM-ACTIVATED CHLORIDE CHANNELS. *Annual Review of Physiology*. 67:719-758.

Hartzell, H.C. 2009. Chloride channels: an historical perspective. . *In* Physiology and Pathology of Chloride Transporters and Channels In the Nervous System: From Molecules to Diseases. F.J.D. Alvarez-Leefmans, E., editor. Academic Press, San Diego. 3-16.

Hartzell, H.C., and C.C. Ruppersburg. 2013. Functional reconstitution of a chloride channel bares its soul. *Proc Natl Acad Sci U S A*. 110:19185-19186.

Hartzell, H.C., K. Yu, Q. Xiao, L.T. Chien, and Z. Qu. 2009a. Anoctamin / TMEM16 family members are Ca2+-activated Cl- channels. *J Physiol Online*. 587:2127-2139.

Hartzell, H.C., K. Yu, Q. Xiao, L.T. Chien, and Z. Qu. 2009b. Anoctamin / TMEM16 family members are Ca^{2+}-activated Cl^- channels. *The Journal of Physiology*. 587.10:2127-2139.

Harville, H.M., S. Held, A. Diaz-Font, E.E. Davis, B.H. Diplas, R.A. Lewis, Z.U. Borochowitz, W. Zhou, M. Chaki, J. MacDonald, H. Kayserili, P.L. Beales, N. Katsanis, E. Otto, and F. Hildebrandt. 2010. Identification of 11 novel mutations in eight BBS genes by high-resolution homozygosity mapping. *Journal of medical genetics*. 47:262-267.

Hattula, K., J. Furuhjelm, A. Arffman, and J. Peranen. 2002. A Rab8-specific GDP/GTP exchange factor is involved in actin remodeling and polarized membrane transport. *Mol Biol Cell*. 13:3268-3280.

Haycraft, C. 2005. Gli2 and Gli3 localize to cilia and require the intraflagellar transport protein polaris for processing and function. *PLoS Genet*. 1:e53.

He, Q., G. Wang, S. Dasgupta, M. Dinkins, G. Zhu, and E. Bieberich. 2012a. Characterization of an apical ceramide-enriched compartment regulating ciliogenesis. *Mol Biol Cell*. 23:3156-3166.

He, Q., G. Wang, S. Dasgupta, M. Dinkins, G. Zhu, and E. Bieberich. 2012b. Characterization of an apical ceramide-enriched compartment regulating ciliogenesis. *Molecular Biology of the Cell*. 23:3156-3166.

Hehnly, H., C.T. Chen, C.M. Powers, H.L. Liu, and S. Doxsey. 2012. The centrosome regulates the Rab11- dependent recycling endosome pathway at appendages of the mother centriole. *Current biology : CB*. 22:1944-1950.

Hengl, T., H. Kaneko, K. Dauner, K. Vocke, S. Frings, and F. Mohrlen. 2010. Molecular components of signal amplification in olfactory sensory cilia. *Proc Natl Acad Sci U S A*. 107:6052-6057.

Hildebrandt, F., T. Benzing, and N. Katsanis. 2011. Ciliopathies. *The New England journal of medicine*. 364:1533-1543.

Hilton, L.K., K. Gunawardane, J.W. Kim, M.C. Schwarz, and L.M. Quarmby. 2013. The kinases LF4 and CNK2 control ciliary length by feedback regulation of assembly and disassembly rates. *Current biology : CB*. 23:2208-2214.

Hoffmann, E.K., I.H. Lambert, and S.F. Pedersen. 2009. Physiology of cell volume regulation in vertebrates. *Physiol Rev*. 89:193-277.

Horst, C.J., D.M. Forestner, and J.C. Besharse. 1987. Cytoskeletal-membrane interactions: a stable interaction between cell surface glycoconjugates and doublet microtubules of the photoreceptor connecting cilium. *J Cell Biol*. 105:2973-2987.

Hu, Q., L. Milenkovic, H. Jin, M.P. Scott, M.V. Nachury, E.T. Spiliotis, and W.J. Nelson. 2010. A septin diffusion barrier at the base of the primary cilium maintains ciliary membrane protein distribution. *Science*. 329:436-439.

Huang, B., M.R. Rifkin, and D.J. Luck. 1977. Temperature-sensitive mutations affecting flagellar assembly and function in Chlamydomonas reinhardtii. *J. Cell Biol.* 72:67-85.

Huang, F., J.R. Rock, B.D. Harfe, T. Cheng, X. Huang, Y.N. Jan, and L.Y. Jan. 2009. Studies on expression and function of the TMEM16A calcium-activated chloride channel. *Proceedings of the National Academy of Sciences*. 106:21413-21418.

Huang, F., X. Wong, and L.Y. Jan. 2012a. International Union of Basic and Clinical Pharmacology. LXXXV: calcium-activated chloride channels. *Pharmacol Rev*. 64:1-15.

Huang, F., H. Zhang, M. Wu, H. Yang, M. Kudo, C.J. Peters, P.G. Woodruff, O.D. Solberg, M.L. Donne, X. Huang, D. Sheppard, J.V. Fahy, P.J. Wolters, B.L. Hogan, W.E. Finkbeiner, M. Li, Y.N. Jan, L.Y. Jan, and J.R. Rock. 2012b. Calcium-activated chloride channel TMEM16A modulates mucin secretion and airway smooth muscle contraction. *Proc Natl Acad Sci U S A*. 109:16354-16359.

Huang, X., T.E. Godfrey, W.E. Gooding, K.S. McCarty, and S.M. Gollin. 2006. Comprehensive genome and transcriptome analysis of the 11q13 amplicon in human oral cancer and synteny to the 7F5 amplicon in murine oral carcinoma. *Genes, Chromosomes and Cancer*. 45:1058-1069.

Huangfu, D., and K.V. Anderson. 2005. Cilia and Hedgehog responsiveness in the mouse. *Proceedings of the National Academy of Sciences of the United States of America*. 102:11325-11330.

Huangfu, D., A. Liu, A.S. Rakeman, N.S. Murcia, L. Niswander, and K.V. Anderson. 2003. Hedgehog signalling in the mouse requires intraflagellar transport proteins. *Nature*. 426:83-87.

Hughes, J., C.J. Ward, B. Peral, R. Aspinwall, K. Clark, J.L. San Millan, V. Gamble, and P.C. Harris. 1995. The polycystic kidney disease 1 (PKD1) gene encodes a novel protein with multiple cell recognition domains. *Nat Genet*. 10:151-160.

Hurd, T.W., S. Fan, and B.L. Margolis. 2011. Localization of retinitis pigmentosa 2 to cilia is regulated by Importin beta2. *J Cell Sci*. 124:718-726.

Hwang, D.G., X. Qian, and J.L. Hornick. 2011. DOG1 Antibody Is a Highly Sensitive and Specific Marker for Gastrointestinal Stromal Tumors in Cytology Cell Blocks. *Am J Clin Pathol*. 135:448-453.

Ishikawa, H., and W.F. Marshall. 2011. Ciliogenesis: building the cell's antenna. *Nat Rev Mol Cell Biol*. 12:222-234.

Jansen, R.-P. 2001. mRNA localization: message on the move. *Nat Rev Mol Cell Biol*. 2:247-256.

Jiang, K., G. Toedt, S. Montenegro Gouveia, Norman E. Davey, S. Hua, B. van der Vaart, I. Grigoriev, J. Larsen, Lotte B. Pedersen, K. Bezstarosti, M. Lince-Faria, J. Demmers, Michel O. Steinmetz, Toby J. Gibson, and A. Akhmanova. 2012. A Proteome-wide Screen for Mammalian SxIP Motif-Containing Microtubule Plus-End Tracking Proteins. *Current biology : CB*. 22:1800-1807.

Joberty, G., C. Petersen, L. Gao, and I.G. Macara. 2000. The cell-polarity protein Par6 links Par3 and atypical protein kinase C to Cdc42. *Nature cell biology*. 2:531-539.

Johnson, K.A., and J.L. Rosenbaum. 1992. Polarity of flagellar assembly in Chlamydomonas. *J. Cell Biol.* 119:1605-1611.

Joo, K., C.G. Kim, M.-S. Lee, H.-Y. Moon, S.-H. Lee, M.J. Kim, H.-S. Kweon, W.-Y. Park, C.-H. Kim, J.G. Gleeson, and J. Kim. 2013. CCDC41 is required for ciliary vesicle docking to the mother centriole. *Proceedings of the National Academy of Sciences*. 110:5987-5992.

Kamentsky, L., T.R. Jones, A. Fraser, M.A. Bray, D.J. Logan, K.L. Madden, V. Ljosa, C. Rueden, K.W. Eliceiri, and A.E. Carpenter. 2011. Improved structure, function and compatibility for CellProfiler: modular high-throughput image analysis software. *Bioinformatics*. 27:1179-1180.

Katoh, M. 2003. FLJ10261 gene, located within the CCND1-EMS1 locus on human chromosome 11q13, encodes the eight-transmembrane protein homologous to C12orf3, C11orf25 and FLJ34272 gene products. *Int.J Oncol*. 22:1375-1381.

Katoh, M. 2005. Identification and characterization of TMEM16H gene in silico. *Int.J Mol.Med*. 15:353-358.

Katsanis, N., J.R. Lupski, and P.L. Beales. 2001. Exploring the molecular basis of Bardet-Biedl syndrome. *Hum Mol Genet*. 10:2293-2299.

Kemphues, K.J., J.R. Priess, D.G. Morton, and N.S. Cheng. 1988. Identification of genes required for cytoplasmic localization in early C. elegans embryos. *Cell*. 52:311-320.

Kim, J., J.E. Lee, S. Heynen-Genel, E. Suyama, K. Ono, K. Lee, T. Ideker, P. Aza-Blanc, and J.G. Gleeson. 2010. Functional genomic screen for modulators of ciliogenesis and cilium length. *Nature*. 464:1048-1051.

Kim, S., and B.D. Dynlacht. 2013. Assembling a primary cilium. *Current opinion in cell biology*. 25:506-511.

Knodler, A., S. Feng, J. Zhang, X. Zhang, A. Das, J. Peranen, and W. Guo. 2010. Coordination of Rab8 and Rab11 in primary ciliogenesis. *Proc Natl Acad Sci U S A*. 107:6346-6351.

Kobayashi, T., and B.D. Dynlacht. 2011. Regulating the transition from centriole to basal body. *J Cell Biol*. 193:435-444.

Kolb, R.J., P.G. Woost, and U. Hopfer. 2004. Membrane trafficking of angiotensin receptor type-1 and mechanochemical signal transduction in proximal tubule cells. *Hypertension*. 44:352-359.

Kottgen, M. 2007. TRPP2 and autosomal dominant polycystic kidney disease. *Biochimica et biophysica acta*. 1772:836-850.

Kottgen, M., B. Buchholz, M.A. Garcia-Gonzalez, F. Kotsis, X. Fu, M. Doerken, C. Boehlke, D. Steffl, R. Tauber, T. Wegierski, R. Nitschke, M. Suzuki, A. Kramer-Zucker, G.G. Germino, T. Watnick, J. Prenen, B. Nilius, E.W. Kuehn, and G. Walz. 2008. TRPP2 and TRPV4 form a polymodal sensory channel complex. *J Cell Biol*. 182:437-447.

Kozminski, K.G., P.L. Beech, and J.L. Rosenbaum. 1995. The Chlamydomonas kinesin-like protein FLA10 is involved in motility associated with the flagellar membrane. *J Cell Biol*. 131:1517-1527.

Kozminski, K.G., K.A. Johnson, P. Forscher, and J.L. Rosenbaum. 1993. A motility in the eukaryotic flagellum unrelated to flagellar beating. *Proc Natl Acad Sci U S A*. 90:5519-5523.

Kuner, T., and G.J. Augustine. 2000. A genetically encoded ratiometric indicator for chloride: capturing chloride transients in cultured hippocampal neurons. *Neuron*. 27:447-459.

Kunzelmann, K., Y. Tian, J. Martins, D. Faria, P. Kongsuphol, J. Ousingsawat, F. Thevenod, E. Roussa, J. Rock, and R. Schreiber. 2011a. Anoctamins. *Pflügers Archiv European Journal of Physiology*. 462:195-208.

Kunzelmann, K., Y. Tian, J.R. Martins, D. Faria, P. Kongsuphol, J. Ousingsawat, F. Thevenod, E. Roussa, J. Rock, and R. Schreiber. 2011b. Anoctamins. *Pflugers Arch*. 462:195-208.

Kuo, I.Y., T.M. DesRochers, E.P. Kimmerling, L. Nguyen, B.E. Ehrlich, and D.L. Kaplan. 2014. Cyst formation following disruption of intracellular calcium signaling. *Proc Natl Acad Sci U S A*. 111:14283-14288.

Lancaster, M.A., and J.G. Gleeson. 2009. The primary cilium as a cellular signaling center: lessons from disease. *Curr. Opin. Genet. Dev*. 19:220-229.

Larkins, C.E., G.D. Aviles, M.P. East, R.A. Kahn, and T. Caspary. 2011. Arl13b regulates ciliogenesis and the dynamic localization of Shh signaling proteins. *Mol Biol Cell*. 22:4694-4703.

Le Gall, A.H., C. Yeaman, A. Muesch, and E. Rodriguez-Boulan. 1995. Epithelial cell polarity: new perspectives. *Seminars in nephrology*. 15:272-284.

Liem, K.F., M. He, P.J. Ocbina, and K.V. Anderson. 2009. Mouse Kif7/Costal2 is a cilia-associated protein that regulates Sonic hedgehog signaling. *Proc. Natl Acad. Sci. USA*. 106:13377-13382.

Liu, A., B. Wang, and L.A. Niswander. 2005. Mouse intraflagellar transport proteins regulate both the activator and repressor functions of Gli transcription factors. *Development*. 132:3103-3111.

Liu, B., J.E. Linley, X. Du, X. Zhang, L. Ooi, and H. Zhang. 2010. The acute nociceptive signals induced by bradykinin in rat sensory neurons are mediated by inhibition of M-type K+ channels and activation of Ca2+-activated Cl- channels. *J Clin Invest*. 120:1240-1252.

Lo Nostro, P., and B.W. Ninham. 2012. Hofmeister phenomena: an update on ion specificity in biology. *Chemical reviews*. 112:2286-2322.

Lu, Q., C. Insinna, C. Ott, J. Stauffer, P.A. Pintado, J. Rahajeng, U. Baxa, V. Walia, A. Cuenca, Y.-S. Hwang, I.O. Daar, S. Lopes, J. Lippincott-Schwartz, P.K. Jackson, S. Caplan, and C.J. Westlake. 2015. Early steps in primary cilium assembly require EHD1/EHD3-dependent ciliary vesicle formation. *Nature cell biology*. 17:228-240.

Lukinavicius, G., L. Reymond, E. D'Este, A. Masharina, F. Gottfert, H. Ta, A. Guther, M. Fournier, S. Rizzo, H. Waldmann, C. Blaukopf, C. Sommer, D.W. Gerlich, H.-D. Arndt, S.W. Hell, and K. Johnsson. 2014. Fluorogenic probes for live-cell imaging of the cytoskeleton. *Nat Meth*. 11:731-733.

Malvezzi, M., M. Chalat, R. Janjusevic, A. Picollo, H. Terashima, A.K. Menon, and A. Accardi. 2013. Ca^{2+}-dependent phospholipid scrambling by a reconstituted TMEM16 ion channel. *Nat. Commun*. 4:2367.

Mangoo-Karim, R., M. Ye, D.P. Wallace, J.J. Grantham, and L.P. Sullivan. 1995. Anion secretion drives fluid secretion by monolayers of cultured human polycystic cells. *Am J Physiol*. 269:F381-388.

Maric, D., C.L. Epting, and D.M. Engman. 2010. Composition and sensory function of the trypanosome flagellar membrane. *Current opinion in microbiology*. 13:466-472.

Marshall, W.F., and S. Nonaka. Cilia: Tuning in to the Cell's Antenna. *Current Biology*. 16:R604-R614.

Martín-Belmonte, F., W. Yu, A.E. Rodríguez-Fraticelli, A. Ewald, Z. Werb, M.A. Alonso, and K. Mostov. 2008. Cell-Polarity Dynamics Controls the Mechanism of Lumen Formation in Epithelial Morphogenesis. *Current Biology*. 18:507-513.

Martin, K.C., and A. Ephrussi. 2009. mRNA Localization: Gene Expression in the Spatial Dimension. *Cell*. 136:719-730.

Matter, K., and M.S. Balda. 2003. Signalling to and from tight junctions. *Nat Rev Mol Cell Biol*. 4:225-237.

May, S.R. 2005. Loss of the retrograde motor for IFT disrupts localization of Smo to cilia and prevents the expression of both activator and repressor functions of Gli. *Dev. Biol*. 287:378-389.

Mazzone, A., S.T. Eisenman, P.R. Strege, Z. Yao, T. Ordog, S.J. Gibbons, and G. Farrugia. 2012. Inhibition of cell proliferation by a selective inhibitor of the Ca(2+)-activated Cl(-) channel, Ano1. *Biochem Biophys Res Commun*. 427:248-253.

McCaffrey, L.M., and I.G. Macara. 2011. Epithelial organization, cell polarity and tumorigenesis. *Trends in Cell Biology*. 21:727-735.

McCartney, B.M., and R.G. Fehon. 1996. Distinct cellular and subcellular patterns of expression imply distinct functions for the Drosophila homologues of moesin and the neurofibromatosis 2 tumor suppressor, merlin. *J Cell Biol*. 133:843-852.

McGrath, J., S. Somlo, S. Makova, X. Tian, and M. Brueckner. 2003. Two populations of node monocilia initiate left-right asymmetry in the mouse. *Cell*. 114:61-73.

Meder, D., A. Shevchenko, K. Simons, and J. Füllekrug. 2005. Gp135/podocalyxin and NHERF-2 participate in the formation of a preapical domain during polarization of MDCK cells. *The Journal of Cell Biology*. 168:303-313.

Miettinen, M., Z.F. Wang, and J. Lasota. 2009. DOG1 antibody in the differential diagnosis of gastrointestinal stromal tumors: a study of 1840 cases. *Am J Surg Pathol*. 33:1401-1408.

Mochizuki, T., G. Wu, T. Hayashi, S.L. Xenophontos, B. Veldhuisen, J.J. Saris, D.M. Reynolds, Y. Cai, P.A. Gabow, A. Pierides, W.J. Kimberling, M.H. Breuning, C.C. Deltas, D.J. Peters, and S. Somlo. 1996. PKD2, a gene for polycystic kidney disease that encodes an integral membrane protein. *Science*. 272:1339-1342.

Moffitt, J.R., Y.R. Chemla, and C. Bustamante. 2010. Methods in statistical kinetics. *Methods in enzymology*. 475:221-257.

Mostov, K.E. 2003. Epithelial polarity and morphogenesis. *Methods*. 30:189-190.

Moyer, J.H. 1994. Candidate gene associated with a mutation causing recessive polycystic kidney disease in mice. *Science*. 264:1329-1333.

Muanprasat, C., N.D. Sonawane, D. Salinas, A. Taddei, L.J. Galietta, and A.S. Verkman. 2004. Discovery of Glycine Hydrazide Pore-occluding CFTR Inhibitors: Mechanism, Structure-Activity Analysis, and In Vivo Efficacy. *Journal of General Physiology*. 124:125-137.

Nachury, M. 2007. A core complex of BBS proteins cooperates with the GTPase Rab8 to promote ciliary membrane biogenesis. *Cell*. 129:1201-1213.

Nachury, M.V. 2014. How do cilia organize signalling cascades?

Nachury, M.V., A.V. Loktev, Q. Zhang, C.J. Westlake, J. Peranen, A. Merdes, D.C. Slusarski, R.H. Scheller, J.F. Bazan, V.C. Sheffield, and P.K. Jackson. 2007. A core complex of BBS proteins cooperates with the GTPase Rab8 to promote ciliary membrane biogenesis. *Cell*. 129:1201-1213.

Nachury, M.V., E.S. Seeley, and H. Jin. 2010. Trafficking to the ciliary membrane: how to get across the periciliary diffusion barrier? *Annual review of cell and developmental biology*. 26:59-87.

Nakajima, K.-i., N. Niisato, and Y. Marunaka. 2012. Enhancement of tubulin polymerization by Cl−-induced blockade of intrinsic GTPase. *Biochem Biophys Res Commun*. 425:225-229.

Nakajima, T., T. Sugimoto, and Y. Kurachi. 1992. Effects of anions on the G protein-mediated activation of the muscarinic K+ channel in the cardiac atrial cell membrane. Intracellular chloride inhibition of the GTPase activity of GK. *Journal of General Physiology*. 99:665-682.

Nakamura, F., M.R. Amieva, and H. Furthmayr. 1995. Phosphorylation of Threonine 558 in the Carboxyl-terminal Actin-binding Domain of Moesin by Thrombin

Activation of Human Platelets. *Journal of Biological Chemistry*. 270:31377-31385.

Namkung, W., Z. Yao, W.E. Finkbeiner, and A.S. Verkman. 2011. Small-molecule activators of TMEM16A, a calcium-activated chloride channel, stimulate epithelial chloride secretion and intestinal contraction. *FASEB J*. 25:4048-4062.

Nauli, S.M., F.J. Alenghat, Y. Luo, E. Williams, P. Vassilev, X. Li, A.E. Elia, W. Lu, E.M. Brown, S.J. Quinn, D.E. Ingber, and J. Zhou. 2003. Polycystins 1 and 2 mediate mechanosensation in the primary cilium of kidney cells. *Nat Genet*. 33:129-137.

Nelson, W.J. 2003. Adaptation of core mechanisms to generate cell polarity. *Nature*. 422:766-774.

Nilius, B., J. Eggermont, T. Voets, G. Buyse, V. Manolopoulos, and G. Droogmans. 1997. Properties of volume-regulated anion channels in mammalian cells. *Progress in Biophysical and Molecular Biology*. 68:69-119.

Novick, P., C. Field, and R. Schekman. 1980. Identification of 23 complementation groups required for post-translational events in the yeast secretory pathway. *Cell*. 21:205-215.

Oh, E.C., and N. Katsanis. 2012. Cilia in vertebrate development and disease. *Development*. 139:443-448.

Oh, S.-J.H., S.J.;Jung, J.;Yu, K.;Kim, J.,Choi, J.Y.;Hartzell, H.C.;Roh, E.J.; Lee, C.J. in press. MONNA, a potent and selective blocker for TMEM16A/Anoctamin-1. *Molecular Pharmcology*. 84:726-735.

Oh, S.J., S.J. Hwang, J. Jung, K. Yu, J. Kim, J.Y. Choi, H.C. Hartzell, E.J. Roh, and C.J. Lee. 2013. MONNA, a potent and selective blocker for transmembrane protein with unknown function 16/anoctamin-1. *Mol Pharmacol*. 84:726-735.

Ong, A.C.M. 2013. Primary cilia and renal cysts: does length matter ? *Nephrology Dialysis Transplantation*:Aug 9. [Epub ahead of print].

Orozco, J.T. 1999. Movement of motor and cargo along cilia. *Nature*. 398:674.

Osathanondh, V., and E.L. Potter. 1964. Pathogenesis of Polycystic Kidneys. Type 4 Due to Urethral Obstruction. *Archives of pathology*. 77:502-509.

Ousingsawat, J., J.R. Martins, R. Schreiber, J.R. Rock, B.D. Harfe, and K. Kunzelmann. 2009. Loss of TMEM16A Causes a Defect in Epithelial Ca2+-dependent Chloride Transport. *Journal of Biological Chemistry*. 284:28698-28703.

Pacheco-Alvarez, D., and G. Gamba. 2011. WNK3 is a putative chloride-sensing kinase. *Cellular physiology and biochemistry : international journal of experimental cellular physiology, biochemistry, and pharmacology*. 28:1123-1134.

Pan, J., T. Seeger-Nukpezah, and E.A. Golemis. 2013. The role of the cilium in normal and abnormal cell cycles: emphasis on renal cystic pathologies. *Cellular and molecular life sciences : CMLS*. 70:1849-1874.

Pan, J., and William J. Snell. 2014. Organelle Size: A Cilium Length Signal Regulates IFT Cargo Loading. *Current Biology*. 24:R75-R78.

Patel, V., R. Chowdhury, and P. Igarashi. 2009. Advances in the pathogenesis and treatment of polycystic kidney disease. *Curr. Opin. Nephrol. Hypertens.* 18:99-106.

Pazour, G.J., B.L. Dickert, Y. Vucica, E.S. Seeley, J.L. Rosenbaum, G.B. Witman, and D.G. Cole. 2000. Chlamydomonas IFT88 and Its Mouse Homologue, Polycystic Kidney Disease Gene Tg737, Are Required for Assembly of Cilia and Flagella. *The Journal of Cell Biology*. 151:709-718.

Pazour, G.J., B.L. Dickert, and G.B. Witman. 1999. The DHC1b (DHC2) isoform of cytoplasmic dynein is required for flagellar assembly. *J. Cell Biol.* 144:473-481.

Pazour, G.J., and J.L. Rosenbaum. 2002. Intraflagellar transport and cilia-dependent diseases. *Trends Cell Biol*. 12:551-555.

Pazour, G.J., J.T. San Agustin, J.A. Follit, J.L. Rosenbaum, and G.B. Witman. 2002. Polycystin-2 is localized to kidney cilia and its ciliary level is elevated in orpk mice with polycystic kidney disease. *Curr. Biol.* 12:R378-R380.

Pazour, G.J., and G.B. Witman. 2003. The vertebrate primary cilium is a sensory organelle. [Review] [49 refs]. *Current opinion in cell biology*. 15:105-110.

Pazour, G.J.B., R.A. 2008. Targeting proteins to the Ciliary Membrane. *Current topics in developmental biology*. 85:115-149.

Pedemonte, N., and L.J. Galietta. 2014. Structure and Function of TMEM16 Proteins (Anoctamins). *Physiol Rev*. 94:419-459.

Pedersen, L.B., S. Geimer, and J.L. Rosenbaum. 2006. Dissecting the molecular mechanisms of intraflagellar transport in chlamydomonas. *Current biology : CB*. 16:450-459.

Pedersen, L.B., and J.L. Rosenbaum. 2008. Intraflagellar transport (IFT) role in ciliary assembly, resorption and signalling. *Current topics in developmental biology*. 85:23-61.

Perez-Cornejo, P., A. Gokhale, C. Duran, Y. Cui, Q. Xiao, H.C. Hartzell, and V. Faundez. 2012a. Anoctamin 1 (Tmem16A) Ca2+-activated chloride channel stoichiometrically interacts with an ezrin-radixin-moesin network. *Proc Natl Acad Sci U S A.* 109:10376-10381.

Perez-Cornejo, P., A. Gokhale, C. Duran, Y. Cui, Q. Xiao, H.C. Hartzell, and V. Faundez. 2012b. Anoctamin 1 (Tmem16A) Ca2+-activated chloride channel stoichiometrically interacts with an ezrin–radixin–moesin network. *Proceedings of the National Academy of Sciences*. 109:10376-10381.

Piel, M., P. Meyer, A. Khodjakov, C.L. Rieder, and M. Bornens. 2000. The respective contributions of the mother and daughter centrioles to centrosome activity and behavior in vertebrate cells. *J Cell Biol.* 149:317-330.

Piperno, G., and K. Mead. 1997. Transport of a novel complex in the cytoplasmic matrix of Chlamydomonas flagella. *Proc. Natl Acad. Sci. USA.* 94:4457-4462.

Porter, M.E., R. Bower, J.A. Knott, P. Byrd, and W. Dentler. 1999. Cytoplasmic dynein heavy chain 1b is required for flagellar assembly in Chlamydomonas. *Mol. Biol. Cell.* 10:693-712.

Praetorius, H.A., J. Frokiaer, S. Nielsen, and K.R. Spring. 2003. Bending the primary cilium opens Ca2+-sensitive intermediate-conductance K+ channels in MDCK cells. *J Membr Biol.* 191:193-200.

Praetorius, H.A., and K.R. Spring. 2001. Bending the MDCK cell primary cilium increases intracellular calcium. *J. Membr. Biol.* 184:71-79.

Pugacheva, E.N., S.A. Jablonski, T.R. Hartman, E.P. Henske, and E.A. Golemis. 2007. HEF1-Dependent Aurora A Activation Induces Disassembly of the Primary Cilium. *Cell*. 129:1351-1363.

Qian, F., F.J. Germino, Y. Cai, X. Zhang, S. Somlo, and G.G. Germino. 1997. PKD1 interacts with PKD2 through a probable coiled-coil domain. *Nat Genet*. 16:179-183.

Qin, H., J.L. Rosenbaum, and M.M. Barr. 2001. An autosomal recessive polycystic kidney disease gene homolog is involved in intraflagellar transport in C. elegans ciliated sensory neurons. *Curr. Biol.* 11:1-20.

Rajagopal, M., P.P. Kathpalia, J.H. Widdicombe, and A.C. Pao. 2012. Differential effects of extracellular ATP on chloride transport in cortical collecting duct cells. *American journal of physiology. Renal physiology*. 303:F483-491.

Rasche, S., B. Toetter, J. Adler, A. Tschapek, J.F. Doerner, and S. Kurtenbach. 2010. Tmem16b is specifically expressed in the cilia of olfactory sensory neurons. *Chem Senses*. 35:239-245.

Ray, K., B. Bhattacharyya, and B.B. Biswas. 1984. Anion-induced increases in the affinity of colcemid binding to tubulin. *European journal of biochemistry / FEBS*. 142:577-581.

Reczek, D., M. Berryman, and A. Bretscher. 1997. Identification of EBP50: A PDZ-containing Phosphoprotein that Associates with Members of the Ezrin-Radixin-Moesin Family. *The Journal of Cell Biology*. 139:169-179.

Reiter, J.F., O.E. Blacque, and M.R. Leroux. 2012. The base of the cilium: roles for transition fibres and the transition zone in ciliary formation, maintenance and compartmentalization. *EMBO Reports*. 13:608-618.

Rieder, C.L., C.G. Jensen, and L.C. Jensen. 1979. The resorption of primary cilia during mitosis in a vertebrate (PtK1) cell line. *Journal of ultrastructure research.* 68:173-185.

Rock, J.R., M. Cecilia Lopez, H.V. Baker, and B.D. Harfe. 2007a. Identification of genes expressed in the mouse limb using a novel ZPA microarray approach. *Gene Expression Patterns*. 8:19-26.

Rock, J.R., C.R. Futtner, and B.D. Harfe. 2008. The transmembrane protein TMEM16A is required for normal development of the murine trachea. *Develop. Biol.* 321:141-149.

Rock, J.R., M.C. Lopez, H.V. Baker, and B.D. Harfe. 2007b. Identification of genes expressed in the mouse limb using a novel ZPA microarray approach. *Gene Expr Patterns*. 8:19-26.

Rock, J.R., W.K. O'Neal, S.E. Gabriel, S.H. Randell, B.D. Harfe, R.C. Boucher, and B.R. Grubb. 2009. Transmembrane Protein 16A (TMEM16A) Is a Ca2+-regulated Cl– Secretory Channel in Mouse Airways. *Journal of Biological Chemistry*. 284:14875-14880.

Rodriguez-Boulan, E., and I.G. Macara. 2014. Organization and execution of the epithelial polarity programme. *Nat Rev Mol Cell Biol*. 15:225-242.

Rogers, K.K., P.D. Wilson, R.W. Snyder, X. Zhang, W. Guo, C.R. Burrow, and J.H. Lipschutz. 2004. The exocyst localizes to the primary cilium in MDCK cells. *Biochem Biophys Res Commun*. 319:138-143.

Roh, M.H., S. Fan, C.J. Liu, and B. Margolis. 2003. The Crumbs3-Pals1 complex participates in the establishment of polarity in mammalian epithelial cells. *J Cell Sci*. 116:2895-2906.

Rohatgi, R., L. Milenkovic, and M.P. Scott. 2007. Patched1 regulates hedgehog signaling at the primary cilium. *Science*. 317:372-376.

Romanenko, V.G., M.A. Catalan, D.A. Brown, I. Putzier, H.C. Hartzell, A.D. Marmorstein, M. Gonzalez-Begne, J.R. Rock, B.D. Harfe, and J.E. Melvin. 2010a. Tmem16A encodes the Ca^{2+}-activated Cl^- channel in mouse submandibular salivary gland acinar cells. *J Biol Chem*. 285:12990-13001.

Romanenko, V.G., M.A. Catalán, D.A. Brown, I. Putzier, H.C. Hartzell, A.D. Marmorstein, M. Gonzalez-Begne, J.R. Rock, B.D. Harfe, and J.E. Melvin. 2010b. Tmem16A Encodes the Ca2+-activated Cl− Channel in Mouse Submandibular Salivary Gland Acinar Cells. *Journal of Biological Chemistry*. 285:12990-13001.

Rosenbaum, J.L., and F.M. Child. 1967. Flagellar regeneration in protozoan flagellates. *J. Cell Biol*. 34:345-364.

Rosenbaum, J.L., and G.B. Witman. 2002. Intraflagellar transport. *Nat Rev Mol Cell Biol*. 3:813-825.

Ruat, M., H. Roudaut, J. Ferent, and E. Traiffort. 2012. Hedgehog trafficking, cilia and brain functions. *Differentiation*. 83:S97-S104.

Ruiz, C., J.R. Martins, F. Rudin, S. Schneider, T. Dietsche, C.A. Fischer, L. Tornillo, L.M. Terracciano, R. Schreiber, L. Bubendorf, and K. Kunzelmann. 2012. Enhanced Expression of ANO1 in Head and Neck Squamous Cell Carcinoma Causes Cell Migration and Correlates with Poor Prognosis. *PLoS ONE*. 7:e43265.

Saotome, I., M. Curto, and A.I. McClatchey. 2004. Ezrin Is Essential for Epithelial Organization and Villus Morphogenesis in the Developing Intestine. *Developmental Cell*. 6:855-864.

Satir, P., and S.T. Christensen. 2007. Overview of structure and function of mammalian cilia. *Annu Rev Physiol*. 69:377-400.

Scholey, J.M., and K.V. Anderson. 2006. Intraflagellar Transport and Cilium-Based Signaling. *Cell*. 125:439-442.

Schreiber, R., I. Uliyakina, P. Kongsuphol, R. Warth, M. Mirza, J.R. Martins, and K. Kunzelmann. 2010. Expression and Function of Epithelial Anoctamins. *Journal of Biological Chemistry*. 285:7838-7845.

Schroder, J.M., J. Larsen, Y. Komarova, A. Akhmanova, R.I. Thorsteinsson, I. Grigoriev, R. Manguso, S.T. Christensen, S.F. Pedersen, S. Geimer, and L.B. Pedersen. 2011. EB1 and EB3 promote cilia biogenesis by several centrosome-related mechanisms. *J Cell Sci*. 124:2539-2551.

Schroeder, B.C., T. Cheng, Y.N. Jan, and L.Y. Jan. 2008a. Expression Cloning of TMEM16A as a Calcium-Activated Chloride Channel Subunit. *Cell*. 134:1019-1029.

Schroeder, B.C., T. Cheng, Y.N. Jan, and L.Y. Jan. 2008b. Expression Cloning of TMEM16A as a Calcium-Activated Chloride Channel Subunit. *Cell*. 134:1019-1029.

Seeger-Nukpezah, T., J.L. Little, V. Serzhanova, and E.A. Golemis. 2013. Cilia and cilia-associated proteins in cancer. *Drug discovery today. Disease mechanisms*. 10:e135-e142.

Seeley, E.S., and M.V. Nachury. 2010. The perennial organelle: assembly and disassembly of the primary cilium. *J Cell Sci*. 123:511-518.

Sharma, N., Z.A. Kosan, J.E. Stallworth, N.F. Berbari, and B.K. Yoder. 2011. Soluble levels of cytosolic tubulin regulate ciliary length control. *Molecular Biology of the Cell*. 22:806-816.

Sharma, N., E.B. Malarkey, N.F. Berbari, A.K. O'Connor, G.B. Vanden Heuvel, M. Mrug, and B.K. Yoder. 2013. Proximal Tubule Proliferation Is Insufficient to Induce Rapid Cyst Formation after Cilia Disruption. *Journal of the American Society of Nephrology*. 24:456-464.

Shestakova, E.A., R.H. Singer, and J. Condeelis. 2001. The physiological significance of β-actin mRNA localization in determining cell polarity and directional motility. *Proceedings of the National Academy of Sciences*. 98:7045-7050.

Shiwarski, D.J., C. Shao, A. Bill, J. Kim, D. Xiao, C.A. Bertrand, R.S. Seethala, D. Sano, J.N. Myers, P. Ha, J. Grandis, L.A. Gaither, M.A. Puthenveedu, and U. Duvvuri. 2014. To "grow" or "go": TMEM16A expression as a switch between tumor growth and metastasis in SCCHN. *Clinical cancer research : an official journal of the American Association for Cancer Research*. 20:4673-4688.

Signor, D. 1999. Role of a class DHC1b dynein in retrograde transport of IFT motors and IFT raft particles along cilia, but not dendrites, in chemosensory neurons of living Caenorhabditis elegans. *J. Cell Biol.* 147:519-530.

Simon, S., F. Grabellus, L. Ferrera, L.J. Galietta, B. Schwindenhammer, T. Muehlenberg, G. Taeger, G. Eilers, J. Treckmann, F. Breitenbuecher, M. Schuler, T. Taguchi, J.A. Fletcher, and S. Bauer. 2013. DOG1 regulates growth and IGFBP5 in gastrointestinal stromal tumors. *Cancer Research*.

Slavotinek, A.M., E.M. Stone, K. Mykytyn, J.R. Heckenlively, J.S. Green, E. Heon, M.A. Musarella, P.S. Parfrey, V.C. Sheffield, and L.G. Biesecker. 2000. Mutations in MKKS cause Bardet-Biedl syndrome. *Nat Genet.* 26:15-16.

Sloboda, R.D., and L. Howard. 2007. Localization of EB1, IFT polypeptides, and kinesin-2 in Chlamydomonas flagellar axonemes via immunogold scanning electron microscopy. *Cell motility and the cytoskeleton.* 64:446-460.

Solinet, S., K. Mahmud, S.F. Stewman, K. Ben El Kadhi, B. Decelle, L. Talje, A. Ma, B.H. Kwok, and S. Carreno. 2013. The actin-binding ERM protein Moesin binds to and stabilizes microtubules at the cell cortex. *J Cell Biol.* 202:251-260.

Sorokin, S. 1962. Centrioles and the formation of rudimentary cilia by fibroblasts and smooth muscle cells. *J Cell Biol.* 15:363-377.

Speck, O., S.C. Hughes, N.K. Noren, R.M. Kulikauskas, and R.G. Fehon. 2003. Moesin functions antagonistically to the Rho pathway to maintain epithelial integrity. *Nature*. 421:83-87.

Stanich, J.E., S.J. Gibbons, S.T. Eisenman, M.R. Bardsley, J.R. Rock, B.D. Harfe, T. Ordog, and G. Farrugia. 2011a. Ano1 as a regulator of proliferation. *American*

Journal of Physiology - Gastrointestinal and Liver Physiology. 301:G1044-G1051.

Stanich, J.E., S.J. Gibbons, S.T. Eisenman, M.R. Bardsley, J.R. Rock, B.D. Harfe, T. Ordog, and G. Farrugia. 2011b. Ano1 as a Regulator of Proliferation. *Am J Physiol Gastrointest Liver Physiol*. 301:G1044-1051.

Stauber, T., and T.J. Jentsch. 2013. Chloride in vesicular trafficking and function. *Annu Rev Physiol*. 75:453-477.

Stephan, A.B., E.Y. Shum, S. Hirsh, K.D. Cygnar, J. Reisert, and H. Zhao. 2009. ANO2 is the cilial calcium-activated chloride channel that may mediate olfactory amplification. *Proc Natl Acad Sci U S A*. 106:11776-11781.

Suzaki, T., H. Sakai, S. Endo, I. Kimura, and Y. Shigenaka. 1978. Effects of Various Anions, Glutamate and GTP on Microtubule Assembly In Vitro. *Journal of Biochemistry*. 84:75-81.

Suzuki, J., T. Fujii, T. Imao, K. Ishihara, H. Kuba, and S. Nagata. 2013. Calcium-dependent phospholipid scramblase activity of TMEM16 protein family members. *J Biol Chem*. 288:13305-13316.

Suzuki, J., M. Umeda, P.J. Sims, and S. Nagata. 2010. Calcium-dependent phospholipid scrambling by TMEM16F. *Nature*. 468:834-838.

Szalontai, B., G. Nagy, S. Krumova, E. Fodor, T. Pali, S.G. Taneva, G. Garab, J. Peters, and A. Der. 2013. Hofmeister ions control protein dynamics. *Biochimica et biophysica acta*. 1830:4564-4572.

Takao, D., T. Nemoto, T. Abe, H. Kiyonari, H. Kajiura-Kobayashi, H. Shiratori, and S. Nonaka. 2013. Asymmetric distribution of dynamic calcium signals in the node of mouse embryo during left-right axis formation. *Dev Biol*. 376:23-30.

Takizawa, P.A., J.L. DeRisi, J.E. Wilhelm, and R.D. Vale. 2000. Plasma Membrane Compartmentalization in Yeast by Messenger RNA Transport and a Septin Diffusion Barrier. *Science*. 290:341-344.

Tanos, B.E., H.J. Yang, R. Soni, W.J. Wang, F.P. Macaluso, J.M. Asara, and M.F. Tsou. 2013. Centriole distal appendages promote membrane docking, leading to cilia initiation. *Genes & development*. 27:163-168.

Tarran, R. 2004. Regulation of airway surface liquid volume and mucus transport by active ion transport. *Proc Am Thorac Soc*. 1:42-46.

Tarran, R., M.E. Loewen, A.M. Paradiso, J.C. Olsen, M.A. Gray, and B.E. Argent. 2002. Regulation of murine airway surface liquid volume by CFTR and Ca2+-activated Cl- conductances. *J Gen Physiol*. 120:407-418.

Taschner, M., S. Bhogaraju, and E. Lorentzen. 2012. Architecture and function of IFT complex proteins in ciliogenesis. *Differentiation; research in biological diversity*. 83:S12-S22.

Terashima, H., Picollo, A., Accardi, A. . 2013. Purified TMEM16A is sufficient to form Ca^{2+} activated Cl- channels. *Proc. Natl. Acad. Sci.* in press.

TerBush, D.R., T. Maurice, D. Roth, and P. Novick. 1996. The Exocyst is a multiprotein complex required for exocytosis in Saccharomyces cerevisiae. *The EMBO Journal*. 15:6483-6494.

Tran, P. 2008. THM1 negatively modulates mouse sonic hedgehog signal transduction and affects retrograde intraflagellar transport in cilia. *Nature Genet*. 40:403-410.

Tucker, R.W., A.B. Pardee, and K. Fujiwara. 1979. Centriole ciliation is related to quiescence and DNA synthesis in 3T3 cells. *Cell*. 17:527-535.

Turunen, O., T. Wahlström, and A. Vaheri. 1994. Ezrin has a COOH-terminal actin-binding site that is conserved in the ezrin protein family. *The Journal of Cell Biology*. 126:1445-1453.

Valente, E.M., R.O. Rosti, E. Gibbs, and J.G. Gleeson. 2014. Primary cilia in neurodevelopmental disorders. *Nature reviews. Neurology*. 10:27-36.

Veland, I.R., A. Awan, L.B. Pedersen, B.K. Yoder, and S.T. Christensen. 2009. Primary cilia and signaling pathways in mammalian development, health and disease. *Nephron Physiol*. 111:39-53.

Verkman, A.S., and L.J. Galietta. 2009. Chloride channels as drug targets. *Nat Rev.Drug Discov*. 8:153-171.

Vieira, O.V., K. Gaus, P. Verkade, J. Fullekrug, W.L. Vaz, and K. Simons. 2006. FAPP2, cilium formation, and compartmentalization of the apical membrane in polarized Madin-Darby canine kidney (MDCK) cells. *Proc Natl Acad Sci U S A*. 103:18556-18561.

Wallace, D.P., J.J. Grantham, and L.P. Sullivan. 1996. Chloride and fluid secretion by cultured human polycystic kidney cells. *Kidney Int*. 50:1327-1336.

Walther, Z., M. Vashishtha, and J.L. Hall. 1994. The Chlamydomonas FLA10 gene encodes a novel kinesin-homologous protein. *J. Cell Biol*. 126:175-188.

Wang, G., K. Krishnamurthy, and E. Bieberich. 2009. Regulation of primary cilia formation by ceramide. *Journal of Lipid Research*. 50:2103-2110.

Wang, M., H. Yang, L.Y. Zheng, Z. Zhang, Y.B. Tang, G.L. Wang, Y.H. Du, X.F. Lv, J. Liu, J.G. Zhou, and Y.Y. Guan. 2012. Downregulation of TMEM16A calcium-activated chloride channel contributes to cerebrovascular remodeling during hypertension by promoting basilar smooth muscle cell proliferation. *Circulation*. 125:697-707.

Weinman, E.J., R.A. Hall, P.A. Friedman, L.-Y. Liu-Chen, and S. Shenolikar. 2006. THE ASSOCIATION OF NHERF ADAPTOR PROTEINS WITH G PROTEIN–COUPLED RECEPTORS AND RECEPTOR TYROSINE KINASES*. *Annual Review of Physiology*. 68:491-505.

Westlake, C.J., L.M. Baye, M.V. Nachury, K.J. Wright, K.E. Ervin, L. Phu, C. Chalouni, J.S. Beck, D.S. Kirkpatrick, D.C. Slusarski, V.C. Sheffield, R.H. Scheller, and P.K. Jackson. 2011. Primary cilia membrane assembly is initiated by Rab11 and transport protein particle II (TRAPPII) complex-dependent trafficking of Rabin8 to the centrosome. *Proc Natl Acad Sci U S A*. 108:2759-2764.

Wheatley, D.N. 1995. Primary cilia in normal and pathological tissues. *Pathobiology : journal of immunopathology, molecular and cellular biology*. 63:222-238.

Wheatley, D.N., A.M. Wang, and G.E. Strugnell. 1996. EXPRESSION OF PRIMARY CILIA IN MAMMALIAN CELLS. *Cell Biology International*. 20:73-81.

Wheway, G., D.A. Parry, and C.A. Johnson. 2014. The role of primary cilia in the development and disease of the retina. *Organogenesis*. 10:0--1.

Wilkerson, P.M., and J.S. Reis-Filho. 2013. The 11q13-q14 amplicon: clinicopathological correlations and potential drivers. *Genes Chromosomes Cancer*. 52:333-355.

Wilson, P.D. 2004. Polycystic kidney disease. *The New England journal of medicine*. 350:151-164.

Wilson, P.D., A.C. Sherwood, K. Palla, J. Du, R. Watson, and J.T. Norman. 1991. Reversed polarity of Na(+) -K(+) -ATPase: mislocation to apical plasma membranes in polycystic kidney disease epithelia. *Am J Physiol*. 260:F420-430.

Witman, G.B. 1975. The site of in vivo assembly of flagellar microtubules. *Ann. NY Acad. Sci.* 253:178-191.

Wolff, J., D.L. Sackett, and L. Knipling. 1996. Cation selective promotion of tubulin polymerization by alkali metal chlorides. *Protein science : a publication of the Protein Society*. 5:2020-2028.

Yan, X., and X. Zhu. 2013a. Branched F-actin as a negative regulator of cilia formation. *Exp Cell Res*. 319:147-151.

Yan, X., and X. Zhu. 2013b. Branched F-actin as a negative regulator of cilia formation. *Experimental Cell Research*. 319:147-151.

Yang, H., A. Kim, T. David, D. Palmer, T. Jin, J. Tien, F. Huang, T. Cheng, S.R. Coughlin, Y.N. Jan, and L.Y. Jan. 2012. TMEM16F forms a Ca2+-activated cation channel required for lipid scrambling in platelets during blood coagulation. *Cell*. 151:111-122.

Yang, Y.D., H. Cho, J.Y. Koo, M.H. Tak, Y. Cho, W.-S. Shim, S.P. Park, J. Lee, B. Lee, B.-M. Kim, R. Raouf, Y.K. Shin, and U. Oh. 2008a. TMEM16A confers receptor-activated calcium-dependent chloride conductance. *Nature*. 455:1210-1215.

Yang, Y.D., H. Cho, J.Y. Koo, M.H. Tak, Y. Cho, and W.S. Shim. 2008b. TMEM16A confers receptor-activated calcium-dependent chloride conductance. *Nature*. 455:1210-1215.

Yang, Y.D., H. Cho, J.Y. Koo, M.H. Tak, Y. Cho, W.S. Shim, S.P. Park, J. Lee, B. Lee, B.M. Kim, R. Raouf, Y.K. Shin, and U. Oh. 2008c. TMEM16A confers receptor-activated calcium-dependent chloride conductance. *Nature*. 455:1210-1215.

Yee, Laura E., and Jeremy F. Reiter. 2015. Ciliary Vesicle Formation: A Prelude to Ciliogenesis. *Developmental Cell*. 32:665-666.

Yoder, B.K., X. Hou, and L.M. Guay-Woodford. 2002. The polycystic kidney disease proteins: polycystin-1, polycystin-2, polaris, and cystin, are co-localized in renal cilia. *J. Am. Soc. Nephrol.* 13:2508-2516.

Yonemura, S., M. Hirao, Y. Doi, N. Takahashi, T. Kondo, S. Tsukita, and S. Tsukita. 1998. Ezrin/Radixin/Moesin (ERM) Proteins Bind to a Positively Charged Amino Acid Cluster in the Juxta-Membrane Cytoplasmic Domain of CD44, CD43, and ICAM-2. *The Journal of Cell Biology*. 140:885-895.

Yonemura, S., T. Matsui, S. Tsukita, and S. Tsukita. 2002. Rho-dependent and -independent activation mechanisms of ezrin/radixin/moesin proteins: an essential role for polyphosphoinositides in vivo. *Journal of Cell Science*. 115:2569-2580.

Yoshiba, S., H. Shiratori, I.Y. Kuo, A. Kawasumi, K. Shinohara, S. Nonaka, Y. Asai, G. Sasaki, J.A. Belo, H. Sasaki, J. Nakai, B. Dworniczak, B.E. Ehrlich, P.

Pennekamp, and H. Hamada. 2012. Cilia at the node of mouse embryos sense fluid flow for left-right determination via Pkd2. *Science*. 338:226-231.

Yoshimura, S., J. Egerer, E. Fuchs, A.K. Haas, and F.A. Barr. 2007. Functional dissection of Rab GTPases involved in primary cilium formation. *J Cell Biol*. 178:363-369.

Yu, K., C. Duran, Z. Qu, Y.-Y. Cui, and H.C. Hartzell. 2012a. Explaining Calcium-Dependent Gating of Anoctamin-1 Chloride Channels Requires a Revised Topology / Novelty and Significance. *Circulation Research*. 110:990-999.

Yu, K., C. Duran, Z. Qu, Y.Y. Cui, and H.C. Hartzell. 2012b. Explaining calcium-dependent gating of anoctamin-1 chloride channels requires a revised topology. *Circ Res*. 110:990-999.

Yu, K., J.M. Whitlock, K. Lee, E.A. Ortlund, Y. Yuan Cui, and H.C. Hartzell. 2015. Identification of a lipid scrambling domain in ANO6/TMEM16F.

Yuan, S., L. Zhao, M. Brueckner, and Z. Sun. 2015. Intraciliary Calcium Oscillations Initiate Vertebrate Left-Right Asymmetry. *Current Biology*. 25:556-567.

Zhang, Q., J. Hu, and K. Ling. Molecular views of Arf-like small GTPases in cilia and ciliopathies. *Experimental Cell Research*.

Zhou, J. 2009. Polycystins and primary cilia: primers for cell cycle progression. *Annu. Rev. Physiol*. 71:83-113.

Zuo, X., B. Fogelgren, and J.H. Lipschutz. 2011a. The Small GTPase Cdc42 Is Necessary for Primary Ciliogenesis in Renal Tubular Epithelial Cells. *Journal of Biological Chemistry*. 286:22469-22477.

Zuo, X., B. Fogelgren, and J.H. Lipschutz. 2011b. The small GTPase Cdc42 is necessary for primary ciliogenesis in renal tubular epithelial cells. *J Biol Chem*. 286:22469-22477.

Zuo, X., W. Guo, and J.H. Lipschutz. 2009. The exocyst protein Sec10 is necessary for primary ciliogenesis and cystogenesis in vitro. *Mol Biol Cell*. 20:2522-2529.